REPORT DOCUMENTATION PAGE

Form Approved
OMB No. 0704-0188

PLEASE DO NOT RETURN YOUR FORM TO THE ABOVE ORGANIZATION.

1. REPORT DATE *(DD-MM-YYYY)*	2. REPORT TYPE	3. DATES COVERED *(From - To)*
19/12/2012	Final	15/07/2007-14/07/2012

4. TITLE AND SUBTITLE
Biologically-Inspired Flight for Micro Air Vehicles

5a. CONTRACT NUMBER

5b. GRANT NUMBER
FA9550-07-1-0540

5c. PROGRAM ELEMENT NUMBER

6. AUTHOR(S)
Kenneth Breuer, Sharon Swarz, Jaime Peraire, Mark Drela, David Willis, Cynthia Moss, Belinda Batten

5d. PROJECT NUMBER

5e. TASK NUMBER

5f. WORK UNIT NUMBER

7. PERFORMING ORGANIZATION NAME(S) AND ADDRESS(ES)
Brown University, School of Engineering, Box D, 182 Hope Street, Providence, RI 02912

8. PERFORMING ORGANIZATION REPORT NUMBER

9. SPONSORING/MONITORING AGENCY NAME(S) AND ADDRESS(ES)
AF OFFICE OF SCIENTIFIC RESEARCH
875 NORTH RANDOLPH STREET, RM 3112
ARLINGTON VA 22203
Dr. Douglas Smith/RSA

10. SPONSOR/MONITOR'S ACRONYM(S)

11. SPONSOR/MONITOR'S REPORT NUMBER(S)
AFRL-OSR-VA-TR-2012-1256

12. DISTRIBUTION/AVAILABILITY STATEMENT
Distribution A: Approved for Public Release

13. SUPPLEMENTARY NOTES

14. ABSTRACT
A summary of results from five university teams, working over five years is presented. Broadly speaking, we have conducted animal flight tests, neurophysiology of bat flight, model experiments motivated by animal flights (membrane wings, flapping wings, etc), computational simulations of flapping flight at multiple levels of fidelity, and experiments and theory of flapping flight control systems.

15. SUBJECT TERMS
bats, flapping flight, unsteady aerodynamics, neurophysiology, control theory.

16. SECURITY CLASSIFICATION OF:			17. LIMITATION OF ABSTRACT	18. NUMBER OF PAGES	19a. NAME OF RESPONSIBLE PERSON
a. REPORT	b. ABSTRACT	c. THIS PAGE			Kenneth Breuer
U	U	U	U		19b. TELEPHONE NUMBER *(Include area code)* 401-863-2870

Reset

Standard Form 298 (Rev. 8/98)
Prescribed by ANSI Std. Z39.18

Bio-Inspired Flight for Micro Air Vehicles

Final Report of the AFOSR-MURI

Grant Number: FA9550-07-1-0540

Kenneth Breuer (PI) & Sharon Swartz (Brown University)
Jaime Peraire & Mark Drela (MIT)
David Willis (University of Massachusetts, Lowell)
Cynthia Moss (University of Maryland),
Belinda Batten (Oregon State University)

September 2012

PREFACE

This report is the final report for the AFOSR –Funded MURI program "Bio-Inspired Flight for Micro Air Vehicles", Grant FA9550-07-1-0540, monitored by Drs. Douglas Smith and Willard Larkin. The program officially started in May 2007, and this report is the summary of our activities from that date to the end of the program in July 2012.

The report is comprised of individual chapters from each of the five universities that are part of the MURI program: Brown University (Lead institution), the Massachusetts Institute of Technology and University of Massachusetts in Lowell (together), the University of Maryland and Oregon State University. Although the report has been formatted in a uniform style, each chapter was written separately. At the end of each chapter, a summary page listing active personnel, publications, awards and other relevant data is included for convenience.

All attempts have been made to make this material an accurate and fair record of our activities. However, it represents work in progress and should not be considered as an archival document. The individual researchers should be consulted for more details and further explanation of the material described herein.

Kenneth Breuer (PI) and Sharon Swartz (Brown University)

Jaime Peraire and Mark Drela (Massachusetts Institute of Technology)

David Willis (University of Massachusetts Lowell)

Cynthia Moss (University of Maryland)

Belinda Batten (Oregon State University)

(cover photo: Nickolay Hristov and Tatjana Hubel)

BROWN UNIVERSITY

INTRODUCTION

It goes without saying that it is almost impossible to summarize a five year program in only a few pages. For a detailed review of the Brown University efforts, one is advised to review some of the many papers that have been published and presented as a result of the MURI funding. These are listed in the supplementary material at the end of the chapter. What follows, however, are some of the highlights of our MURI research.

KINEMATICS OF BAT FLIGHT

A major contribution of portion of the effort at Brown University concerned the understanding how bats employ wing motion and structural design to achieve high levels of flight performance. This project successfully developed techniques to make the first fully detailed 3D kinematic descriptions bat wings in flight. We applied these methods to a number of important issues:

- modulation of the wing motion patterns forward flight, turns, and landing maneuvers;
- flight in bats that are morphologically similar but differ greatly in body size;
- wing kinematics in relation to changes in flight velocity and load carrying, and,
- we have compared a range of bat species to uncover patterns of wing movement related to differences among bat taxa that differ morphologically.

In each case, our work has demonstrated that wing motions of bat flight differ substantially from those of birds and insects, providing key information concerning the range of biological variation in flapping flight. We have shown that 3D dynamic complexity of bat airfoil geometry is enormous, and is characterized by varying planform, time- and span-varying camber, and high levels of wing bending and twist. We have shown that bats modulate kinematics to change the way lift is generated with increasing body size, that individual variation in kinematic patterns can be substantial, and that some interspecific differences in kinematic patterns are profound, while others are subtle.

We also explored the structural and mechanical basis for the physical capabilities of wings, and at the end of the support period, energetic aspects of the velocity-dependence of kinematic and aerodynamics in bat flight. Key finding from these studies include :

- bat wing skin is characterized by unique elastin structures that pre-loaded in compression when the wing is folded, reducing the magnitude of net tensile force required to fully stretch the wing in flight
- active muscle actuation of the joints of the bat handwing have been lost multiple times during bat evolution, suggesting that the musculoskeletal system of the bat wing represents a design compromise for maintaining flight control while simultaneously reducing wing mass

COMPLEXITY OF WING MOTIONS

Wing form of bats in flight is characterized by high levels of three-dimensional complexity that changes dynamically during the wingbeat cycle. Photograph by Richard Wainwright.

We began our work on the kinematics of bat flight by exploring the consequences of how one carries out kinematic reconstruction of the rapid three-dimensional folding, bending, and rotational wing movements employed by bats to generate aerodynamic force. Models of this system, be they focused on neuromuscular control, aerodynamic function, or energetics, can only be as accurate as the kinematic reconstructions upon which they are based. Bat flight has the potential to be extremely dimensionally complex. A bat wing membrane is maneuvered skeletally by a jointed leg, a shoulder, an elbow, a wrist, and by five fingers, each with several joints. Adding up joints alone, this provides 420 degrees of kinematic freedom per wing. Additionally, movement is influenced by the flexibility of the bony elements within the wing, the orientation-dependent compliance of the membranes, their interactions with the surrounding fluid, and by movements of the numerous tendons and muscles within the membranes themselves.

We applied proper orthogonal decomposition (POD) to wing kinematics of a bat flying in a wind tunnel to quantifying dimensional complexity of movement during steady flight over a range of speeds. We examined whether the dimensional complexity of bat movement changes with speed by looking at the number of POD modes required to closely reproduce the original movement, then used POD to quantify the relative dimensional complexities captured by using different numbers of anatomical markers in studies of bat kinematics. We used POD to assess the similarity of motion of joint angles throughout the skeleton to find functional groups of joints that are actuated in synchrony by the flying bat. We predicted that joints moving in synchrony should be located close together on the wing because units controlled together for aerodynamic purposes would likely appear close together, and because units controlled by a common part of the neuromuscular control hierarchy should presumably be near one another.

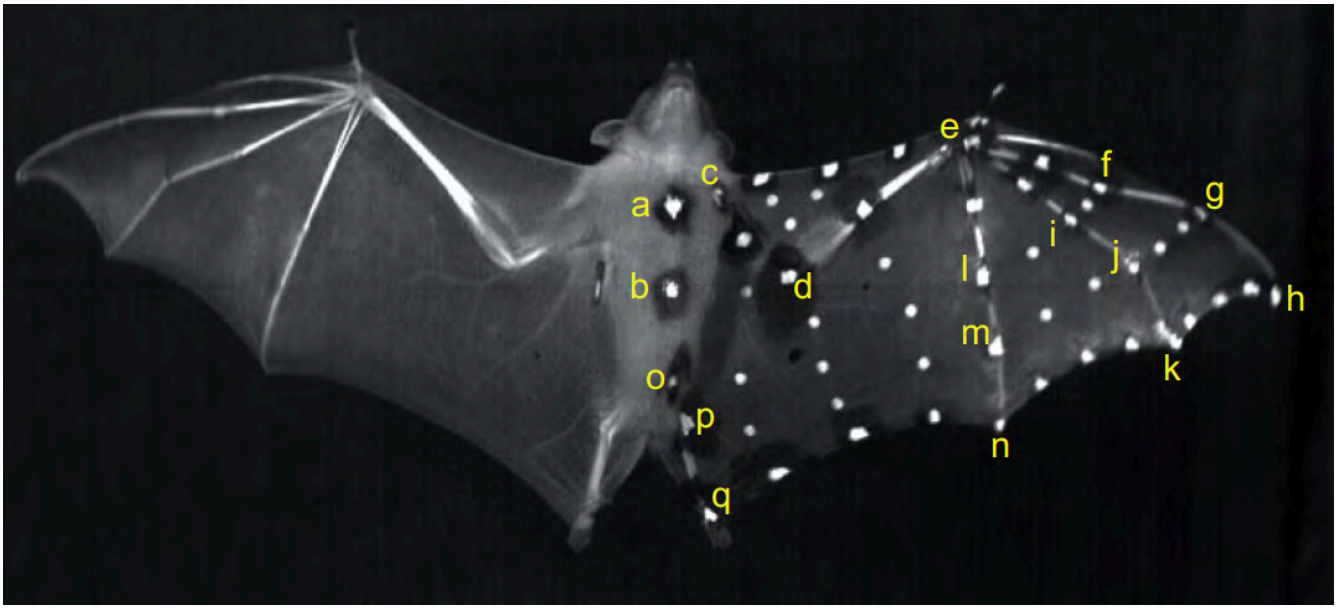

Image of lesser dog-faced fruit bat, *Cynopterus brachyotis*, in flight, from records of one of three high-speed video cameras that captured motion at speeds from approximately 3 to 7.5 m/s , illustrating 17 anatomical markers employed for POD analysis.

We found that dimensional complexity of kinematics had no significant dependence on forward velocity. More kinematic complexity is captured with more markers, but approximately 95% of the full marker set kinematic complexity is recovered with thirteen markers, and the incremental information added beyond nine markers is relatively small. The dimensional complexity captured for any subset of markers depended strongly on the particular subset employed, however. We found that sternum and knee moved in a manner distinct from that

of the forelimb markers, and that the fifth digit contributes relatively little information that is independent of that of the remainder of the wing. The shoulder and hip also showed a high level of independent motion, although this could relate to the nature of the muscle interposed between the marker and the joint. Marker sets that include more than one marker along a digit instead of using digit tips only recover significantly more complexity.

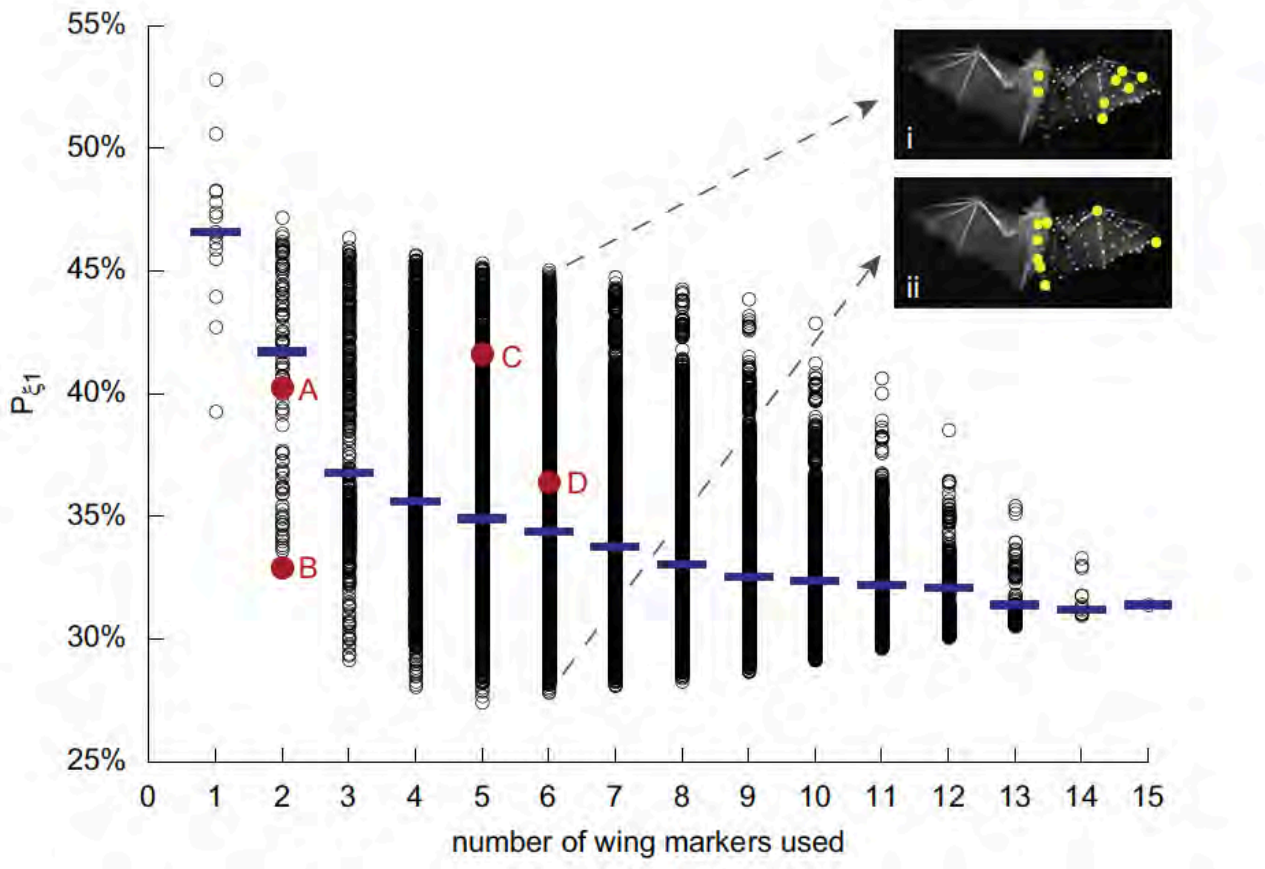

Percent recovery by the first POD mode ($P_{\xi 1}$) for the 32,767 different marker combinations possible using both sternum markers and 1–15 wing markers. Each black circle represents the mean value for a set of markers (n 1/4 9 trials), and each blue bar represents the median $P_{\xi 1}$-value for all marker position permutations with that number of wing markers. When six wing markers are used, the placement of those markers can result in any of 5005 $P_{\xi 1}$-values, from relatively poor capture of kinematic dimensional complexity, where a single mode recovers 45.1% of the original motion, to better capture of dimensional complexity, where mode 1 recovers just 27.8% . The six marker sets corresponding to those Px1-values are shown. Wing marker configurations from other published studies are shown as red circles.

We also found strong patterning in the timing of joint movements. Three major joint groups emerged that shared common motion timing within the wingbeat cycle. The first group includes the angles between digit V and its neighboring long bones (the forearm and digit IV), along with the metacarpophalangeal angles of digits III and IV, and rotation of the humerus. The second group (joint angles 4, 8, 9, and 10) includes the carpometacarpal angle of digits III, IV, and V, along with the elbow angle. The third group (joint angles 1, 2, 17, 19, and 20) includes the elevation/depression (dorsoventral) and protraction/retraction (craniocaudal) of the humerus, the elevation/depression of the femur, femoral rotation, and the knee angle. These joint angles may change together because multiple joints are controlled by muscle-tendon structures that cross more than one

joint, or groups of muscles may be innervated by a single motor pool from the nervous system. Alternatively, the motions of some joints may influence motion at other joints because the wing membrane is a single continuous structure. It may also be possible that motor programs in the central nervous system command multiple joints to carry out movement in synchrony to for the task of effective, efficient aerodynamic force generation. These three explanations are in no way exclusive, and any or all of these explanations may underlie the existence of highly correlated clusters of joint angles. Testing among these alternatives will require further and more detailed study, particularly of muscular control of the bat wing (currently in progress in AFOSR FA9550-12-1-0301 DEF, Dynamics of Bat Wing Musculature).

TURNING AND LANDING

Maneuverability is a key aspect of flight performance for both animals and engineered aircraft. Many bats inhabit and navigate rapidly through cluttered environments and the ability change flight direction likely plays an important role in obtaining food and avoiding predation. Accordingly, maneuvering performance could strongly influence many aspects of bat natural history, from habitat selection to foraging strategy. Traditional analyses of the basis maneuvering in bats and birds have employed fixed-wing models although flying animals turn using unsteady dynamics, violating the assumptions of steady-state aerodynamic theory. During this MURI, we carried out flight studies that substantially advanced understanding of how bats carry out unsteady flight behaviors, such as turning, landing, and takeoff.

Slow Turns

To successfully complete a turn, an animal must translate its center of mass (CoM) along the flight path (i.e. change its flight direction) and rotate its body around its CoM to align its body orientation with the new flight direction. Two basic strategies to produce a turning force include banked, or rolling, and crabbed, or yawing, turns. Banked turns are more common both for fixed-wing aircraft and in animal flight, and have been observed in fruit flies, locusts, dragonflies, gliding frogs, gliding mammals, and birds. Crabbed turns are also widespread in the biological world, and have also been seen in flies, dragonflies, and gliding frogs and mammals. For both banked and crabbed turns, body rotation results from an asymmetry in aerodynamic forces between left and right wings, an asymmetry in the inertial forces produced by the two wings or a combination of both. Aerodynamically generated force asymmetries can arise from differential changes in wing shape, such as changes in wing surface area, angle of attack, or camber. Alternatively, they may be due to differences in the kinematics of the left and right wings, as when the wings differ in relative velocity. It is also possible for aerodynamic force asymmetry to arise through a combination of wing shape and motion. By contrast, inertially generated force asymmetries can be produced only by differences in motion between left and right wings. Inertial forces can produce net changes in body orientation over a wingbeat cycle even when no external torques are applied due to conservation of angular momentum.

We used kinematic analysis to determine the mechanistic basis of turning flight in the lesser dog-faced fruit bat, *Cynopterus brachyotis* (see Iriarte-Díaz, J. and Swartz, S. M. 2008. Kinematics of slow turn maneuvering in the fruit bat *Cynopterus brachyotis*. *J Exp Biol* 211, 3478-3489.)

We employed high-speed multi-camera imaging of animals carrying out 90° turns in a custom-designed flight corridor under controlled conditions. Changes in bearing occur almost entirely during the downstroke, not the upstroke, portion of the wingbeat cycle. Body orientations changes continuously in a sinusoidal fashion, in synchrony with the wingbeat cycle. Bats roll into a bank at the beginning of the turn. Angular velocities increased throughout the upstroke, peaking near the upstroke-downstroke transition, then declining. Although bats change heading and bearing in a similar fashion, there is a clear temporal offset between them; changes in heading precede changes in flight path in the turn. At the end of the downstroke, the difference between the heading and bearing angle diminishes to near zero.

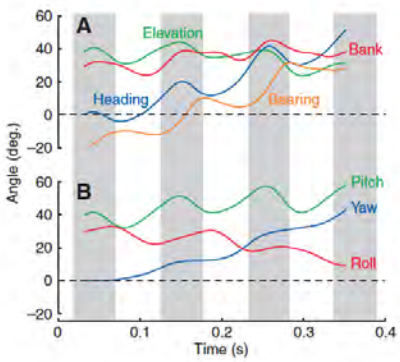

A) Bearing and orientation angles (heading, bank and elevation; and B) body angles (yaw, pitch and roll; B) for a representative right turn. Shading indicates downstroke.

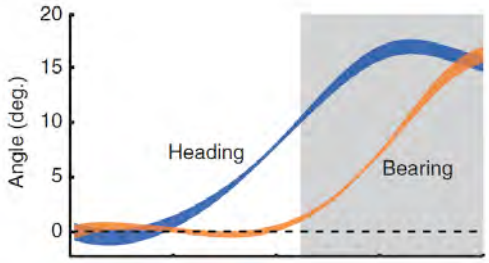

We observe small but statistically significant differences the kinematics and posture/3D geometry of the wings on the inside and outside of the turn. Mean tip speed of the inside wing was 7% faster (difference = 0.27±0.15 ms^{-1}; paired *t*-test, t_{31}=1.82, *P*=0.08), and the angle of attack of the inside wing during downstroke was 9% greater than the outside wing (difference = 2.7±0.9°, paired *t*-test, t_{31}=3.15, *P*<0.01). The asymmetry in stroke plane angle during turning was 10.8±2.8° (paired *t*-test, t_{31}=3.86, *P*<0.001), indicating that the outside wing moved more parallel to the long axis of the body than the inside wing, which had an overall direction more oriented towards the midline.

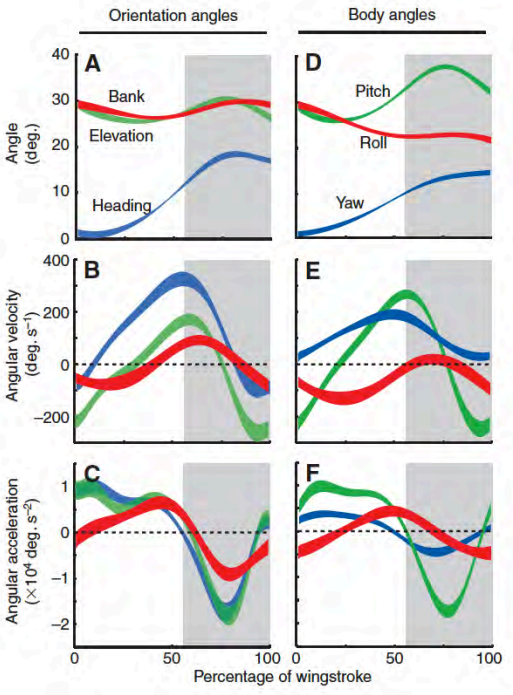

Angle, angular velocities and angular accelerations for the orientations angles (heading, elevation and bank) (A–C) and the body angles (yaw, pitch and roll) (D–F). The width of the traces represents the means ± s.e.m. Shading indicates downstroke.

In a banked turn, change in direction angle is expected to be proportional to the bank angle, but in a crabbed turn, change in direction relates to rate of change in heading rather than heading orientation. In *Cynopterus brachyotis*, heading angular velocity and mean bank angle during the downstroke are significantly correlated with the peak rate of change in direction. The partial correlation between heading rate and bearing rate when controlling for bank angle was $r_{heading|bank}$=0.80 (two-tailed *t*-test, *P*<0.0001), whereas the partial correlation between bank angle and bearing rate when controlling for heading angular velocity was $r_{bank|heading}$=0.14 (two tailed t-test, P>0.05). On average, $A_{c,bank}/A_{c,total}$, the estimated centripetal

acceleration produced by the degree of bank relative to the centripetal acceleration necessary to produce the observed change in flight direction, accounted for only 74.0±4.9% of the total acceleration required, but this varied considerably with the bank contribution as small as 10% and as much as 90% of the necessary centripetal acceleration depending on the specific turn.

Landing

Turning to a more complex aspect of maneuvering capabilities, we conducted the first detailed analysis of the mechanics of landing in bats. Bats typically roost in a head-under-heels position, but few species are capable of hovering, so achieving this inverted posture requires an acrobatic flip that brings the claws of the toes in contact with the ceiling in a manner that minimized impact forces to the lightly built hindlimbs. We quantitatively described landing kinematics and ceiling impact forces, and determined whether landing strategies vary among three bat species: *Cynopterus brachyotis*, the lesser dog-faced fruit bat, a medium-sized tree-roosting species of the Old World fruit bat lineage, and two cave-roosting New World fruit bats, *Carollia perspicillata*, Seba's short-tailed fruit bat, similar in size to *C. brachyotis* and *Glossophaga soricina*, Pallas' long-tongued bat, a smaller-bodied animal of less than half the body mass of the other two bats.

We found bats employed two distinct modes of landing: four or two 'point' landings. In a four-point landing, a bat arrived at the ceiling with the wings partially folded, the forelimbs extended laterally and anteriorly and the hindlimbs extended laterally and caudally from the body. After making contact with the ceiling with both the wings and the, the bat suspended itself by the limbs that grasped the ceiling, and subsequently, let go with its thumbs to assume a typical, head-down roosting posture. In some four-point landings, the bat's head struck the ceiling simultaneously with, or immediately before, the wrists and feet.

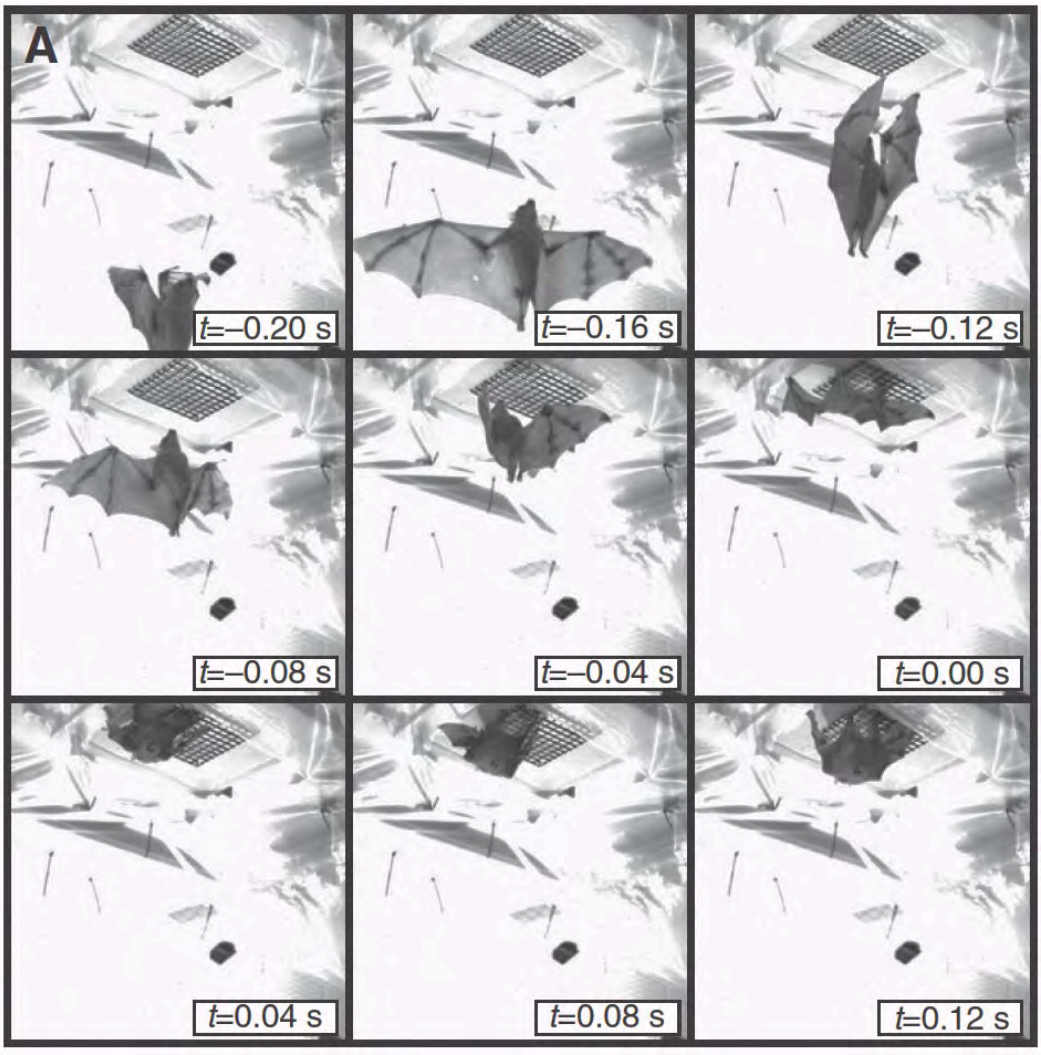

Four–point landing by *Cynopterus brachyotis.*

Two-point landings were implemented by bats moving the left and right wings and

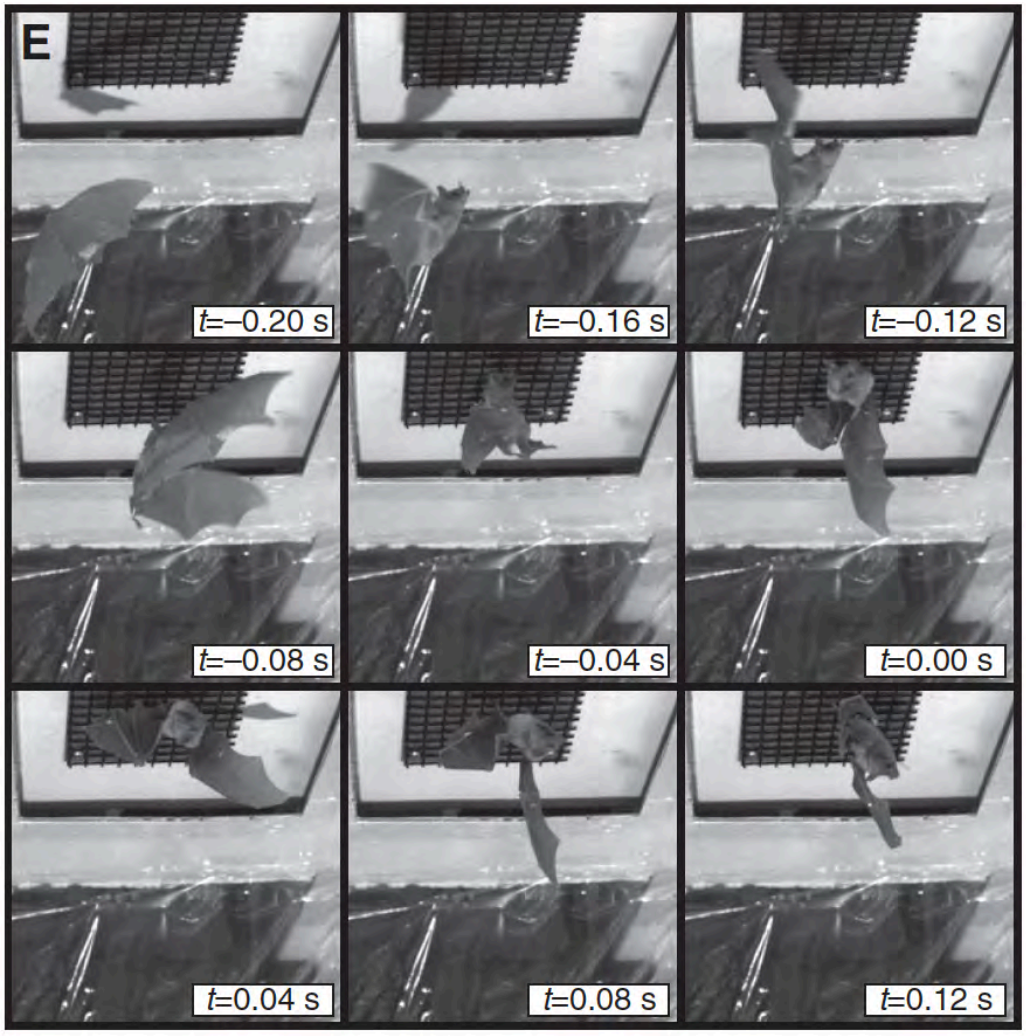

Two–point landing by *Glossophaga soricina.*

limbs asymmetrically. These bats either brought their hindlimbs anteriorly along the right side of their body (right-handed two-point landing) or along the left side of the body (left-handed two-point landing).

When bats landed on the ceiling, there was an initial peak in vertical force associated with the first impact of the body with the ceiling, then a second peak after ceiling began to support when the vertical component of the force, directed away from the ceiling, reached its first peak.

After landing, *C. perspicillata* and *G. soricina* swung back and forth by their toes, causing periodic oscillations in ceiling reaction forces. The magnitude of the impact forces varied significantly among species, with greater forces observed in the *C. brachyotis,* the species that employed four-point landings, than in *C. perspicillata* and *G. soricina,* the two species that used two-point landings.

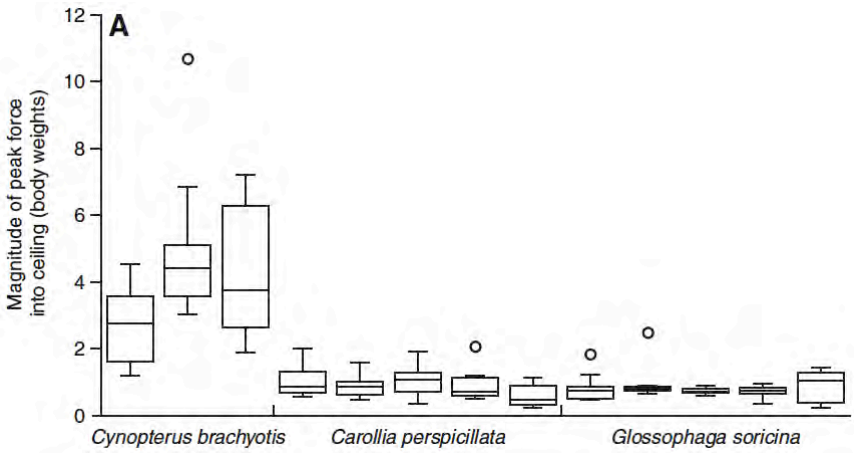

Box plot of peak impact force into ceiling at landing over the course of each trial for 13 individual sampled in this study. Each individual occupies a position on the x-axis, N-10 trials per individual.

CARRYING LOAD AND KINEMATIC VARIABILITY

Under this program, we have explored how bats in flight are able to respond to the challenges presented by carrying loads representing a significant portion of their body mass. We designed experiments that required bats to fly vertically while carrying loads of saline injected into the body cavity, a method that closely mimics natural loading, and does not interfere with the normal movements of wings in any way, unlike external load carrying . We developed a model based on actuator disk theory, and estimated the mechanical power expended by the bats as they flew, partitioned into different estimated costs of hovering, climbing and kinetic energy. We found that even our most heavily loaded bats were capable of upward flight, but as the magnitude of the load increased, flight performance diminished. Although the cost of flight increased with loading, bats did not vary total induced power across loading treatment. Bats produced more power chiefly by increasing their wingbeat frequency, although we also observed trends toward changes in other kinematic parameters, such as increased wing extension and changes in the orientation of the wingbeat stroke plane. Wingbeat amplitude decreased somewhat, in contrast to predictions and to observations from birds. However, given that the bats increase wingbeat frequency, increasing amplitude in addition may be energetically disadvantageous or beyond the limits of the musculoskeletal system.

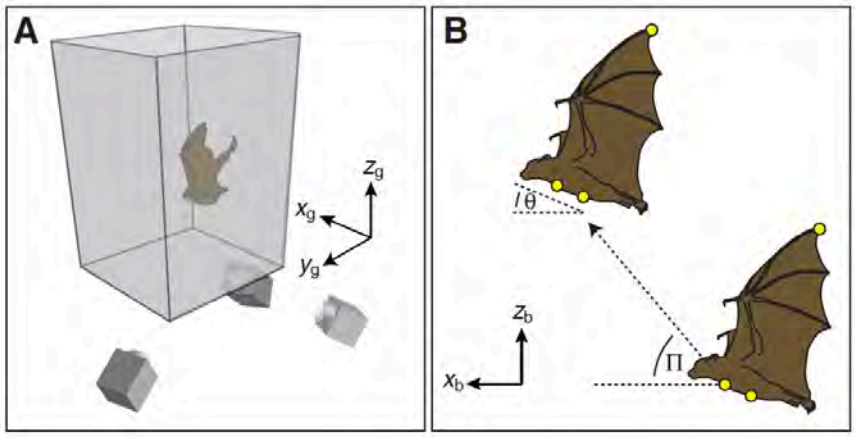

Experimental setup for the study of load carrying in bats, designed to closely mimic natural behavior.

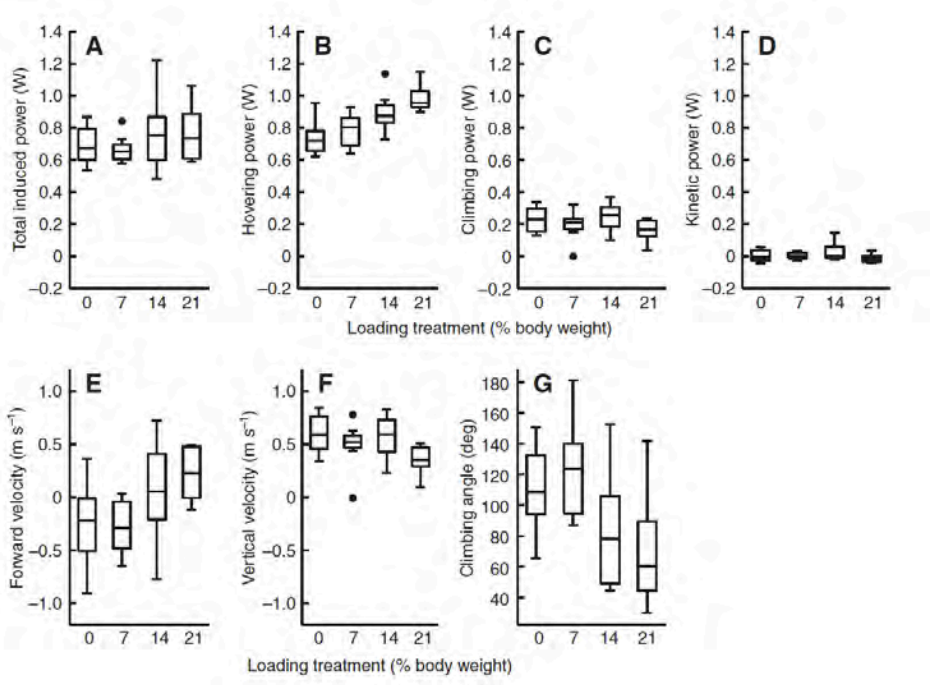

Power and flight performance across four different treatments of added weight (0, 7, 14 and 21% mass added). Total induced power (PT) did not change with loading, despite an increase in the hovering power. Climbing power (PPE) decreased slightly with loading, and kinetic power (PKE) did not change with loading. Forward flight velocity (Vx) increased with loading and vertical velocity (Vz) decreased. As a result, climbing angle (P) decreased with loading.

In this study, we applied a 20% increase in mass to *Cynopterus brachyotis*, the lesser dog-faced fruit bat, reconstructed the 3D wing kinematics, and looked at how they changed with the additional mass. Bats showed a marked change in wing kinematics in response to loading, but changes varied substantially among individuals. Each bat adjusted a different combination of kinematic parameters to increase lift, indicating that aerodynamic force generation can be modulated in multiple ways in bats, animals with complex wing structure and sophisticated neural control mechanisms.

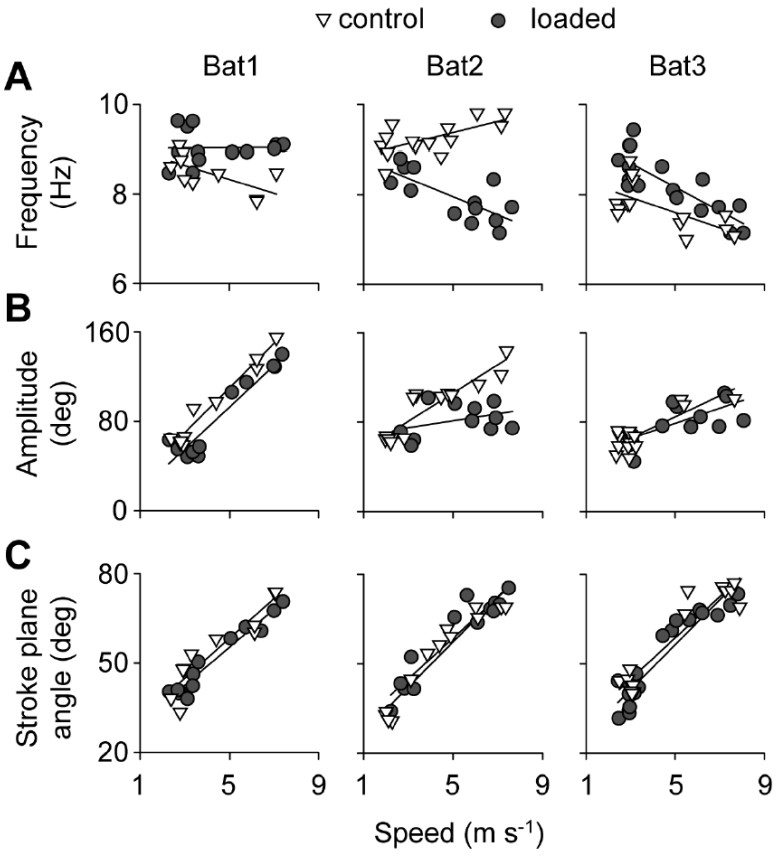

Wing motion parameters for bats in control and loaded conditions. Relationship between wingbeat frequency (A), wingbeat amplitude (B), and stroke plane angle (C) with flight speed. Open triangles represent control flights, grey circles represent loaded flights. Each point represents the mean value for a particular trial, using both wind tunnel and flight corridor flights.

We subdivide the changes we observed into two main kinematic strategies: bats either changed the motion of the wings, or changed the configuration of the wings. Wing motion was modulated primarily by increases in wingbeat frequency. Wing geometry was adapted by increasing wing area and camber. These changes in wing geometry are distinctive, and differ from patterns observed in insects and birds. The complex, individual-dependent response to increased loading in our bats points to an underappreciated aspect of locomotor control, in which the inherent complexity of the biomechanical system allows for kinematic plasticity. The kinematic plasticity and functional redundancy observed in bat flight can have evolutionary consequences, such as an increase potential for morphological and kinematic diversification due to weakened locomotor trade-offs. These strategies also could be adapted in the design of autonomous vehicles intended to carry variable payloads.

To gain further insight into the complex interconnections among kinematics, aerodynamic force production, and load, we carried out a comparative study of kinematics of six bat species representing a 40-fold body size range (M_b = 0.0278–1.152 kg), and compared wing posture overall wing kinematics to predictions based on scaling theory.

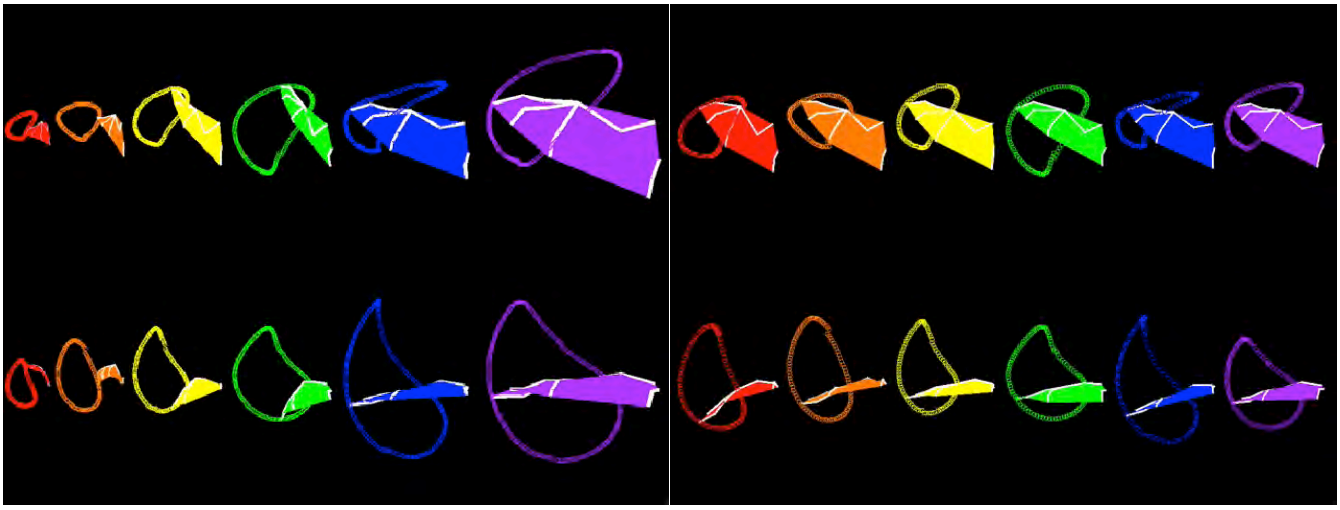

Wing motion in six species of pteropodid bats, in top view (top row) and head on (bottom row). The left panel shows wings and motions in correct relative size, and in the right panel wings are scaled to comparable wingspan, with motion scaled accordingly. Species are: *Cynopterus brachyotis* (red, body mass approx. 0.32 kg), *Rousettus aegyptiacus* (orange, body mass approx. 0.14 kg), *Pteropus pumilis* (yellow, body mass approx. 0.19 kg), *Eidolon helvum* (green, body mass approx. 0.30 kg), *Pteropus hypomelanus* (blue, body mass approx. 0.58 kg), *Pteropus vampyrus* (purple, body mass approx. 1.05 kg).

We found that maximum wingspan (b_{max}) and maximum wing area (S_{max}) scaled with somewhat positive allometry, and wing loading (Q_s) with negative allometry ($b_{max} \propto M_b^{0.423}$; $S_{max} \propto M_b^{0.768}$; $Q_s \propto M_b^{0.233}$) than has in comparison to previous studies that were based on measurements from specimens stretched out flat on a horizontal surface. Our results suggest that larger bats open their wings more fully than small bats do in flight, and that for bats, body measurements alone cannot be used to predict the conformation of the wings in flight. This body size-dependence of wing conformation has not been recorded previously.

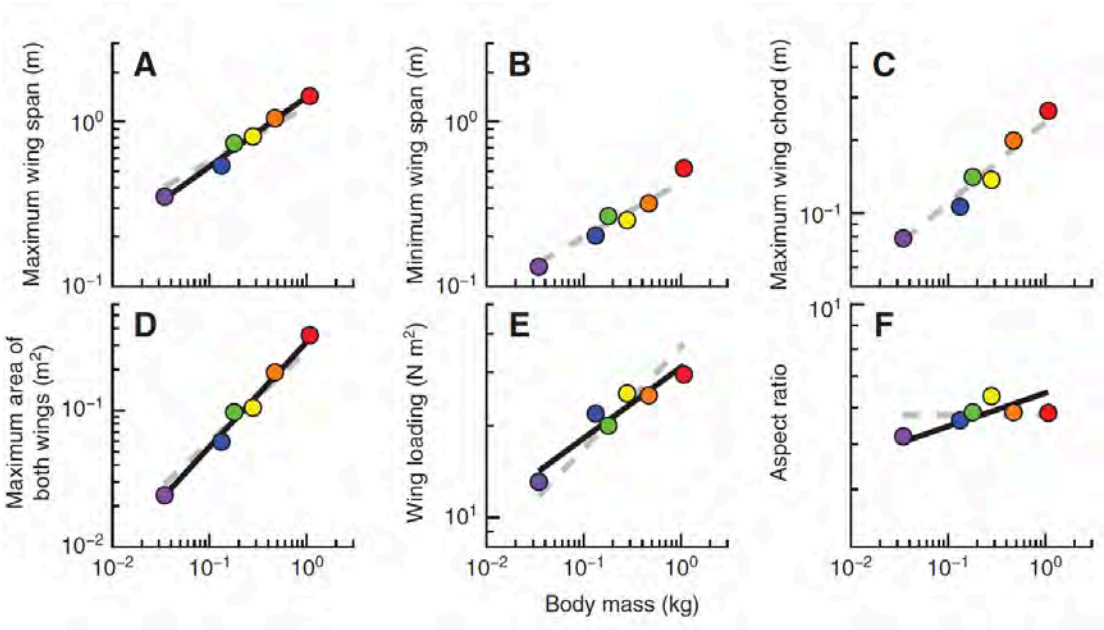

Log–log phylogenetic GLS RMA regressions of wing shape parameters against body mass after phylogenetic correction. Circles represent medians for each species. Expected slopes under isometry are denoted by the grey dashed line. Where data approached or achieved statistically significant allometry, the best fit line is shown in black. (A) Maximum wingspan, (B) minimum wingspan, (C) wing chord, (D) maximum wing area, (E) wing loading, and (F) aspect ratio.

Several kinematic variables, including downstroke ratio, wing stroke amplitude, stroke plane angle, wing camber and Strouhal number, did not change significantly with body size, demonstrating that many aspects of wing kinematics are

similar across this range of body sizes, at least in this group of relatively closely related species. Whereas aerodynamic theory suggests that preferred flight speed should increase with mass, we did not observe an increase in preferred flight speed with mass, but instead saw that these animals flew at similar absolute flight speeds despite substantial differences in size. Larger bats had also higher lift coefficients (C_L) than did small bats ($C_l \propto M_b^{0.170}$). The slope of the wingbeat period (T) to body mass regression was significantly more shallow than expected under isometry ($T \propto M_b^{0.180}$), and angle of attack (AoA) increased significantly with body mass [AoA $\propto$ log $M_b^{7.738}$]. None of the bats in our study flew at constant speed, so we used multiple regression to isolate the changes in wing kinematics that correlated with changes in flight speed, horizontal acceleration and vertical acceleration. We uncovered several significant trends that were consistent among species. Our results demonstrate that for medium- to large-sized bats, the ways that bats modulate their wing kinematics to produce thrust and lift over the course of a wingbeat cycle are independent of body size.

FLIGHT ENERGETICS

To complement our work on the kinematic and aerodynamics of bat flight, at the end of our project, we made direct measurements of the speed-dependence of the metabolic cost of flight in unrestrained flight in a wind tunnel. Using Seba's short tailed fruit bats, *Carollia perspicillata*, as our study species, we probed flight metabolism at air speeds from 1 to 7 m s^{-1}. Aerodynamic theory predicts that flight for fixed-wing aircraft requires more energy at low and high speeds compared with intermediate speeds, and this theory has often been extended to predict speed-dependent metabolic rates and optimal flight speeds for flying animals. However, it has not previously been possible to robustly test the theoretical U-shaped flight power curve for bats.

We took advantage of the recent development of a greatly improved method, the labeled sodium bicarbonate technique, to measure oxygen consumption during flight experiments. This technique allows quantification of an animal's CO_2 production rate while performing activities of only several minutes duration, without restricting the animal's movements. In this method, investigators administer ^{14}C- or ^{13}C-labeled sodium bicarbonate to an animal prior to the onset of the experiment, and assess the enrichment in labeled C of exhaled breath before and after the activity of interest by quantifying the washout rate of the label and deviations from that rate. Fractional turnover of ^{13}C can be converted into metabolic rate and power, based, in this case, on the assumption that bats oxidized glycogen during short flights. The labeled Na-bicarbonate method is particularly powerful for studies of flight metabolism because of the difficulties of measuring oxygen consumption during animal flight. In addition to the many challenges of recording metabolic rate from moving animals, flight imposes additional constraints. In particular, the types of apparatus usually used for making metabolic measurements, such as respirometry masks worn around an animal's head or respirometers that an animal approaches during feeding in hovering or hovering-like behavior, often impose additional metabolic costs on an animal's flight or restrict normal motions of flight. The sodium bicarbonate method eliminates all necessity for such devices, instead requiring only a small injection prior to the exercise period, followed by the imposition of a period of rest after exercise, during which time the animal's exhaled breath can be regularly sampled for oxygen and carbon dioxide analysis.

We found that power requirements of flight varied with air speed in a U-shaped manner in five out of seven individuals, but energy turnover was independent of air speed in two individuals. Power is somewhat higher at the lowest airspeeds, with a tendency to decline at moderate speeds, and to increase at the highest speeds from which we were able to obtain data. In nature, *Carollia* are able to achieve higher flight speeds, and it is possible that metabolic power continues to increase at higher flight speed. The variation we see among individuals differs from patterns of speed-dependent energy use seen in birds, but is consistent with our observations of kinematic variability among individuals flight during load carrying.

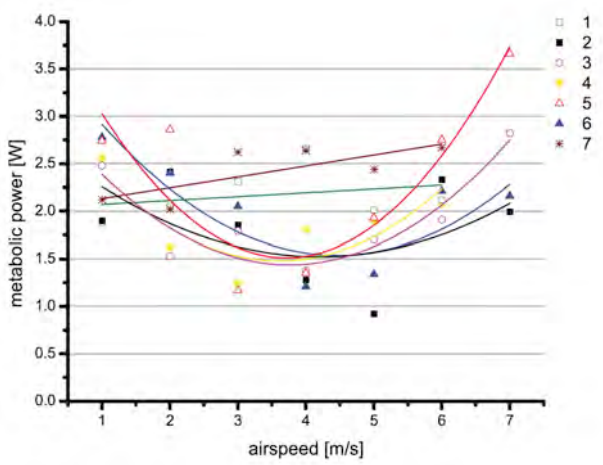

Relationship between metabolic power (W) and air speed (m s^{-1}) in seven *Carollia perspicillata* with best fit regressions.

We also compared measured metabolic power to values predicted by a widely used model of aerodynamic power requirements for animal flight developed by Pennycuick. Empirical measurement of power requirements of flight were close to values predicted by Pennycuick's aerodynamic model for lower speeds, but differed at higher speeds, including minimum power speed, and even more for maximum range speed. This suggests that these common theoretical models are likely incomplete or inaccurate in some meaningful respects, and predictions of flight power based on simple theoretical modeling of this kind along should be viewed with some caution. Further studies should be carried out to explore flight metabolism over a greater range of flight conditions and in a broader range of bat species that represent a larger sample of the diversity of body sizes, wing form, wing kinematics, etc. It will also be informative to compare the metabolic power of flight to aerodynamic power, computed from wake measurements obtained in PIV experiments, and we expect to be able to conduct these analyses in the near future.

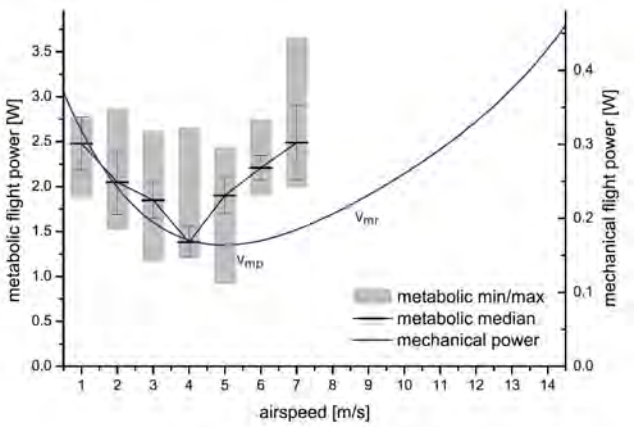

Metabolic power (W) in relation to air speed in *Carollia perspicillata*, in comparison to mechanical power vs. air speed as predicted by Pennycuick's model, measured metabolic power, shown in box plots (with minimum and maximum values) for a given air speed, matches closely at low speeds, but increasingly diverges from predicted values at moderate to higher speeds.

WING MEMBRANE STRUCTURE AND MECHANICS

WING MEMBRANE STRUCTURE

The primary of the aerodynamic surface in bats, the wing membrane, is skin, modified for exceptional compliance and anisotropy. The extraordinary compliance of bat skin makes it possible for the wing to change shape during flight not only because of the motions of the highly jointed skeleton, the structural framework of the wing membrane, but also because of deformations of the skin itself when it is subjected to dynamically changing aerodynamic forces. In this project, we have developed new methods for the study of bat wing skin that are beginning to provide fundamental insight into the function of this remarkable structure. Better understanding of the diversity of bat wing membranes is key to unraveling the diversity of bat flight performance.

We developed a novel method to visualize, document and describe important aspects of bat wing structural architecture. First, wings are extended and affixed to an armature-wire frame with suture thread and photographed to record the natural patterning of corrugation induced in the skin by the tension in the fibers.

Dorsal view of fresh mounted *Glossophaga soricina* with corrugations imposed by tension in fiber network.

Then, to explore the internal structure of the fiber architecture, We photograph the wing membrane skin using a polarizing lens filter on a copy stand-mounted Nikon D300 camera after placing the wing specimen under a large sheet of polarizing film (TECHSPEC NT45-204) on a light table; by progressively rotating the lens filter, we optimize the illumination of different connective tissue fiber populations. Because collagen and elastin, the primary connective tissue structural constituents of the wing are birefringent, we have found that they appear at heightened contrast when viewed through polarizing filters.

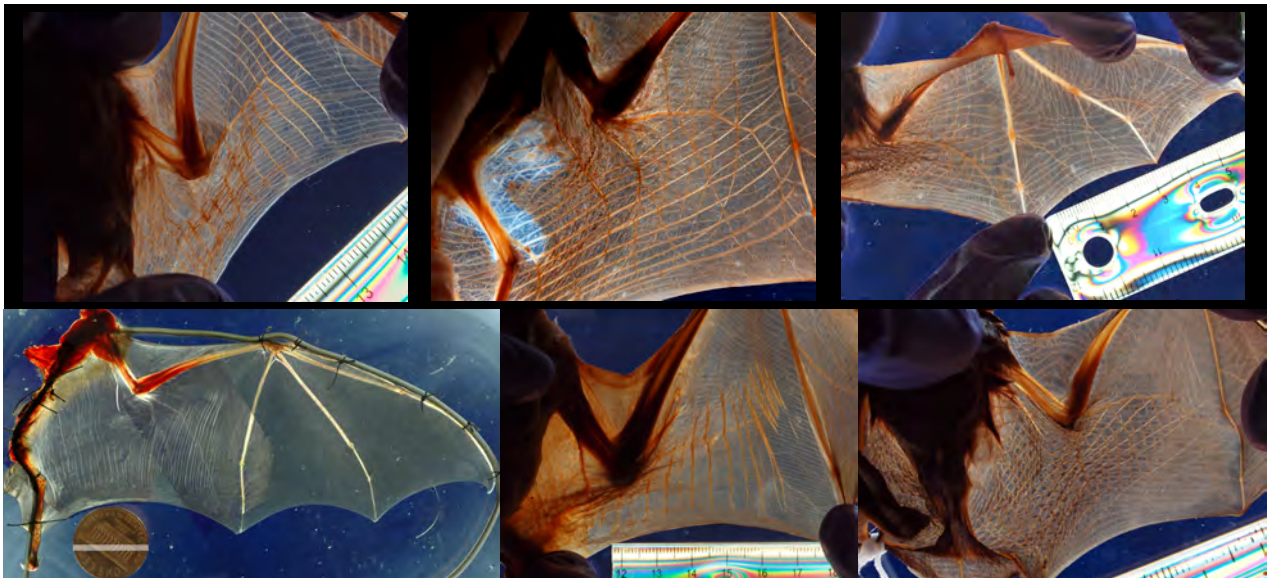

Polarized light photographs of six bat species demonstrate a portion of the interspecific variability in connective tissue and muscle architecture.

For fresh tissue specimens, we can further enhance the specimen quality: to remove as much tissue opacity and pigmentation as possible, we can chemically treat them clear them by with acetone and methyl salicylate.

Cleared *Glossophaga soricina* wing imaged without (left) and with (right) polarizing filters.

These techniques are allowing us to understand the large-scale patterns in bat wing tissue architecture. For example, in the species we have surveyed to date, the number and length of intrinsic muscles of the wing membrane, the plagiopatagiales, appear body size-independent, but their diameter scales in proportion to mass$^{0.33}$. The capacity of muscles to generate force is proportional to cross-sectional area, hence we would predict an increase in diameter with body mass, but with a scaling coefficient of only 0.33 and no increase in muscle number with body mass, it appears that larger animals have substantially less muscle force within the wing, normalized to body size, than do smaller bats. The pattern for the

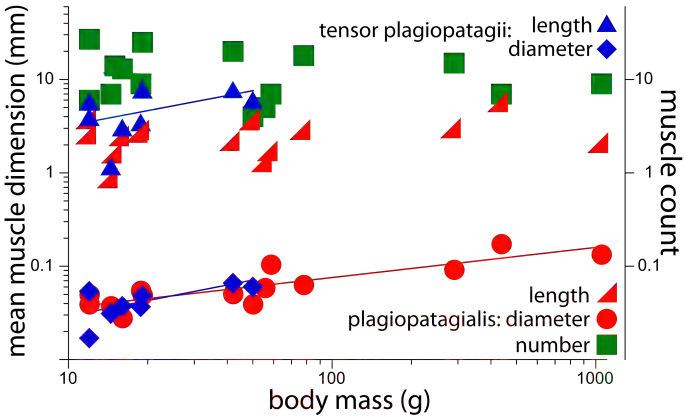

intrinsic wing muscles in the region of the ankle is somewhat different; the scaling of the tensor plagiopatagii muscles is steeper, proportional to body mass$^{0.54}$. Full significance of these results awaits further study, but suggests that these two intrinsic muscle groups may be functionally distinct in their roles in flight.

FUNCTION IN INTRINSIC WING MUSCLES

Bat wings possess distinctive muscles that run within the skin and attach into the connective tissue network. These muscles, which originate and insert within the membrane itself, lacking direct connection to the skeleton, are known as the *plagiopatagiales*; they are found in all bat species examined to date, and are restricted to the armwing or plagiopatagium, where they run parallel to digit V, the 'pinkie' finger. It has been traditional thought that they help control the camber armwing, and recent work has proposed that this may be implemented by modulating the stiffness of the membrane skin.

To better understand the potential role of these muscles in flight control, a key first step is to ascertain their patterns of activation in relation to the timing of wing movements in flight. Electromyography or EMG is a technique that allows investigators to directly measure and record the activity of skeletal muscles by detecting the electrical potential generated by muscle cells when they activated. Recording muscle activity from the plagiopatagiales during flight is challenging in several ways. The muscles in question are very small, near the size limit for successful implantation of bipolar EMG electrodes. EMG recording is subject to movement artifact, and flapping wings pose great difficulties in this regard. Many EMG recordings are made attaching the animal or human subject to a lightweight electrical cable, which poses potential difficulties when the test subjects flies in a three-dimensionally complex path. Our lab has devoted considerable effort to developing suitable methods to meet these challenges. During the course of this project, we succeeded in recording in-flight EMG from wing muscles, including the plagiopatagiales, using both conventional hard-wired EMG and our own custom-designed radio-frequency telemetry system in our wind tunnel and flight corridor. Our FM transmitter employs is tunable over a +/-2 MHz range; the signal is not digitized on board, hence there is no constraint on sampling rate. The system is long-lived (battery life = approx. ten hours), lightweight (transmitter mass = 1.5 g), and low cost; each board plus components costs less than $45 and signals can be received with a consumer-grade radio. On-board amplification is 100X.

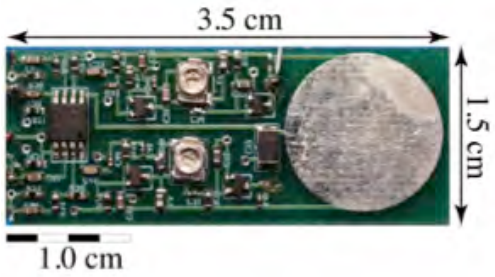

EMG transmitter built in the Swartz/Breuer labs. Mass = 1.5 g.

For bats well-adapted to fly in wind tunnels, however, we find the quality of data obtained from light-weight cables may be as good as we obtain from wireless experiments, as has been the case in EMG studies of hummingbirds. Using a cabled data and recording from bats flying in the Brown wind tunnel, we can are aobly to observe the activation of plagiopatagiales muscles during takeoff (far right, white area), multiple wingbeats (alternating grey and white) and landing (far left, white area), with electrodes in adjacent muscles showing highly congruent activity patterns. During steady flight, muscle activity occurs primarily during the downstroke, a pattern that is consistent with the idea that the muscles act to regulate camber. The plagiopatagiales also show bursts of irregular activity during takeoff and landing; the functional role of the muscles during these behaviors remains uncertain. Future work will build on the results obtained to date, and will address velocity dependence of plagiopatagiales activity, coordination of activity to firing in other wing muscles, relationship of

intrinsic muscle activity to activity of other important flight muscles (pectoralis major, trapezius, spinodeltoid, biceps, triceps) and key kinematic parameters, such as timing of top of upstroke, maximum wing extension, maximum camber, etc.

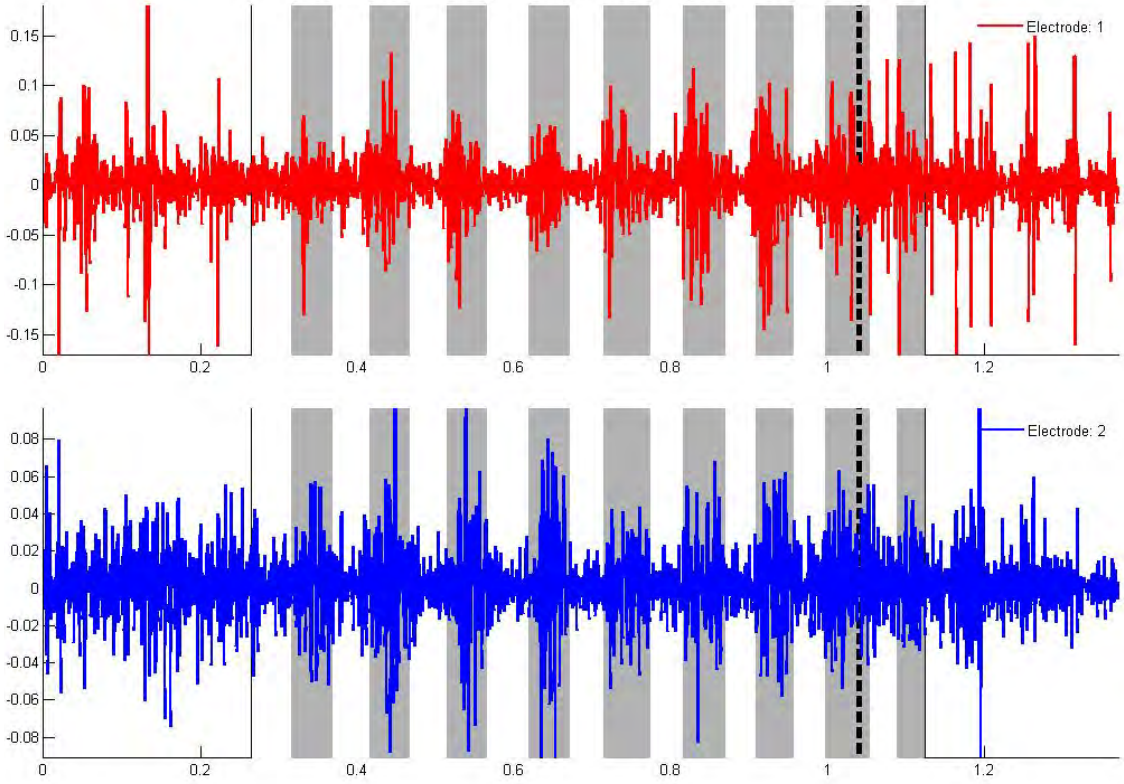

Representative EMG recorded from two adjacent plagiopatagiales muscles of *Artibeus jamaicensis*, the Jamaican fruit bat, taking off (far left), flying steadily for nine wingbeat cycles (alternating grey and white bars, grey indicates downstroke), and then landing (far right). Time in seconds on x-axis, voltage (millivolts) on y-axis.

AERODYNAMICS OF BAT FLIGHT USING PIV

A significant portion of the effort at Brown University was focused on the quantitative measurement of bat flight, and the velocity fields associated with animal flight. This is in addition to the kinematics measurements described in the earlier section. Much of the early work focused on the development of real-time PIV techniques for aerodynamic measurements, while the latter work, which still continues, focuses on measurement of wake and wing flow structures associated with different modalities of bat flight. In these areas we accomplished the following:

- Development of the first techniques for time-resolved PIV measurements of wakes behind freely flying animals
- Trefftz plane measurements of velocity fields behind several species of bats (*Cynopterus, Tararida, Myotis , Eptesicus* and *Artibeus*)
- Demonstration of wake features common to bat flight, including tip vortices, starting and stopping vortices, a near-body vortex associated with wing-body interaction and short-lived vortex pair at the

wing tip, associated with the upper wing reversal. These features are observed in all bat wakes except for those of high-speed fliers

- On-wing measurement of velocity fields for *Eptesicus fuscus,* and analysis of the generation of vortex structures during the wing beat cycle.

TREFFTZ PLANE PIV MEASUREMENTS

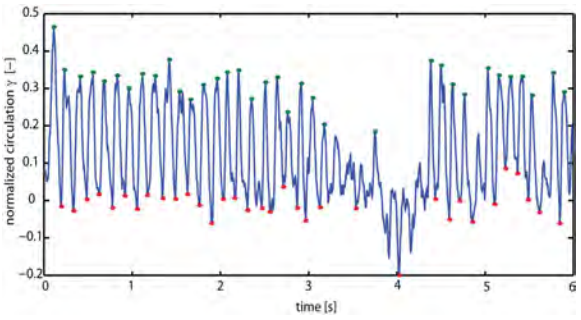

Circulation as a function of time from a freely flying bat in the wind tunnel

In our first series of experiments, we focused on synchronized time-resolved measurements of the wing kinematics and wake velocities for a medium sized bat, *Cynopterus brachyotis*, flying at low-medium speed in a closed-return wind tunnel. Measurements of the motion of the body and wing joints, as well as the resultant wake velocities in the Trefftz plane, are recorded at 200 Hz (approximately 24-28 measurements per wing beat). Circulation profiles are found to be quite repeatable, although variations in the flight profile are visible in the wake vortex structures. The figure to the left shows the normalized circulation for about 40 wing beat cycles. The circulation has almost constant strength over the middle half of the wing beat (as defined by the vertical motion of the wrist, beginning with the downstroke). This emphasizes the importance of time-resolved PIV measurements and kinematics in order to detect variability in the circulation and to be able to correlate these with changes in acceleration and maneuvering (middle of the recorded trial).

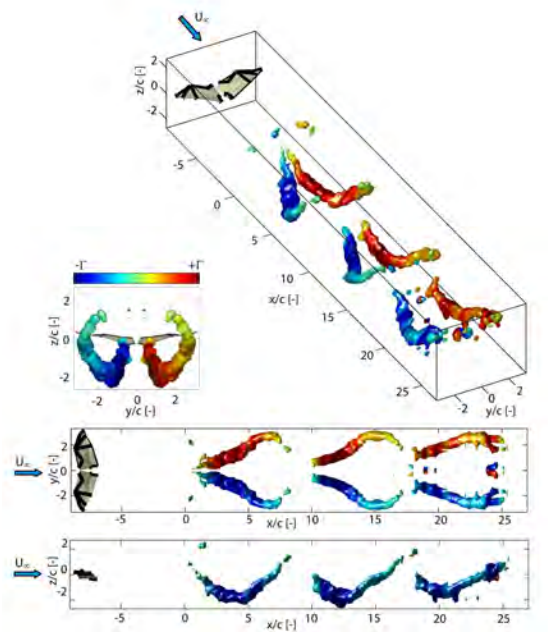

Vortex wake structure measured using time resolved PIV behind *Cynopterus brachyotis.*

A strong streamwise vortex is shed from the wingtip, growing in strength during the downstroke, and persisting during much of the upstroke. At relatively low flight speeds (3.4 m/s), a closed vortex structure behind the bat is postulated. We have followed up the initial measurements with PIV measurements on two other species – *Tadarida brasiliensis* and *Myotis fuscus* (results not shown here). Most recent results are of *Artibeus jamaicensis*, in which the data was used for estimation of flight energetics (presented later in this chapter)

PIV-MEASUREMENT OF THE AIR FLOW AROUND A BAT WING

The Trefftz plane flow field measurements helped us to develop a good understanding of the lift generation during different parts of the wing beat cycle as well as for different regions of the wing. However, to complete the understanding of the three-dimensional wake structures, additional views are

necessary. Thus we now align the laser light sheet parallel to the freestream in order to measure, using time-resolved PIV (200 Hz), the air flow in the region of the left wing of the animals.

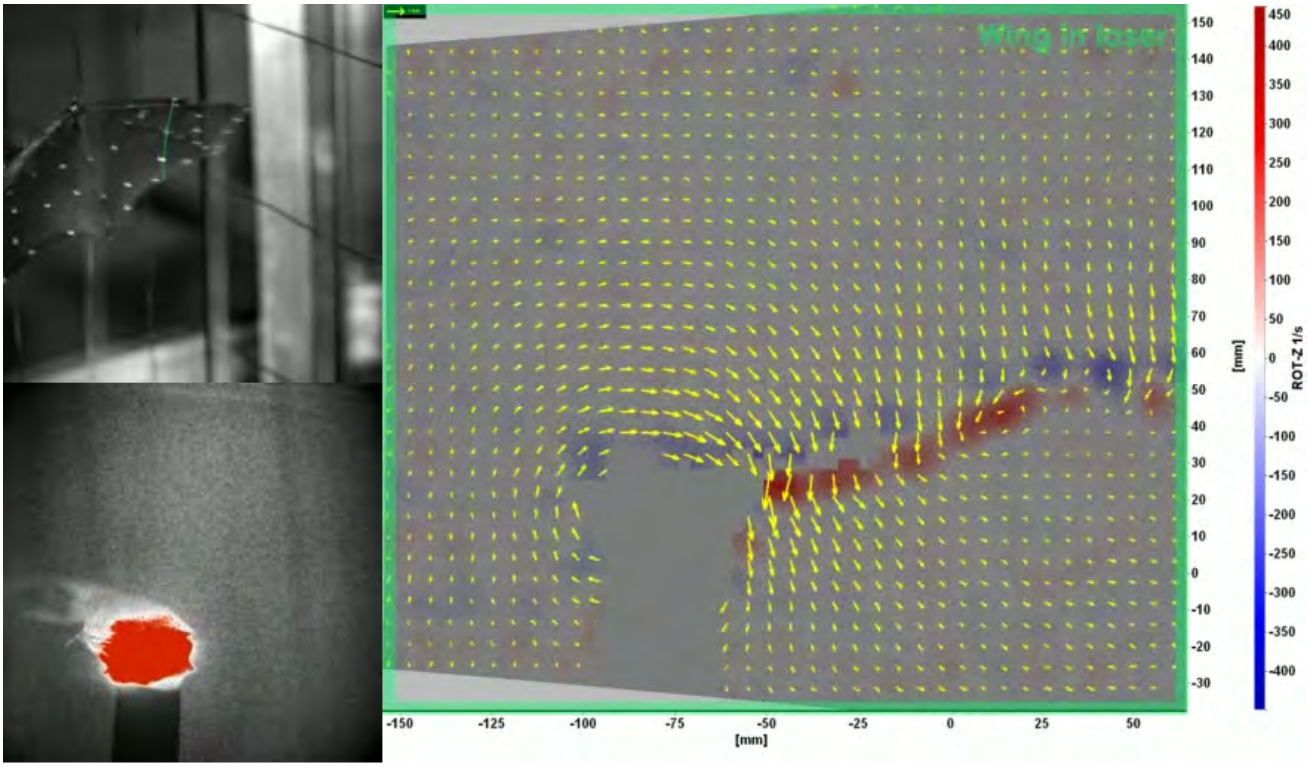

On-wing PIV results showing the bat in the wind tunnel (top left), the raw PIV image (bottom left) and the resultant PIV frame with the velocity vectors and vorticity contours

A preliminary study with one individual big brown bat (*Eptesicus fuscus*) was successfully conducted in the summer of 2010 and was repeated in more detail in the summer of 2012. We measured the flow field for speed range of 4.5 m/s to 7 m/s over the entire span of the left wing. Characteristic flow structures were observed consistently at different spanwise positions, including the starting and stopping vortices at the beginning and end of the downstroke, as well as other vortex and wake features. These data have identified flow structures that have confirmed conclusions that we drew out of the previous Trefftz plane measurements and will help to add detail to the nature and timing of the lift generation as well as increase our understanding of the generation of thrust and the presence of drag, respectively. The data is currently being analyzed.

PIV ESTIMATES OF THE POWER REQUIRED FOR FLIGHT

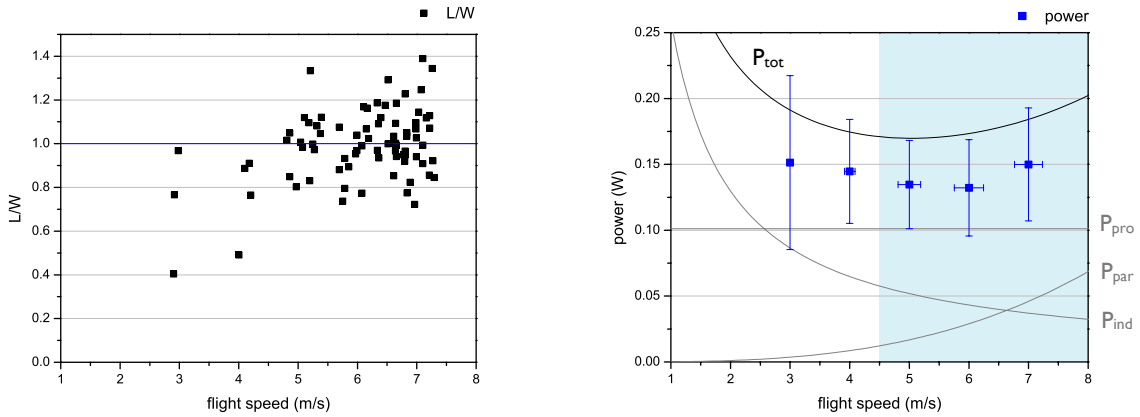

Lift, normalized by weight (left), and aerodynamic power (right), plotted versus the flight speed and compared against the Pennycuick prediction for flight power

Using our newly developed high-accuracy system for Trefftz plane measurements (discussed later in the chapter with regard to technqiues), we have completed a series of measurements of three components of velocity, time resolved in the wake behind the Jamaican fruit bat, *Artibeus jamaicensis.* The data has been processed with great care to extrapolate the velocities outside the measurement regime (using the knowledge that the velocities are induced by the trailing vortex wake, and that outside the core wake, the flow is irrotational), and the complete kinetic energy in the wake has been computed. Two remarkable results have been achieved. The first indicates that the wake can account for lift support. This seems obvious, but it is worth noting that in all previous wake measurements, both in our group and the Lund group, wake velocities have not truly accounted for lift support, a failure due to the inaccuracies of Trefftz plane measurements prior to our improved split laser sheet measurement methods. The second result is that the power in the wake appears to lie in the "elbow" of the predicted power curve, falling slight lower than the classic Pennycuick prediction (shown), and higher than the more complex Raynor prediction (not shown here). This data is currently being written up for publication.

PHYSICAL MODEL TESTING

TESTING OF A ROBOTIC BAT WING

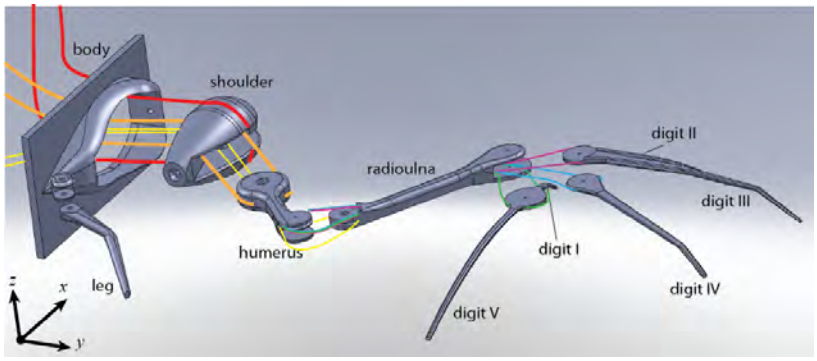

Robotic model of bat wing, showing skeletal structure and actuation system of pulleys, enablling motion in three degrees of freedom

Live bats come in a variety of ecological niches, from those that chase insects through tree branches, to those that carry fruit for miles back to their roosts, to those that catch fish, to those that migrate thousands of miles south for the winter. These different species have different wing morphologies as well as employ a variety of kinematics while flying to accomplish their goals. To study the effect of different wing morphologies and kinematics we must be able to systematically vary each variable independently. To achieve this we have built a robotic wing with many of the basic kinematic capabilities of bat wings.

The shape of the wing was modeled after the most thoroughly-studied bat in the lab, *Cynopterus brachyotis*. The body and skeleton was rapid prototyped out of ABS plastic, and the membrane was made from poly-di-methyl-siloxane (PDMS). The robotic wing has seven joints controlled by three servo motors, providing three active degrees of freedom: the shoulder can move on an up and down axis and a fore and aft axis, and the elbow and wrist joints flex synchronously extending and retracting the wing (**Error! Reference source not found.**). The mechanism is inspired by biology where the servo motors actuate the joints through cables the same way a muscle actuates a joint through tendons. Together the joints and motors allow us to vary the wing beat frequency, amplitude, stroke plane, downstroke ratio, and retraction during upstroke all with biologically relevant values.

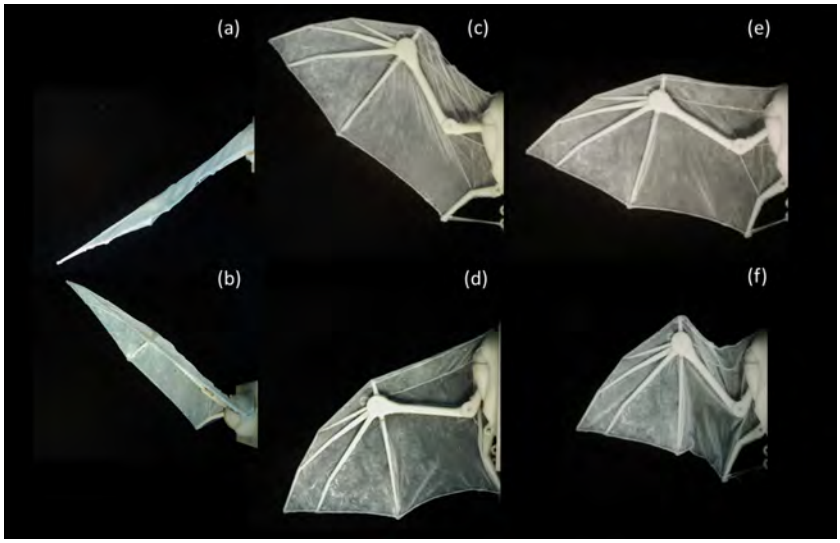

Still photgraphcs from robotic wing motion, illustrating flapping, sweep and retraction

Using this robot we sought to determine the aerodynamic force generated by and power required to flap the wings with different kinematic parameters. The wing was mounted in the ceiling of a wind tunnel on a low drag air bearing support. Lift and drag were measured using load cells, while power to flap was recorded from the torque input to the servo motors.

Results are shown below, which illustrates the lift and thrust generated as well as the input power required, all as functions of a variety of kinematic parameters: frequency, amplitude, stroke plane and downstroke ratio. As

one might suspect, the power scales with frequency cubed, and we were gratified to see that weight support, and a balance between drag and thrust both occur at around 6 Hz, which is comparable to the value observed in the live animals. The dependence of aerodynamic forces on stroke plane behaves as one might expect – increasing the stroke plane serves to rotate the force vector, increasing the thrust.

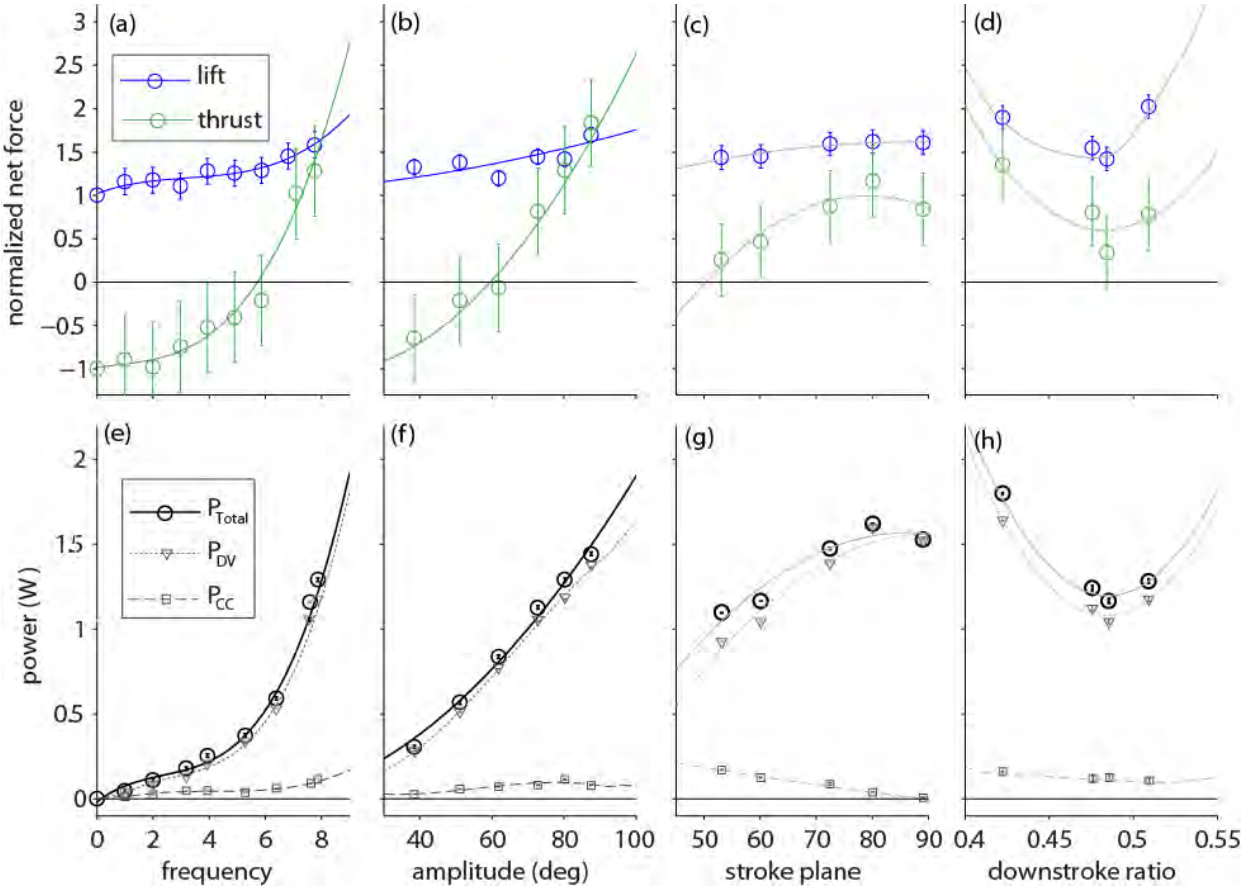

Net force (lift and thrust) and input Power, as functions of flapping frequency, ampliude, stroke plane and downstroke ratio.

A SELF-EXCITED FLAPPING WING MODEL: FROM GLIDING TO POWERED FLIGHT

We also explored more "impressionistic" aerodynamic models that are less connected to bat flight, but are inspired by biological flight problems. An example of this is a project in which we used a wing model to explore an aeroelastic instability that may have aided early bats in the transition from gliding to flapping flight over fifty million years ago. The wing model is composed of a flat plate with a hinged trailing flap. The wing is cantilevered to the main body to enable a flapping motion with a specific natural frequency. At low wind speed the wing is stationary, but above a critical wind speed the flap start to oscillate, generating an oscillating lift force on the main wing. The oscillating lift force results on a self-excited flapping motion of the wing.

In a series of detailed experiments, we measured the drag and lift forces, and kinematics as we varied the natural frequency of the wing model (by varying the shoulder stiffness), the angle of attack, and the wind speed. The critical velocity when the model undergoes in a flapping state depends linearly with the natural frequency. The amplitude of oscillation for the main wing and flap follow a sinusoidal motion. A positive angle of attack on the wing results in a positive lift force with a respective lift coefficient. But this lift coefficient is

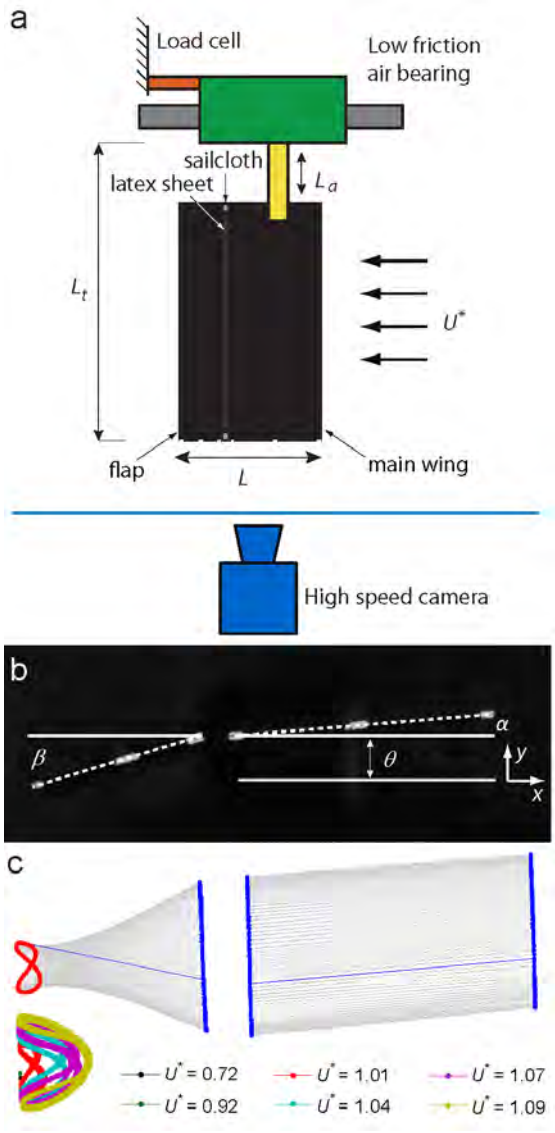

significantly enhanced (between 25% and 16%) once the wing starts to flap. The flapping motion in addition to increase the lift coefficient increases the drag coefficient of the wing. Our results have valuable implications on the evolution of powered biological flight. Based on our results that indicate that passive flapping wing can increase the lift generation compared to a non-flapping wing, we hypothesize that early bats may have used a self-excited aeroelastic mechanism that originate from the animals' flexible wing to increase lift generation and this passive motion eventually led to powered flight. Although this is accompanied by a lower lift to drag ratio (which would have decreased the length of the total glide), the increased lifting capability would have enabled larger body mass and/or transport of more food and hence might have been a positive selective pressure.

Schematic of the natural flapper experimental setup. The flap is attached to the main body with sailcloth. The wing model was mounted in a low friction air bearing. A uniaxial load cell was used to record the drag force and lift force. A high speed camera synchronized with the load cell was used to capture the kinematics. The natural frequency of the wing was varied with the length of the cantilever. (b) Image of the high speed camera. Broken white line shows the wing tip edge. α is the angle of attack based on the main wing, β is the angle of the flap and θ is the angle of oscillation of the main body. (c) Motion of the flapper above the critical velocity. Inset show the trailing edge motion for different wind speeds.

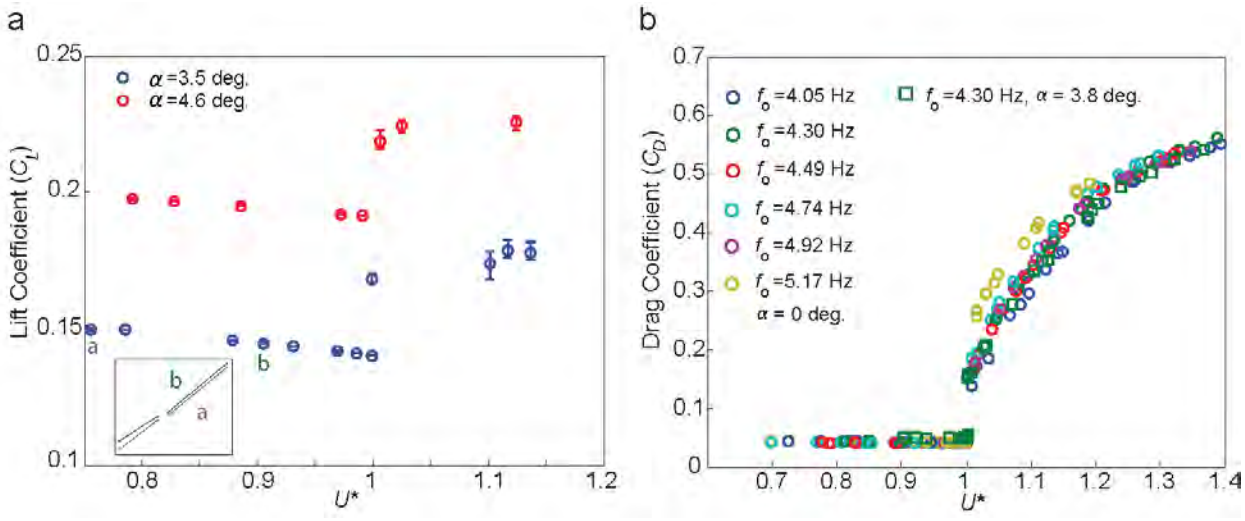

(a) Lift coefficient versus velocity for α = 3.5 and α = 4.6. There is a jump on the lift coefficient once the wing starts to oscillate (U^*>1) . Inset shows the flapper configuration at α =3.5 deg. at two subcritical air speeds. (b) Drag coefficient versus velocity.

COMPUTATIONAL STUDIES OF LIFT ENHANCEMENT VIA FLAPPING

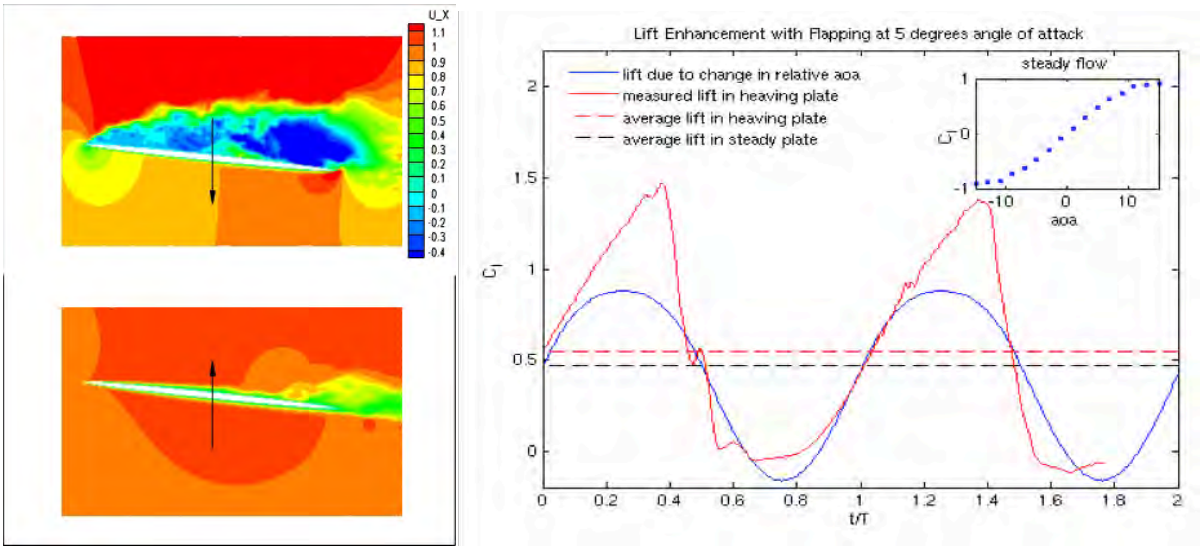

(Left) Instantaneous streamwise velocity contours of the plate during downstoke (top) and upstroke (bottom). (Right) C_l vs. time for the measured heaving plate at 5 degrees and that predicted due to relative angle of attack. The dashed lines show the mean C_l for the heaving and steady flows. The inset is the angle of attack vs. C_l computed for steady, non-moving plates.

In order to better understand the results of the experiment described above, we performed high-fidelity computations on a simplified flapping model. These simulations isolate the high-lift mechanism, and provide the detailed and time-resolved dynamics of the flow. The computational model is an ellipse of aspect ratio 50, which approximates the thin flat-plate on the leading edge of the flapper. The plate is fixed at an angle of attack, and then prescribed a sinusoidal heaving motion whose non-dimensional amplitude and frequency closely match that of the experiments. A large-eddy simulation (LES) with a fully resolved boundary layer, allows an accurate three-dimensional computation at a turbulent Reynolds number of 40,000. In addition, baseline computations are performed at fixed angles of attack for the steady, non-moving plate. Each

simulation takes approximately 100 hours of computational time utilizing 64 processors on the Army Research Lab's SGI Altix ICE 8200 cluster.

The plate is heaved vertically in a sinusoidal motion. The top image shows the instantaneous streamwise velocity contours during the downstroke, and the bottom image is a snapshot of the upstroke. During the downstroke, the boundary layer is separated and contains a coherent vortex structure that moves downstream. This vortex structure corresponds to an extended low pressure region over the length of the chord, and a peak in the lift coefficient (red solid line) in he figure above. Compared with the flow over a non-moving plate at 5 degrees, the heaving motion increases the lift by approximately 16%. However since the plate is moving, the relative angle of attack changes with time and depends on the mean angle of attack and the vertical velocity of the plate. However, the measured lift of the heaving plate is greater than the lift calculated using the relative angle of attack (blue solid line in the figure above) and the lift coefficients of the corresponding steady flows. Thus, the acceleration and unsteady motion of the plate promote a higher lift than predicted from the non-moving or steady angle of attacks. Although the kinematics of the self-propelled flapper consist of a main airfoil and attached flap, these computations indicate that the lift enhancement may be predominantly due to the heaving motion rather than the more complicated flow dynamics surrounding the flap.

THE MECHANICS OF MEMBRANE WINGS

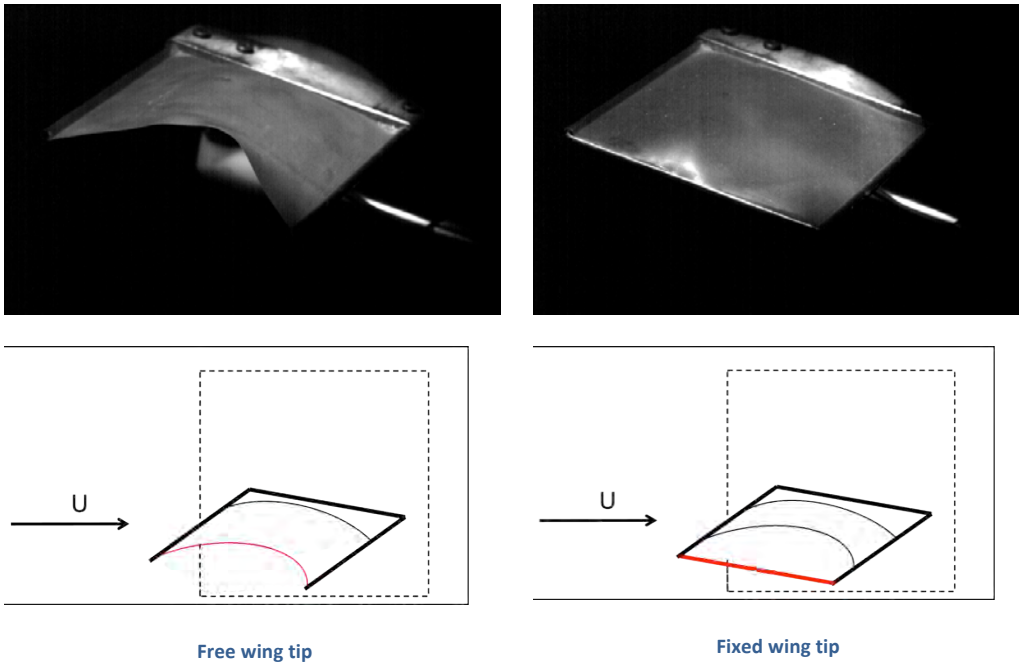

Photographs of membrane wings under identical aerodynamic conditions exhibit behavior heavily dependent upon the membrane support. The wing with unsupported wing tip exhibits much larger camber than its fully supported version.

One of the key features unique to bats is their highly compliant membrane wings. Wing compliance allows self-cambering, soft stall, and sustained performance at large angles of incidence. Because they are lightweight, membrane wings are also an attractive option for Micro Air Vehicle design.

The interaction between the vortices shed from the leading edge and wing tip interact with the membrane to select vibration modes. The interaction between the membrane dynamics and the boundary layer is a suspected mechanism for maintaining attached flow in aggressive aerodynamic conditions. The shape and dynamics of the membrane wing is heavily dependent upon how the membrane's support. We want to understand the relationship between the membrane dynamics, the flow structures and how they combine to affect the aerodynamic performance of a membrane wing. Although these experiments are just getting underway, our approach combines direct force measurement, high-speed membrane displacement measurements, and Particle Image Velocimetry on rectangular membrane wings with different perimeter support.

TECHNIQUES AND TOOL DEVELOPMENT

ACCURATE MEASUREMENT OF STREAMWISE VORTICES

Measuring the aerodynamic forces on an animal in free flight poses some unique challenges. Because the animal cannot be directly instrumented, forces must be indirectly measured by observing the wake. One such method for determining forces is to measure the circulation in the Trefftz plane using Particle Image Velocimetry. Previous PIV wake measurements have characterized the flow structures behind bats under varying flight conditions; however, the measured forces have failed to resolve weight support. We explored the challenge of Trefftz plane PIV measurements by conducting a case study on a fixed wing. We modified the traditional PIV setup to increase the accuracy of measurement and determined the conditions under which aerodynamic forces can and cannot be resolved.

The major challenge of Trefftz plane PIV measurements is that the freestream quickly advects wake structures through the investigation plane. In typical flight conditions, the strength of the wake structures are an order of magnitude less than the freestream; hence, the dynamic range of the PIV experiment is very low. We increased the dynamic range of the measurement by moving the interrogation plane with the freestream, allowing the flow structures to be resolved.

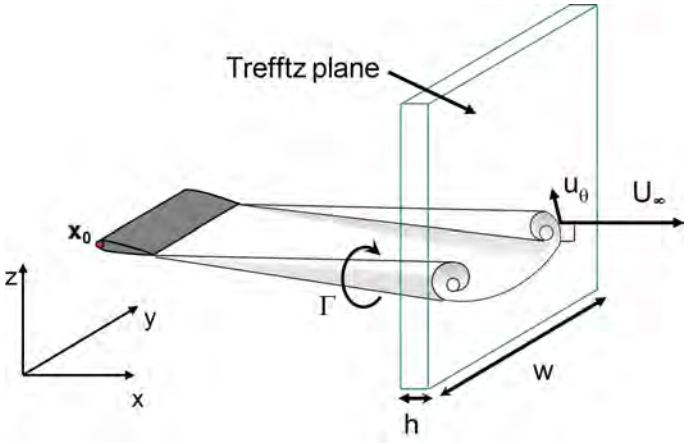

The roll-up of a vortex sheet behind a flyer into streamwise trailing vortices. Measurement of the circulation in the Trefftz plane is sufficient to determine lift.

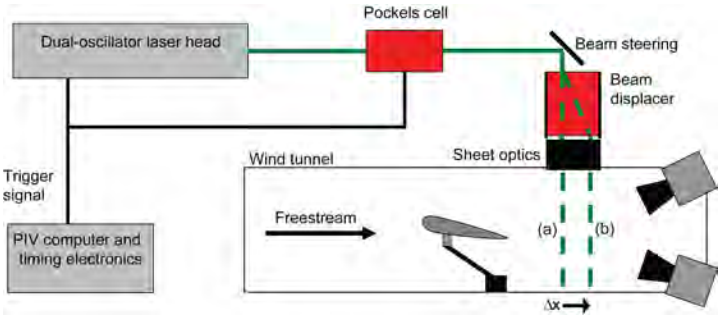

The laser sheet is displaced with the freestream. High-speed, repeatable displacement is achieved by adding a Pockels cell and a beam displacer. The electro-optical components are capable of operating at 200Hz.

The traditional PIV configuration is comprised of an interrogation plane illuminated by a double-pulsed laser. Moving the interrogation plane with the freestream requires changing the laser path by a fixed distance with precision timing. Furthermore, the implementation must be capable of a fast repetition rate (200Hz). We implemented a Pockels cell and polarizing beam displacer to achieve precise, jitter-free displacement of the interrogation plane. We conducted wake measurements on a fixed wing using both traditional and our improved PIV techniques.

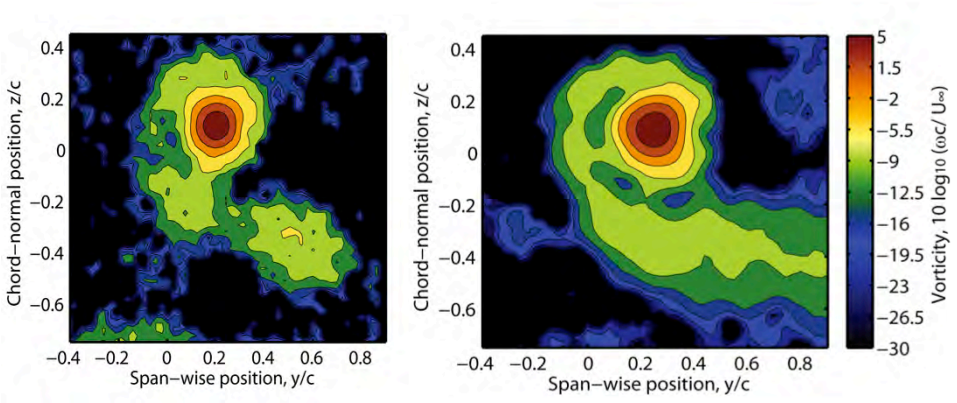

The trailing vortex was measured using traditional PIV and the dual-plane technique. The region behind the left wing-tip is shown. Vorticity is shown on a logarithmic scale to emphasize the low level structure outside the core.

We compared the measurements of the wake behind a fixed wing as it rolls into trailing vortices. The trailing vortices have a strong core region, and an outer spiral tail of low-level vorticity. Both techniques capture the core of the trailing vortex; however, unlike the dual-plane measurement, the traditional PIV measurement was not capable of resolving the flow outside the core. The strong, defining features of the wake can be captured by the traditional PIV method in the Trefftz plane; however, to capture the total strength of the wake and estimate aerodynamic forces, the low level details must be resolved. The evolution of the trailing vortex location agrees favorably between the two experimental methods. Despite similar measurement of the wake structure, the traditional PIV technique failed to capture the lift. The dual-plane technique did capture the expected wake strength.

The measurement of aerodynamic forces behind free flying bats requires resolution of the details in the wake. Implementing the dual-plane PIV technique provides the measurement resolution necessary to capture the full strength of the wake structures.

THREE-DIMENSIONAL RECONSTRUCTION OF BAT FLIGHT KINEMATICS

Central to our MURI into the flight mechanics of bats is the ability to accurately reconstruct the three-dimensional wing and body kinematics. We reconstruct the elaborate motions of bats from high-speed videos of bats. Despite a growing interest in recovering the motion of biological systems, 3D motion reconstruction methods predominantly focus on the capture and reconstruction of human motion. As such, there are fewer sophisticated methods for analysis of animal locomotion. The fast wing and body motions of flying animals place serious requirements on both the hardware and software systems

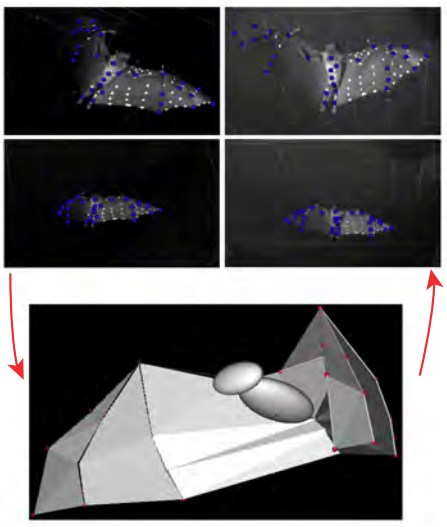

Reducing multiple camera views to a "digital bat" is time consuming, but critical to much biomechanics research

used to reconstruct their three-dimensional motion. Bats pose a particular challenge: the elaborate wing beats of bats result from the coordination of more than 24 wing joints as well as the deformation of a thin membrane covering their wing skeleton. The complex wing motionresults in significant self-occlusion that makes direct tracking of marker locations tedious.

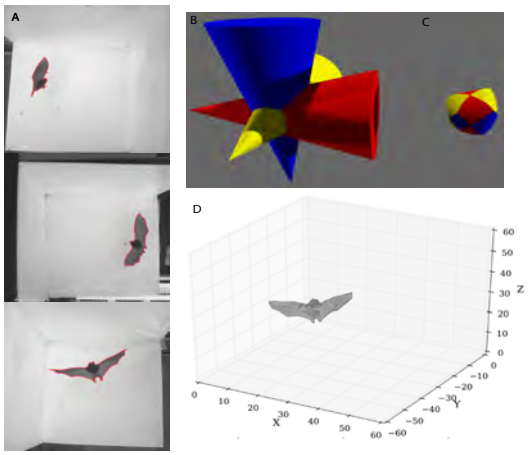

A. We are able to automatically extract the bats' silhouettes. B. Using the camera calibration we are able to both predict silhouettes cast by a model as well as C. directly approximate the shape of the flying animal.

During the MURI program, we have developed a method to reconstruct and analyze the flight kinematics of freely flying bats from multiple view video. Our tracking system is developed to allow tracking of complex models that incorporate known biomechanical constraints. The framework accommodates generalized models, is able to track from several types of image properties - e.g. image features, markers, and we are extending it work work with silhouettes. Furthermore, by modeling the dynamics of the biological systems, we are also able to directly recover not only the motion of these animals, but also infer the external and internal forces that act upon these animals to generate this motion. Our method is a top-down model-based approach built upon the Square Root Unscented Kalman Filter.

To augment image feature and marker-based tracking our tracking framework allows for the detection and incorporation of silhouettes into tracking. By controlling the lighting and the background of flight experiments we are able to automatically identify the outline - or silhouette - of bats in image sequences. Using the known camera calibration we are able to both predict silhouettes cast by a model as well as directly approximate the bat's shape from the silhouettes alone. In addition - the computational model that we build tracking upon is able to predict and refine a detailed silhouette outline thus incorporating this image feature directly into the model-based tracking pipeline

CONCLUDING REMARKS

The MURI program at Brown has been successful beyond our most ambitious expectations. The support has built a significant collaboration between the physical and biological sciences, it has spurred the development of novel and creative new tools for the measurement of live animal flight biomechanics and has inspired numerous projects in bio-inspired flight, unsteady aerodynamics, biological materials and simplified models for low Reynolds number flapping flight and Micro Air Vehicles. The MURI program has successfully trained numerious students and post doctoral research scientists who have gone on to research careers in universities, government research laboratories and private industry.

As a result of the MURI program, the key personnel at Brown (Profs Breuer and Swartz) have developed lasting research collaborations with the other MURI team members as well as with other researchers at AFRL labs, around the US and the world. Several other AFOSR research projects have been initiated as a result of the MURI program, enabling the work to continue. For all these, we express our deep and sincere thanks to the program managers at AFOSR who had the vision and skill to initiate and to manage the AFOSR MURI on bio-inspired flight – Rhett Jeffries, Willard Larkin and Douglas Smith.

SUPPLEMENTARY DATA

PERSONNEL SUPPORTED (AT LEAST IN PART) BY MURI PROJECT

Faculty:

- Kenneth Breuer
- Sharon Swartz

Post Doctoral Researchers

- Oscar Curet
- Attila Bergou
- Jenifer Franck
- Nicolai Hristov
- Tatjana Hubel
- Rhea von Busse
- Chen Chiu

Graduate Students

- Joe Bahlman
- Jorn Cheney
- Cosima Schunk
- Arnold Song
- Rye Waldman

PUBLICATIONS RESULTING FROM WORK SUPPORTED BY MURI FUNDING

Book Chapters:

1. Dumont, E. L. and Swartz, S. M. 2009. Biomechanical approaches and ecological research. In Ecological and Behavioral Methods fr the Study of Bats (T. H. Kunz, ed.) pp. 436-458. Johns Hopkins University Press.

2. Albertani R, Hubel, T. Y., Swartz, S. M., Breuer, K. S. and Evers, J. 2011. In-flight wing-membrane strain measurements on bats. In: Proulx, T. (ed) Experimental and Applied Mechanics. Springer, New York, pp. 437-455.

3. Swartz, S. M., Iriarte-Díaz, J., Riskin, D. K., and K. S. Breuer. "A bird? A plane? No, it's a bat: an introduction to the biomechanics of bat flight". in: Gunnell, G. F., and Simmons, N. B., Editors: Evolutionary history of bats: Fossils, molecules, and morphology. *Cambridge University Press* (2012).

Papers appeared, or in press in Archival Journals:

1. D. K. Riskin, D. J. Willis, J. Iriarte-Diaz, T. L. Hedrick, M. Kostandov, J. Chen, D. H. Laidlaw, K. S. Breuer, and S. M. Swartz. Quantifying the complexity of bat wing kinematics, *Journal of Theoretical Biology* 254, 604 (2008), (http://dx.doi.org/10.1016/j.jtbi.2008.06.011).
2. Iriarte-Díaz, J. and Swartz, S. M. 2008. Kinematics of slow turn maneuvering in the fruit bat Cynopterus brachyotis. *Journal of Experimental Biology* 211, 3478-3489. (http://dx.doi.org/10.1242/jeb.017590)
3. Swartz, S. M. D. J. Willis, and K. S. Breuer. 2008. Aeromechanics in aeroecology: Flight biology in the aerosphere. Integrative and Comparative Biology, 48: 85-98 (http://dx.doi.org/10.1093/icb/icn054)
4. A. Song, X. Tian, E. Israeli, R. Galvao, K. Bishop, S. Swartz, and K. Breuer. Aeromechanics of membrane wings with implications for animal Flight, *AIAA Journal* 46, 2096 (2008), (http://dx.doi.org/10.2514/1.36694).
5. T. Y. Hubel, N. I. Hristov, S. M. Swartz, and K. S. Breuer. Time-resolved wake structure and kinematics of bat flight, Expt. Fluids. 46, 933 (2009), (http://dx.doi.org/10.1007/s00348-009-0624-7).
6. M. Molki and K. Breuer. Oscillatory motions of a prestrained compliant membrane caused by fluid-membrane interaction, *Journal of Fluids and Structures* 26, 339 (2010), (http://dx.doi.org/10.1016/j.jfluidstructs.2009.11.003).
7. Riskin, D. K., J. W. Bahlman, T. Y. Hubel, J. M. Ratcliffe, T. H. Kunz, and S. M. Swartz. 2009. Bats go head-under-heels: The biomechanics of landing on a ceiling. Journal of Experimental Biology. 212:945-953. (http://dx.doi/org/ 10.1242/jeb.026161)
8. Chen, J., D. K. Riskin, T. Y. Hubel, D. J. Willis, A. Song, H. Liu, K. S. Breuer, S. M. Swartz, and D. H. Laidlaw. 2010. Exploration of bat wing morphology through a strip method and visualization. Special Interest Group on Graphics and Interactive Techniques (SIGGRAPH).
9. T. Y. Hubel, D. K. Riskin, S. M. Swartz, and K. S. Breuer. Wake structure and wing kinematics: the flight of the lesser dog-faced fruit bat, *Cynopterus brachyotis*, *Journal of Experimental Biology* 213, 3427 (2010), (http://dx.doi.org/10.1242/jeb.043257).
10. D. K. Riskin, J. Iriarte-Diaz, K. M. Middleton, K. S. Breuer, and S. M. Swartz. The effect of body size on the wing movements of pteropodid bats, with insights into thrust and lift production, *Journal of Experimental Biology* 213, 4110 (2010), (http://dx.doi.org/10.1242/jeb.043091).
11. D. Willis, J. Bahlman, K. Breuer, and S. Swartz. Energetically optimal short-range gliding trajectories for gliding animals, AIAA Journal 49, 2650 (2011), (http://dx.doi.org/10.2514/1.j051070).
12. L. C. MacAyeal, D. K. Riskin, S. M. Swartz, and K. S. Breuer. Climbing flight performance and load carrying in lesser dog-faced fruit bats (*Cynopterus brachyotis*), Journal of Experimental Biology 214, 786 (2011), (http://dx.doi.org/10.1242/jeb.050195).
13. J. Iriarte-Diaz, D. K. Riskin, D. J. Willis, K. S. Breuer, and S. M. Swartz. Whole-body kinematics of a fruit bat reveal the influence of wing inertia on body accelerations, Journal of Experimental Biology 214, 1546 (2011), (http://dx.doi.org/10.1242/jeb.037804).
14. Bergou, A. J., S. M. Swartz, K. S. Breuer, and G. Taubin. 2011. 3D Reconstruction of bat flight kinematics from sparse multiple views. IEEE International Conference on Computer Vision Theory. doi:10.1109/ICCVW.2011.6130443
15. R. M. Waldman and K. S. Breuer. Accurate measurement of streamwise vortices using dual-plane PIV, Experiments in Fluids (2012), (http://dx.doi.org/10.1007/s00348-012-1368-3).

16. J. Iriarte-Diaz, D. K. Riskin, K. S. Breuer, and S. M. Swartz. Kinematic plasticity during flight in fruit bats: Individual variability in response to loading, PLoS ONE 7, e36665 (2012), (http://dx.doi.org/10.1371/journal.pone.0036665).
17. J. Colorado, A. Barrientos, C. Rossi, and K. S. Breuer. Biomechanics of smart wings in a bat robot: morphing wings using SMA actuators, Bioinspir. and Biomim. 7, 036006 (2012), (http://dx.doi.org/10.1088/1748- 3182/7/3/036006).
18. D. K. Riskin, A. Bergou, K. S. Breuer, and S. M. Swartz. Upstroke wing flexion and the inertial cost of bat flight, Proceedings of the Royal Society B: Biological Sciences (2012), (http://dx.doi.org/10.1098/rspb.2012.0346).
19. T. Y. Hubel, N. I. Hristov, S. M. Swartz, and K. S. Breuer. Changes in kinematics and aerodynamics over a range of speeds in *Tadarida brasiliensis*, the brazilian free-tailed bat, J R Soc Interface (2012), (http://dx.doi.org/10.1098/rsif.2011.0838).
20. O. Curet, SM Swartz and KS Breuer "An aeroelastic instability provides a possible basis for the transition from gliding to flapping flight" Proc Roy Soc Interface. 2012 (in press).
21. J Bahlman, SM Swartz, D Riskin & KS Breuer "Glide performance and aerodynamics of non-equilibrium glides in northern flying squirrels (*Glaucomys sabrinus*) Proc Roy Soc Interface 2012 (in press).

Papers in preparation, or in review in archival journals:

1. J Bahlman, MS Swartz & KS Breuer "Design and characterization of a multi-articulated robotic bat wing" Bioinspiration and Biomimetics 2012 (in review).
2. Arnold J. Song, Sharon M. Swartz, Daniel K. Riskin, Kenneth S. Breuer "Extreme extensibility of bat wing membranes during flight and the implications for aerodynamic control". (in preparation).
3. J. Bergou, D. K. Riskin, L. Reimnitz, G. Taubin, S. M. Swartz, and K. S. Breuer. "Falling with style: Bats perform complex aerial rotations by modulating solely wing inertia" (in preparation).
4. J Bahlman SM Swartz & KS Breuer "The cost of performance: the influence of wingbeat kinematics on power and aerodynamic force in a bat-inspired robotic flapper" (in preparation).
5. J Bahlman KS Breuer and SM Swartz "Joints without actuators: diversity and biomechanics of the interphalangeal joints in bats." (in preparation).
6. O Curet & KS Breuer "Dynamic testing of the mechanical properties of electrostrictive membranes" (in preparation).
7. Au, V. I., Riskin, D. K., Chiu, C., and Swartz, S. M. The effects of load carrying and obstacle size on maneuvering flight in the Jamaican fruit bat, *Artibeus jamaicensis*
8. Cheney, J. A., Ton, D., Riskin, D. K., Breuer, K. S., and Swartz, S. M. The role of hindlimbs in modulating tension and 3D geometry in the wing membrane of the lesser dog-faced fruit bat, *Cyopterus brachyotis*.
9. Cheney, J. A. and Swartz, S. M. A comparative study of intramembranous muscles of the bat wing membrane.
10. Cheney, J. A., Konow, N., Middleton, K. M., Breuer, K. S., and Swartz, S. M. Activity of the plagiopatagiales muscles in the bat wing membrane in the Jamaican fruit bat, *Artibeus jamaicensis*.
11. Cheney, J. A., Breuer, K. S., and Swartz, S. M. Connective tissue architecture and mechanical properties of bat wing skin – Pre-stressed compliant fibers in a thin, stiff isotropic matrix.
12. Hristov, N. I., Riskin, D. K., Hubel, T. Y., Breuer, K. S. and Swartz, S. M. Kinematics of a fast flying bat: speed dependence of wing movements in the Brazilian free-tailed bat, *Tadarida brasiliensis*.

Conference papers with published proceedings

1. Arnold Song, Xiaodong Tian, Emily Israeli, Ricardo Galvao, Kristin Bishop, Sharon Swartz, and Kenneth Breuer , "The Aero-Mechanics of Low Aspect Ratio Compliant Membrane Wings, with Applications to Animal Flight". Proceedings of AIAA Aerospace Sciences Meeting, Reno NV Jan 2008.
2. Rye M. Waldman, Arnold J. Song, Daniel K. Riskin, Sharon M. Swartz, and Kenneth S. Breuer, "Aerodynamic Behavior of Compliant Membranes as Related to Bat Flight". Proceedings, AIAA Fluid Dynamics Conference, Seattle WA. June 2008.
3. Hubel, TY, Hristov, HI, Riskin, DK, Swartz, SM and Breuer, KS "The aerodynamics of different bat species". Proceedings of the 15th International Bat Research Conference. Prague, CZ Aug 2010.
4. Jian Chen, Daniel K. Riskin, Tatjana Y. Hubel, David Willis, Arnold Song, Hanyu Liu, Kenneth Breuer, Sharon Swartz, and David H. Laidlaw. "Exploration of bat wing morphology through a strip method and visualization". In SIGGRAPH (talk), Los Angeles, July 2010.
5. D. H. Theriault, Z. Wu, N. I. Hristov, S. M. Swartz, K. S. Breuer, T. H. Kunz, and M. Betke. "Reconstruction and analysis of 3D trajectories of Brazilian free-tailed bats in flight." In Workshop on Visual Observation and Analysis of Animal and Insect Behavior, held in conjunction with the 20th International Conference on Pattern Recognition, Istanbul, Turkey, August 2010.
6. J. Bergou, S. M. Swartz, K. S. Breuer, and G. Taubin. 3D reconstruction of bat flight kinematics from sparse multiple views, In Proceedings of the IEEE ICCV Workshop on Dynamic Shape Capture, 2011.
7. J. Bergou, S. Swartz, K. S. Breuer, G. Taubin. 3D Reconstruction and Analysis of Bat Flight Maneuvers from Sparse Multiple View Video, In Proceedings of the 1st IEEE Symposium on Biological Data Visualization, 2011.
8. Curet, O, Swartz, S & Breuer, KS "A self-excited flapping wing: Lift, Drag and the implications for Biological Flight". AIAA Paper 2011-3433. 41st AIAA Fluid Dynamics Conference and Exhibit. Honolulu HI June 2011.
9. Schunk, C, Bahlman, J, Swartz, S & Breuer, KS "Measurement of the wake behind a bat-like flapper, and the influence of flapping frequency on lift generation". AIAA Paper 2011-3116. 41st AIAA Fluid Dynamics Conference and Exhibit. Honolulu HI June 2011.

Conference presentations (without archival proceedings)

1. Arnold Song, Kenneth Breuer Aerodynamics of compliant membrane wings as related to bat and other mammalian flight. Proceedings of APS/DFD Annual Meeting. Salt Lake City, UT. Nov 2007.

   SICB, Jan 2008:

2. SWARTZ, SM; WILLIS, DJ; BOWLIN, MS; BREUER, KS. Aeromechanics in the Aerosphere: Where Physics meets Flight Biology in Aeroecology. Annual Meeting of the Society of Integrative and Comparative Biology. San Antonio TX. Jan 2008.
3. RISKIN, D. K.; WILLIS, D. J.; HEDRICK, T. L.; IRIARTE-DIAZ, J.; LAIDLAW, D. J.; BREUER, K. S.; SWARTZ, S. M. Proper orthogonal decomposition of bat flight kinematics. Annual Meeting of the Society of Integrative and Comparative Biology. San Antonio TX. Jan 2008.
4. Iriarte-Díaz, J., D. K. Riskin, and S. M. Swartz. The effect of loading on flight kinematics of bats: a case of kinematic plasticity.

5. Hubel, T, Swartz, S and Breuer, K. "Wake structure and wing motion in bat flight". Society of Experimental Biology Annual Meeting, Marseilles, France July 2008.

NASBR, Oct 2008:

6. Joseph Wm Bahlman, Kenneth S. Breuer,and Sharon M. Swartz "Size Matters More than How You Use It: Modeling the Effects of Varying Bat Wing Morphology and Kinematics". North American Symposium on Bat Research. Annual Meeting, Scranton PA Oct 2008.
7. Tatjana Y. Hubel, Sharon Swartz and Kenneth Breuer. "The Aerodynamic Flight Pattern of Bats" North American Symposium on Bat Research. Annual Meeting, Scranton PA Oct 2008.
8. Riskin, D. K., J. Iriarte-Díaz, K. S. Breuer, and S. M. Swartz. Allometry of inertial power during flight in pteropodid bats.

9. MacAyeal, L. C.,* D. K. Riskin, and S. M. Swartz. Vertical flight performance and load carrying in lesser dog-faced fruit bats (*Cynopterus brachyotis*)

10. Sullivan, A. C.*, D. K. Riskin, and S. M. Swartz. Influence of upstream vortex structures on flight behavior in *Cynopterus brachyotis*.

11. Robb, A. C.*, S. A. Stamper and S. M. Swartz. Multimodal target facilitates odor discrimination training in lesser dog-faced fruit bats.

APS/DFD Nov 2008:

12. Song, A, Tuttman, M & Breuer, K "Vortex induced motion in compliant structures". APS/DFD Annual Meeting, San Antonio TX. Nov 2008
13. Hubel, T, Breuer, K and Swartz, S. "Wake structure and wing motion in bat flight". APS/DFD Annual Meeting, San Antonio TX. Nov 2008

SICB, Jan 2009

14. SWARTZ, SM; RISKIN, DK; IRIARTE, J; MIDDLETON, KM; BREUER, KS "Scaling of flight characteristics in bats" Annual Meeting of the Society of Integrative and Comparative Biology. Boston MA. Jan 2009
15. WILLIS, D.J.; RISKIN, D.K.; SWARTZ, S.M.; PERAIRE, J.; BREUER, K.S. "Computational modeling of the aeromechanics of a bat (*Cynopterus brachyotis*)". Annual Meeting of the Society of Integrative and Comparative Biology. Boston MA. Jan 2009
16. HUBEL, Tatjana; BREUER, Kenneth; SWARTZ, Sharon "Individual variability in the aerodynamics and kinematics of bat flight". Annual Meeting of the Society of Integrative and Comparative Biology. Boston MA. Jan 2009.
17. CHEN, Jian; RISKIN, Daniel K.; BREUER, Kenneth S.; SWARTZ, Sharon M.; LAIDLAW, David H. "Bookstein coordinate-based shape analysis of bat wing kinematics". Annual Meeting of the Society of Integrative and Comparative Biology. Boston MA. Jan 2009.
18. Bahlman, J. W., D. K. Riskin, J. Iriarte-Díaz, and S. M. Swartz. Aerodynamics of the northern flying squirrel (*Glaucomys sabrinus*).
19. Dickinson, B. T., S. M. Swartz, and B. A. Batten. A mathematical model of the detection of unsteady flow separation by hairs on a bat wing.
20. Iriarte-Díaz, J., D. K. Riskin, and S. M. Swartz. No net thrust on the upstroke: the effect of wing inertia on body accelerations of fruit bats during flight

21. Song A. and Breuer KS "Vortex-induced flapping and twisting of a compliant plate". Fluid and Elasticity, Carry-le-Rouet, France. June 2009.

NASBR Nov. 2009:

22. Nickolay I. Hristov Daniel K. Riskin, Tatjana Y. Hubel, Louise C. Allen, Kenneth S. Breuer and Sharon M. Swartz "How Do Fast Bats Fly: Wing Kinematics of the Brazilian Free-tailed Bat (*Tadarida brasiliensis*) Flying at a Range of Flight Speeds". North American Symposium on Bat Research. Portland OR, Nov 2009.
23. Tatjana Hubel, S. Swartz, N. Hristov, and K. Breuer "How Different is the Flight of Different Bat Species?" North American Symposium on Bat Research. Portland OR, Nov 2009.
24. Cheney, J. A., D. Ton, D. K. Riskin, and S. M. Swartz. Don't forget the legs: hindlimb movement of *Cynopterus brachyotis* during flight.
25. Evans, A., J. A. Cheney, and S. M. Swartz. Material properties of *Glossophaga soricina* wing membrane.

APS/DFD Nov 2009:

26. Song, A & Breuer KS. Vortex shedding interactions with an oscillating flat plate APS/DFD Meeting. Minneapolis MN. Nov 2009
27. Hubel, T, Riskin, D. Swartz, S and Breuer K.S. Similarities and differences in the wake structure generated by different species of bats. APS/DFD Meeting. Minneapolis MN. Nov 2009
28. Waldman R, and Kudo, J, and Breuer, KS. Trailing vortices from low speed flyers. APS/DFD Meeting. Minneapolis MN. Nov 2009

SICB, Jan 2010:

29. RISKIN, DK; IRIARTE-DíAZ, J; MIDDLETON, K; BREUER, KS; SWARTZ, SM "How do bats accelerate? " Soc. Comp. Integ. Bio Annual Meeting Seattle WA Jan 2010
30. MACAYEAL, Leigh C.; RISKIN, Daniel K.; SWARTZ, Sharon M.; BREUER, Kenneth S. "Vertical climbing performance and reserve power in loaded and unloaded Lesser Dog-faced Fruit Bats (*Cynopterus brachyotis*)" . Comp. Integ. Bio Annual Meeting Seattle WA Jan 2010
31. HRISTOV, N.I.; RISKIN, D.K.; HUBEL, T.Y.; ALLEN, L.C.; BREUER, K.S.; SWARTZ, S.M. Kinematics of a fast bat: Changes in wing kinematics with flight speed in the migratory bat (*Tadarida brasiliensis*) . Comp. Integ. Bio Annual Meeting Seattle WA Jan 2010
32. BAHLMAN, Joseph WM; SCHUNK, Cosima; SWARTZ, Sharon M.; BREUER, Kenneth S . The effect of wingbeat frequency on aerodynamic force and wake structure using a bat-like mechanical flapper. . Comp. Integ. Bio Annual Meeting Seattle WA Jan 2010
33. HUBEL, T.Y.; HRISTOV, N.I.; RISKIN, D.K.; SWARTZ, S.M.; BREUER, K.S. Bat flight and hierarchies of variability. Comp. Integ. Bio Annual Meeting Seattle WA Jan 2010
34. Tatjana T Hubel, Daniel K Riskin, Sharon M Swartz & Kenneth S Breuer "The flight of the lesser short-nosed fruit bat". Annual meeting of the Society of Experimental Biology. Prague 2010.

APS/DFD, Nov 2010:

35. Attila Bergou, Daniel Riskin, Gabriel Taubin, Sharon Swartz & Kenneth S. Breuer "Falling with Style - Bat flight maneuvers". APS/DFD Annual Meeting. Long Beach CA, Nov 2010.
36. Jennifer Franck, Charles Peguero, Charles Henoch & Kenneth Breuer "Characteristics of Turbulent flow over Superhydrophobic Surfaces". APS/DFD Annual Meeting. Long Beach CA, Nov 2010.

37. Rye M. Waldman, Jun Kudo & Kenneth S. Breuer "Accurate measurement of streamwise vortices in low speed aerodynamic flows". APS/DFD Annual Meeting. Long Beach CA, Nov 2010.
38. Oscar M. Curet & Kenneth S. Breuer "A self-excited flapper from fluid-structure interaction". APS/DFD Annual Meeting. Long Beach CA, Nov 2010.

SICB, Jan 2011:

39. Schunk, C, Chiu, C, Bahlman, JW, Bergou, A, Cheney, J., Waldman, RM, Curet, O, Albright, E, Swartz, SM, Breuer, KS. "Time-Resolved Measurements Of The Velocity Field Over The Wing Of A Bat During Flight Annual meeting of the Society of Integrative and Comparative Biology (SICB) Salt Lake City, UT. Jan 2011.
40. Bergou, AJ, Riskin, DK, Taubin, G, Swartz, SM, Breuer, KS. "Falling With Style" - The Role Of Wing Inertia In Bat Flight Maneuvers Annual meeting of the Society of Integrative and Comparative Biology (SICB) Salt Lake City, UT. Jan 2011.
41. Bahlman, JW, Swartz, SM, Breuer, KS. Measuring Performance Associated With Increasing Kinematic Complexity In A Robotic Bat Wing. Annual meeting of the Society of Integrative and Comparative Biology (SICB) Salt Lake City, UT. Jan 2011.
42. Cheney, JS, Bearnot, A, Breuer, KS, Swartz, SM. Form And Function In The Wing Membrane Of Bats Annual meeting of the Society of Integrative and Comparative Biology (SICB) Salt Lake City, UT. Jan 2011.
43. Hristov, NI, Hedrick, Tl, Allen, LC, Chadwell, B, Kunz, TH, Breuer, KS, Swartz, SM. Flight Formation And Group Behavior In The Highly Gregarious Brazilian Free-Tailed Bat *Tadarida Brasiliensis.* Annual meeting of the Society of Integrative and Comparative Biology (SICB) Salt Lake City, UT. Jan 2011.
44. Swartz, SM, Breuer, KS. How Can Bats Inspire Robotic Fliers And Micro Air Vehicles? Annual meeting of the Society of Integrative and Comparative Biology (SICB) Salt Lake City, UT. Jan 2011.

45. R. Albertani, T. Hubel, S. M. Swartz, K. S. Breuer, and J. Evers, In-flight wing-membrane strain measure- ments on bats, in Experimental and Applied Mechanics, Volume 6, edited by T. Proulx. Springer New York. 2011. volume 17 of Conference Proceedings of the Society for Experimental Mechanics Series. pp. 437 (http://dx.doi.org/10.1007/978-1-4419-9792-0_68).

APS/DFD, Nov 2011:

46. Bergou, A., J. Franck, G. Taubin, S. Swartz and K. Breuer (2011). "Inertial and Fluid Forces during Bat Flight Maneuvers." APS/DFD Annual Meeting, Baltimore MD
47. Curet, O., S. Swartz and K. Breuer (2011). "Lift force enhancement and fluid-structure interactions on a self-excited flapping wing model." APS/DFD Annual Meeting, Baltimore MD
48. Franck, J., S. Swartz and K. Breuer (2011). "Large-Eddy Simulations of Flapping-Induced Lift Enhancement." APS/DFD Annual Meeting, Baltimore MD
49. Schunk, C., S. Swartz and K. Breuer (2011). "Time-resolved measurements of the velocity field over the wing of bats during flight." APS/DFD Annual Meeting, Baltimore MD
50. Waldman, R., S. Swartz and K. Breuer (2011). "Fluid-structure interactions on compliant membrane wings." APS/DFD Annual Meeting, Baltimore MD

SICB, Jan 2012:

51. Bergou, A. J., J. Franck, L. Reimnitz, D. K. Riskin, G. Taubin, S. M. Swartz, and K. S. Breuer. Inertial and fluid forces during bat flight maneuvers.
52. Chiu, C., K. S. Breuer, and S. M. Swartz. The interactive flight of bats.
53. Von Busse, J. R. S., S. M. Swartz, K. S. Breuer, A. Hedenström, Y. Winter, and C. C. Voigt. Energetics of bat flight.

54. Bahlman, J. W., S. M. Swartz, and K. S. Breuer. Measuring cost of flight associated with varying kinematics in a robotic bat wing.
55. Bergou, A. J., S. M. Swartz, K. S. Breuer, and G. Taubin. 3D Reconstruction and analysis of bat flight maneuvers from sparse multiple view video.
56. Cheney, J. A., A. Bearnot*, K. S. Breuer, S. M. Swartz. Pre-stressed compliant fibers within the wing membrane of Glossophaga soricina, Pallas' long tongued bat.

COMPUTATION

MIT · UML

CONTENTS

SUMMARY

This section provides an overview of the Computation component of the MURI project on Biologically-Inspired Flight for Micro Air Vehicles. MIT led this component, which midway through the project expanded to include UMass Lowell. Goals, approach and results of our work are summarized below, and further details of our results are presented in the next section.

GOALS

The goal of the Computation component of the MURI project was to develop state of the art, multi-fidelity, numerical techniques to address the challenges of unsteady fluid-structure interaction at transitional Reynolds numbers with specific application to understanding, analyzing and optimizing flapping flight for Micro Air Vehicles. The use of a multi-fidelity approach allowed us to address research questions with the appropriate fidelity level.

Computational tools that were modified and developed through this project were:

- Wake Only Energetics – A novel approach to simultaneously predicting optimal energetics and kinematics of flapping wings using the Wake Only method, *HallOpt*.
- ASWING, a lifting line method coupled with beam elements and controls
- FastAero, an unsteady, accelerated panel method with vorte particle wakes. In addition, a quasi-inverse, doublet lattice method (QI-DLM) was developed to generate wing shapes from wake-circulation distributions.
- 3DG, a high order Discontinuous Galerkin Navier-Stokes solver coupled with nonlinear structural models

Using this suite of tools, both design-oriented explorations as well as analysis of animal flight were performed.

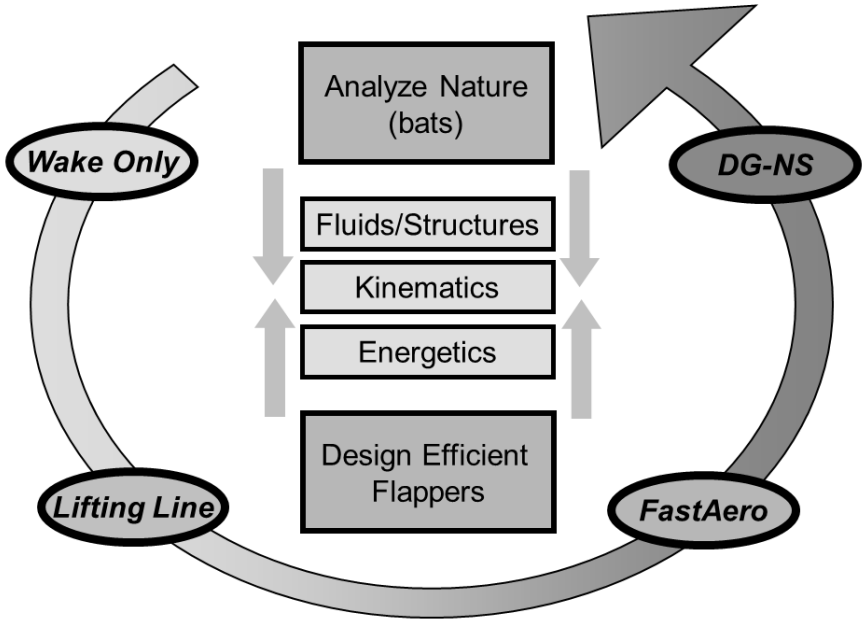

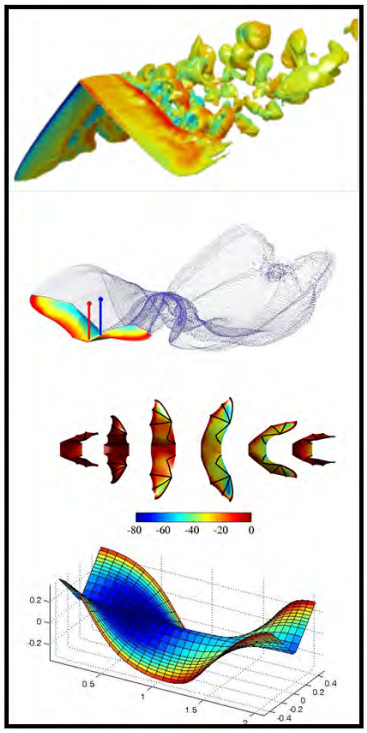

APPROACH

Our approach to developing a multi-fidelity simulation capability for flapping flight was as follows:

1. **Enhance ASWING** to dynamically simulate entire flapping-wing configurations. A more general geometry parameterization was to replace the existing simple joint articulation and thus permit more complex wing motions. The capability to drive the flapping via some general unsteady torque/angle joint relations was to replace simple prescribed joint angles. This would allow more realistic modeling of muscle compliance.

2. **Enhance FastAero** to incorporate a harmonic balance time-periodic solver to take advantage of the cyclic nature of steady flight configurations. In addition, a formal adjoint-based optimization was to be incorporated so that optimal flight configurations could be easily identified. Lastly, strategies for arbitrary separation lines were to be incorporated (using N-S simulations and experimental results). Although this cannot replace a detailed viscous analysis, it can provide a more realistic solution at this level of fidelity and computational efficiency.

3. **Enhance 3DG.** At the beginning of the MURI, our high-order Discontinuous Galerkin Navier-Stokes solver (3DG) was capable of handling rigid body motions using an Arbitrary Lagrangian-Eulerian (ALE) formulation. A more general algorithm allowing for grid deformation was planned to be developed. In an ALE formulation, the motion of the structure needs to be extended into the flow computational domain in such a way that good grid quality is maintained. We were considering several mesh-deformation strategies, including the representation of the computational domain as a soft Neo-Hookean material and integrating the equations for the mesh motion simultaneously with those of the flow.

4. **Develop a coupled Fluid Structure Interaction simulation capability.** Our ASWING and FastAero codes initially included some coupling between the flow and a structural model. If required, we planned to extend these and incorporate an overall structural dynamics model that could also include shell and volume elements. For the 3D NS code, we planned to develop procedures for transferring displacements and loads between the flow and structural models (each having different geometric fidelity). In 2D, a procedure based on an elastic analogy had already been developed, and would be extended to 3D during the MURI.

5. **Develop an unsteady transition model for flapping flight.** As part of the development of predictive theories appropriate to bio-inspired flight at low Reynolds numbers, we planned to develop a new low-Re transition prediction tool, analogous to the extremely successful e^N methods utilized in *XFOIL* and *MSES* codes for higher Re steady flows. We were to extend these theories to unsteady and low-Re by adding a transport equation which observes the necessary invariance. This transition model would then be implemented in our 3DG N-S code.

6. **Conduct numerical simulations to explore the aerodynamic effects of structural compliance, wing based sensors and actuators.** Bats appear to have distributed shear stress and membrane strain sensors, as well as camber-control muscles embedded throughout their flexible wing membrane. During the MURI, we planned to conduct numerical simulations to better understand the function and role of these sensory and control features, including the effect of structural compliance. Close collaboration was planned with partners at Oregon State University.

7. **Compare an experimental membrane wing model to multi-fidelity numerical simulations.** Experimental results from a membrane wing model tested by MURI collaborators at Brown University were to be compared to equivalent numerical simulations, using our multi-fidelity tool set.

8. **Multi-fidelity simulations of articulated flapping flight using kinematic data from bats.** We planned to first investigate this using our multi-fidelity simulation capabilities which can quickly explore a wide variety of articulation geometries, flapping frequencies and unsteady control responses. The most promising approaches were to be studied using higher-order Navier-Stokes simulations.

RESULTS

Here we addresses each of the 8 specific goals listed in the previous section and highlight our key achievements during the MURI. Goals that remain incomplete are noted as such.

1. **Enhancements made to ASWING lifting line code**

    - A preliminary design space study was completed using ASWING for a simple flapping wing.
    - Further enhancements to ASWING code are not yet complete and will be a subject of future research.
    - A wake-only energetics method was developed to link the energetics of flight to flapping kinematics. This tool harnesses a large database of wake-only simulations to make flight energetics predictions.

2. **Enhancements made to FastAero panel code**

    - A strategy using a quasi-inverse doublet lattice method (QI-DLM) formulation with periodic wakes was implemented for determining optimal wing shapes, rather than an adjoint-harmonic balance approach. This approach tightly integrates results from the wake-only method into the multi-fidelity framework, while giving the designer freedoms over design considerations to achieve efficient flight. We believe the present quasi-inverse method provides a unique research contribution in this field.
    - A two-equation, two-dimensional integral boundary layer method similar to that used in XFOIL has been developed for coupling to the quasi-inverse design method. We are currently attempting to incorporate this into the inverse design capability as a strip-wise, weakly coupled indicator of likely separation on the wings. Comparisons to existing Navier-Stokes solutions will be made once this is complete.

3. **Enhancements made to 3DG high-order Navier-Stokes code**

    - A more general grid deformation methodology was developed and implemented for 3DG, allowing computation of flapping wing solutions with arbitrary non-rigid mesh deformations.
    - A mesh-deformation strategy based on solving the equations of Neo-Hookean nonlinear elasticity was developed, implemented and tested in 3DG, allowing robust deformation of 2D or 3D meshes while maintaining grid quality. This approach was a crucial enabler for 3D Navier-Stokes simulations of a flying bat using kinematic data recorded by MURI collaborators at Brown University.

4. **Development of a coupled Fluid Structure Interaction simulation capability**

    - 2D Fluid Structure Interaction capabilities were developed and implemented in our Navier-Stokes solver, enabling numerical studies of the effects of structural compliance and hair sensor feedback control on the thrust and propulsive efficiency of flapping airfoils.
    - 3D Fluid Structure Interaction capabilities have been developed for prescribed structural motions, but coupling between a flow and structural model is currently under development in our 3DG code.
    - 3D Fluid Structure interaction capabilities are currently being developed to incorporate in the quasi-inverse design process. Simplified models incorporating rigid beams, torsional springs and thin membranes are being constructed.

5. **Development of an unsteady transition model for flapping flight**

    - Quantified the growth of Tollmien-Schlichting waves, based on a study of the transition which takes place along a laminar separation bubble in low Reynolds number flows.
    - Investigated cross-flow instabilities present over swept wings. This is an area which had remained essentially unexplored until the MURI effort.

- Found that for separation-induced transition at low Reynolds numbers, it is not possible to treat streamwise and cross-flow instabilities independently for wings with sweep angles between about 10◦ and 40◦. For MAV and animal flight, this has the important implication that the type of transition (TS dominated, cross-flow dominated, or mixed) is a priori unknown as soon as the flow is slightly misaligned with the wing's chord.

6. **Numerical simulations to explore the aerodynamic effects of structural compliance and wing based sensors and actuators**

    - Lower fidelity models were used to explore structural compliance in 2-Dimensions to predict optimal flapping frequency and amplitudes. In addition, the design space for leading edge torsional springs was refined using these lower fidelity tools. Results of these initial explorations provided a reasonable starting point for higher fidelity simulations.

    - Fluid Structure Interaction capabilities were built into our 2D Navier-Stokes solver, which we then used to conduct simulations of a 2D pitching and heaving airfoil with a leading-edge torsional spring to model wing structural compliance. These simulations demonstrated that a simple torsional spring can passively control wing pitch in a very effective manner as measured by thrust generation and propulsive efficiency.

    - Our 2D Navier-Stokes solver was then extended to include a wing hair sensor model developed in collaboration with Ben Dickinson at OSU. This wing hair sensor model was designed to mimic the feedback signal thought to be generated by hair sensors observed on the wings of bats. A Proportional-Differential control law was implemented in our simulation model to drive a leading edge control torque in response to a feedback signal from wing hair sensors.

    - Simulations exploring the performance envelope of this flapping airfoil with active feedback control showed that the feedback controller was able to improve the propulsive efficiency of the flapping airfoil by up to 8%, compared to a flapping airfoil without such a controller. Gust alleviation simulations also demonstrated that the hair sensor feedback controller was capable of greatly reducing the transient lift deviation experienced during a gust encounter.

7. **Comparison of an experimental membrane wing model to multi-fidelity numerical simulations**

    - Collaboration between the Brown University and MIT groups led to preliminary high-order Navier-Stokes simulations of a pitching foil, matching experiments conducted at Brown. However, experimental challenges meant that the collaboration was not followed through and definitive comparisons between the experiments and simulations were not completed.

    - Experimental studies of compliant wing strategies were initiated at UMass Lowell. Several UMass Lowell students visited Dr. Ifju's laboratory at the University of Florida Gainesville to learn how to build bat-inspired and computationally developed membrane-beam composite wings. Similar experimental challenges were experienced in testing these wings, and a revised effort has been initiated to test simpler compliance strategies. This effort continued during a summer faculty fellowship program opportunity. Testing these simpler structurally compliant wings remains an ongoing effort.

8. **Multi-fidelity simulations of articulated flapping flight using kinematic data from bats**

    - FastAero simulations of a flapping bat were conducted using several Brown University kinematic data sets for a new bat species, *Tadarida brasilliensis*, and compared to similar simulations using kinematic data from the *Cynopterus brachyotis*. High outboard loading of the bat wing during slow and moderate speed forward flight was noted in both species, and wake computations compared well with PIV measurements made by Brown University. Simulations of *Cynopterus brachyotis* compared well to observed body accelerations, using a discrete mass model and computed aerodynamic forces.

    - High-order Navier-Stokes simulations of a flapping *Cynopterus brachyotis* are currently under development

and some preliminary simulation results have been obtained. Our 3DG code was used to robustly deform a 3D computational grid according to the equations of Neo-Hookean solid mechanics. We were then able to apply 3DG to an Arbitrary Lagrangian-Eulerian formulation of the Navier-Stokes equations to compute fully 3D flow solutions over a flapping *Cynopterus*.

- We have developed new meshing techniques that allow us to compute deformed meshes more robustly, and are currently applying this technique to refine our preliminary 3D *Cynopterus* flow simulations and perform computations at higher Reynolds numbers closer to the actual bat.
- A series of multi-fidelity computational studies were performed to understand the importance of flapping kinematics on flight performance. These studies were performed from the ground up, using our multi-fidelity tool set. The wing kinematics were dictated by minimum energetics considerations, while the flying wing shape was determined by limiting degrees of freedom in the wing deformation. A series of studies were performed to assess the importance of leading edge angle on flight efficiency, flow structure generation on the outboard wing and the impact of different wing planforms on performance and desired wing deformation. These studies provide insight into flapping wing performance considerations and design.

The chart below summarizes the current status of each of the tasks originally proposed within the computational portion of the MURI.

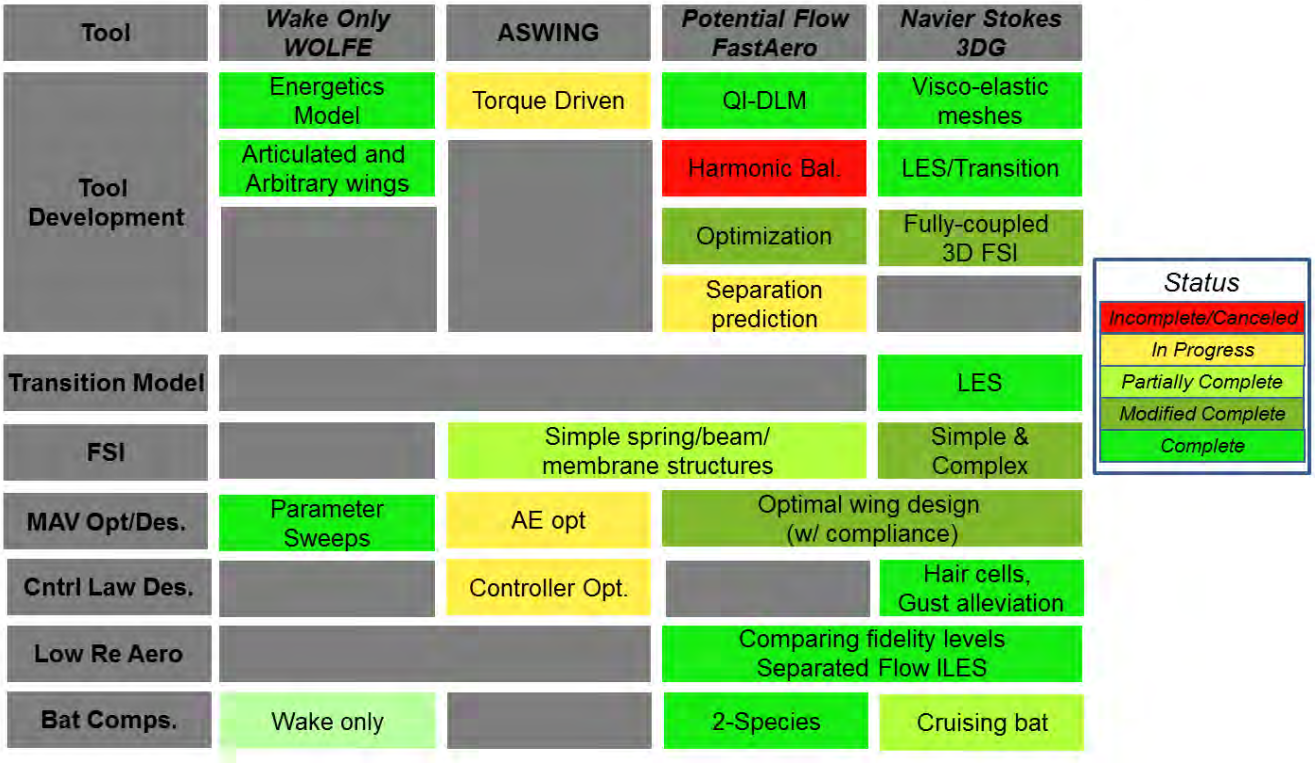

DETAILED RESULTS

The sections below provide further details of the key computational research accomplishments of our MURI project.

MULTI-FIDELITY ANALYSIS OF OPTIMAL FLAPPER DESIGN

Our computational philosophy is to use multiple fidelity levels in an integrated manner to predict, understand and improve flapping flight performance. In this report we describe our progress (1) in understanding biologically inspired flight using computational tools and (2) in understanding and integrating different fidelity levels. Two core strategies for understanding flapping flight are considered in the computational effort:

- A top-down analysis of bat flight to understand natural flight and the implications on Micro Air Vehicle (MAV) design.
- A bottom-up analysis of flapping flight to understand fundamental aspects of flapping flight and determine parametric dependencies.

Several themes are present in the computational research. These include:

- Understanding when lower fidelity tools can be used to adequately represent the problem, and when higher fidelity tools must be used.
- Developing a deeper understanding of optimal energetics flapping flight.
- Understanding the parametric dependencies in optimal energetics flapping flight. This includes kinematics, wing shape and wing morphing during flapping motions.

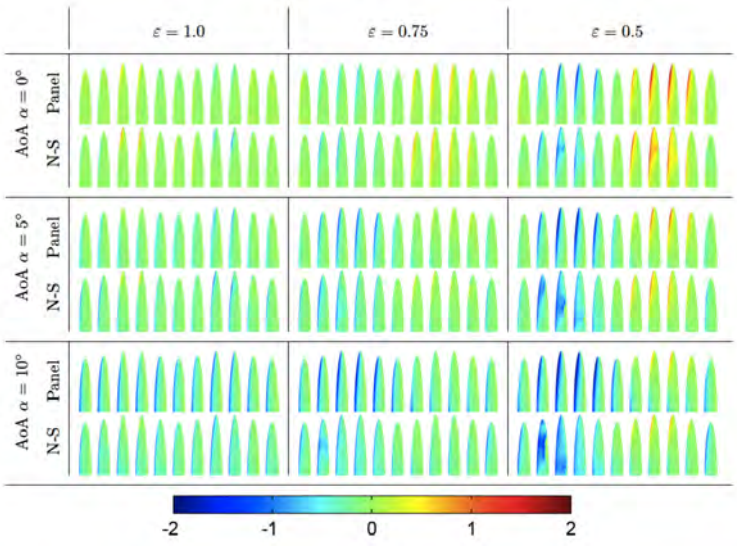

Figure 1: Pressure differential across the wing as computed using *FastAero* (top image of each pair) and Discontinuous Galerkin (bottom image of each pair). The wing is approximately feathered for ε = 1.0; conversely, aggressive wing twist is prescribed when ε = 0.5. The two methods show good agreement for moderate wing twist and angle of attack.

LOW VS. HIGH FIDELITY METHODS FOR FLAPPING WINGS

We performed a computational study[1] to assess the applicability of low-fidelity, potential flow methods to flapping flight. This involved a comparative series of *FastAero* and high-fidelity Discontinuous Galerkin (DG) simulations. This was a collaborative effort between researchers at MIT, UC Berkeley and UMass Lowell.

An elliptical planform wing geometry with a single centerline flapping hinge was selected for this computational comparison. Different wing twist distributions were analytically prescribed in our model of the wing geometry. These wing twist distributions range from benign to aggressive. A series of three angles of attack were also prescribed for each twist distribution.

Our high fidelity simulations required a fairly substantial development effort in high-order solvers for viscous flow on deforming domains. It is widely believed that traditional low-order solvers are insufficient for the simulation of problems involving separated flows, vortex interactions, and other nonlinear effects. But it is also clear that the geometric complexity of real-world problems, even for a simple elliptic wing as in this study, need discretizations based on fully unstructured meshes of tetrahedra. The Discontinuous Galerkin method is a natural choice for these requirements, and our 3DG software package is based on our work on unstructured mesh generation, curved mesh generation using Lagrangian solid mechanics, efficient formulations for viscous terms, parallel preconditioned Newton-Krylov solvers with optimal element ordering, and nonlinear stabilization using a selective artificial viscosity.

For our flapping wing simulations, the deforming domain is handled by an Arbitrary Lagrangian-Eulerian method, which is based on a mapping that describes the moving surfaces and extends smoothly to the entire domain. Various techniques can be used to construct the mapping, and in this work we used a combination of shearing and blending of the given expressions for the wing motion. The problem was discretized using approximately 23 million degrees of freedom, and the systems were integrated in time using a third-order diagonally implicit Runge-Kutta scheme, which required a computation time on the order of days for each simulation, on a parallel computer with 16 compute nodes. Figure 1 illustrates the surface pressure differential results. Additional results are reported by Persson *et al*.[1]

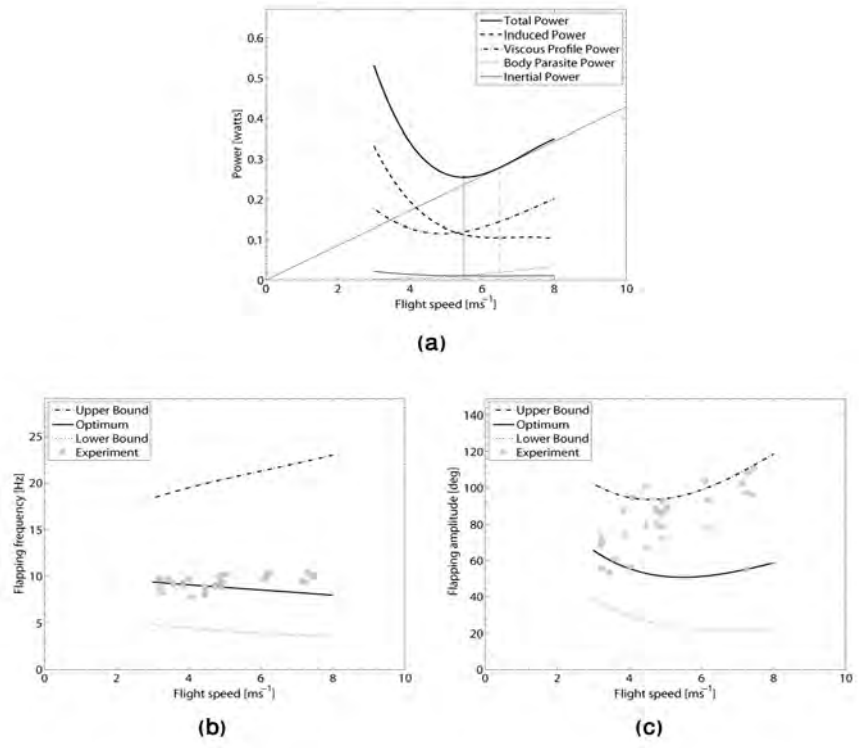

Figure 2: (a) Power, (b) frequency and (c) amplitude vs. flight velocity for the *Cynopterus brachyotis* bat, computed using the wake-only energetics method (compared with experimental data from Brown University).

The results of this computational study indicated that lower fidelity potential flow methods can accurately predict

[1] P.-O. Persson, D. J. Willis and J. Peraire, Numerical Simulation of Flapping Wings using a Panel Method and a High-Order Navier-Stokes Solver, Int. J. Num. Meth. Engrg.,vol. 89, issue 10, pp. 1296-1316, 2012.

flows around flapping wings when there is limited or no flow separation. Conversely, the predictive capability is degraded when substantial separation exists. When weak or intermediate flow separation exists, *FastAero* is capable of predicting trends adequately. From these results, we hypothesize that lower-fidelity inviscid methods can predict the inviscid forces when the flow remains attached or when the flow separates and subsequently reattaches to the wing. We believe this is due to the satisfaction of the trailing edge Kutta condition in both of these cases.

As a result of this computational study, we will attempt to formulate simple separation warnings for our *FastAero* and QI-DLM potential flow analyses using the surface velocity and pressure gradient distribution. While this will not predict the viscous effects, it will provide a first-order indicator of possible flow separation.

WAKE-ONLY ENERGETICS ANALYSIS

We have derived, implemented and refined a novel wake-only energetics method that for the first time predicts the relationship between minimum power flight and the associated wing flapping kinematics. While the method represents the lowest-fidelity computational tool in our framework, the method is the highest-fidelity computational method currently used for broad scale flapping flight energetics predictions, design space construction and analysis.

In addition to the wake-only energetics tool development, we have used the method for several parametric studies of biologically-inspired flapping flight to better understand the parameter space.

WAKE-ONLY ENERGETICS TOOL DEVELOPMENT

The wake-only energetics method derives aerodynamic power and force estimates from the HallOpt wake-only method. We have introduced significant modifications and additional calculations to the original wake-only method in order to predict and achieve a flight force balance model for cruise, descending and climbing flight. The wake-only aerodynamics tool is used to construct a large offline database of optimal circulation wakes. This corresponds to computing wake-only solutions for the large array of potential flapping kinematics to be studied. Despite the low cost of wake-only aerodynamics solutions, the construction of a comprehensive offline database is a computationally intensive task. We have found a way to design the energetics method so that this database is only computed once, and reused for all energetics predictions. Subsequent computations use a flight force balance and the offline database to determine minimum energy flapping kinematics.

One of the key components of the wake-only energetics method is the ability to examine a wide range of flapping constraints, including (1) fixed amplitude and frequency flapping, (2) fixed amplitude flapping, (3) fixed frequency flapping and (4) optimal selection of frequency and amplitude. The flexibility in flapping kinematics has allowed us to highlight the potential disadvantages of traditional fixed amplitude flapping wing MAVs.

The wake-only energetics model has undergone significant improvements over the past two years including deriving an inviscid-viscous decoupled formulation that facilitates aspect ratio and Reynolds number independence. In addition to the many improvements, we are working on a graphical user interface for a preliminary public release of our method.

APPLICATION OF THE WAKE-ONLY ENERGETICS MODEL TO FLAPPING WINGS

The wake-only energetics model has been applied to several different studies ranging from natural flight analysis to preliminary MAV design. These parameter studies are only briefly highlighted here, but are more fully explored in the associated references.

ENERGETICS OF ANIMAL FLIGHT

We have applied the energetics tool to several different species of flying animals including: a bat (*Cynopterus brachyotis*), a cormorant (*Phalacrocorax carbo*), a thrush nightingale (*Luscinia luscinia*) and a budgerigar (*Melopsittacus bundulatus*). The energetics code predictions show good agreement with the available data for these animals (Figure 2). This suggests that minimum energetics flight is likely a considerable factor in the selection of flapping kinematics in nature. Additionally, these results indicate our energetics method is a good initial predictor of flight performance.

FORWARD-AFT FLAPPING KINEMATICS

In addition to simple flapping kinematics we have examined the impact of more complex kinematics that are exhibited by natural flyers. One such series of kinematics is the forward-aft flapping motions that animals exhibit during slow flight (Figure 3). These forward-aft excursions of the wing are especially noticeable in the Brown U. bat flight kinematics data for slower flights. We modified the wake-only method to account for forward-aft flapping motions. Our results indicate that forward-aft flapping kinematics can be extremely effective in reducing power requirements at lower flight speeds; however, at faster flight speeds the benefits diminish.

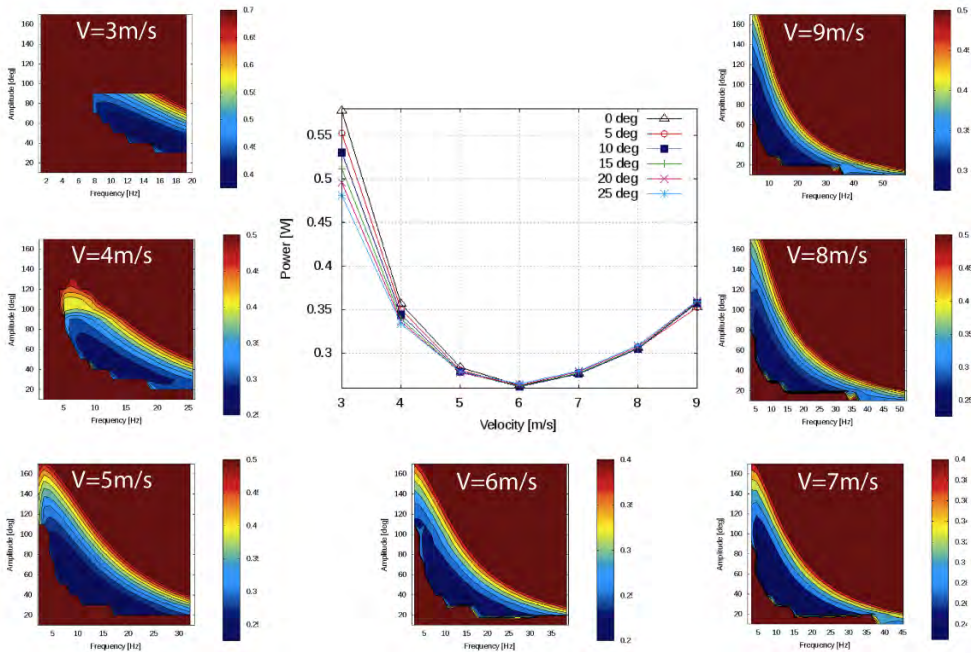

Figure 3: Forward-aft flapping has the ability to substantially reduce power requirements at slower flight speeds. In the case of the *Cynopterus brachyotis* (shown here) forward aft flapping can reduce power requirements at 3m/s by over 20%.

MICRO AIR VEHICLE (MAV) SIZING & MISSION PERFORMANCE

We have also used the energetics model to examine preliminary MAV sizing and mission considerations. For this particular study, we defined two missions: (1) an endurance mission in which the MAV will fly at its minimum power flight condition for the majority of the mission, and (2) a range mission in which the MAV flies at the maximum range velocity for the majority of the mission duration.[3] We performed an operating space sweep (Figure 4) for these two cases along with sensitivity studies. The results show that the traditional aerodynamics conclusion, that aspect ratio should be maximized to minimize energy consumption, does not hold true in the span-constrained endurance mission. In the case of the endurance mission, achieving a higher wing area has advantages over maximizing aspect ratio. While this is a subtle result, it illustrates how these simpler, low-fidelity tools can contribute to the design process.

[3] H. Salehipour, D. J. Willis, A Wake-Only Energetics Model for Preliminary Design of Biologically-Inspired Micro Air Vehicles, *AIAA Atmospheric Flight Mechanics Conference*, Toronto, Canada, August 2010.

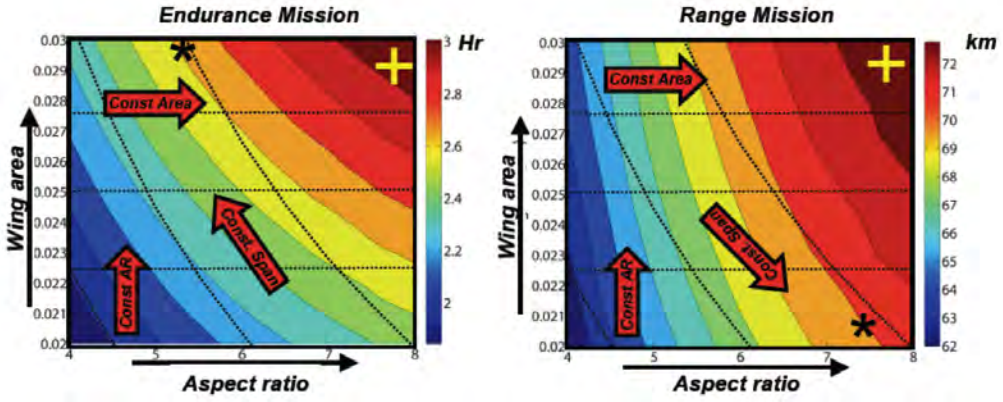

Figure 4: The performance of a bat-like MAV in an endurance based mission vs. a range based mission. Guide-lines are provided for constant span, area and aspect ratio. When a span constraint is applied, the energetics method predicts different aspect ratios for endurance and range missions.

FUTURE EFFORTS

We will continue to explore and document our findings using the wake-only energetics method. This will include performing more extensive design space sweeps, examining new flapping concepts and guiding experiments. In addition, once we have published our results, we aim to release a public version of the energetics code for use in the flapping flight community.

DESIGNING ENERGTICALLY OPTIMAL FLAPPERS

While our wake-only energetics method has allowed us to examine the large flapping-wing design space, the method does not provide details about the flapping wing geometry. We have developed a quasi-inverse wing design tool that can be used to determine flapping wing shapes to generate the desired or target wake-circulation distribution.

Through a collaborative effort (UMass Lowell, MIT, Berkeley), we have simulated several of these wing designs at different fidelity levels. This design and analysis process illustrates the integration of the full range of computational fidelity levels into a single coherent design and analysis framework.

QUASI-INVERSE WING DESIGN USING WAKE CIRCULATION DISTRIBUTIONS

The wake-only energetics method provides an optimal wake-circulation description for each flight speed (Figure 5); however, it does not indicate the wing geometry required to achieve that optimal flight condition. We have developed a quasi-inverse doublet lattice method (QI-DLM) that can be used to determine the morphing flapping-wing shape that produces the target wake-circulation distribution. This is a powerful capability because it allows us to not only determine geometries corresponding to the optimal wake-only results, but it also allows us to design lower degree of freedom wings that produce similar flight qualities as those observed in our bat-flight simulation results.

Our QI-DLM method takes a wake-circulation distribution, a wing planform description and a wing camber strategy as inputs. The QI-DLM method adjusts the wing twist distribution at each timestep of the flapping cycle to achieve the desired shed-wake circulation distribution (with the cambering strategy prescribed). The output from the inverse design is

the wing twist as a function of time (and the camber distribution if a leading edge alignment strategy is used). The methodology of the QI-DLM is described in greater detail in several of our publications[4].

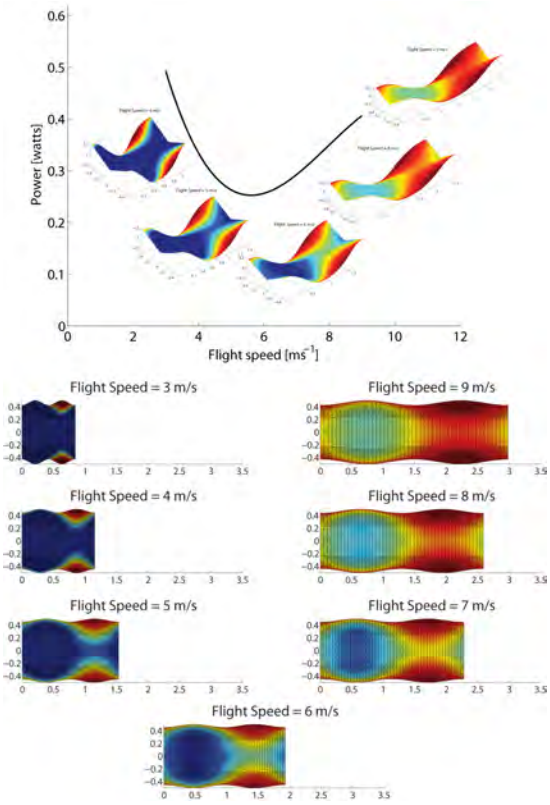

We have applied the QI-DLM methodology to study:

- The effect of the angle between the relative flow and the leading edge
- The effect of wing shape (taper ratio) on twist distribution, angle of attack and desired camber

Figure 5: The minimum power wake-circulation distributions for a collection of different flight velocities. These wake-distributions are qualitatively very similar to bat-wakes at similar speeds. These wakes form the basis for the quasi-inverse wing design process.

DISCONTINUOUS GALERKIN MODELING OF OPTIMAL FLAPPERS

High-fidelity simulations of optimal flapping wings are performed using the 3DG framework, as described above and by Persson *et al*[5]. The main difference is that the wing motions are now given by numerical data from the quasi-inverse design, and cannot be expressed as a closed form expression. Instead, we use a Lagrangian solid mechanics analogy to define the mapping of the deforming domain, where a reference mesh is smoothly deformed to align with the given wing geometry. This process gives a mapping at each substep of the Runge-Kutta time-stepper, and results in numerically defined grid velocities and deformation gradients. For these simulations, we used an unstructured tetrahedral mesh with approximately 5 million degrees of freedom.

[4] P.-O. Persson and D. J. Willis, High Fidelity Simulations of Flapping Wings Designed for Energetically Optimal Flight, *Proc. of the 49th AIAA Aerospace Sciences Meeting and Exhibit*, January 2011, AIAA-2011-568.

[5] P.-O. Persson, D. J. Willis and J. Peraire, Numerical Simulation of Flapping Wings using a Panel Method and a High-Order Navier-Stokes Solver, *Int. J. Num. Meth. Engrg.,vol. 89, issue 10, pp. 1296-1316, 2012.*

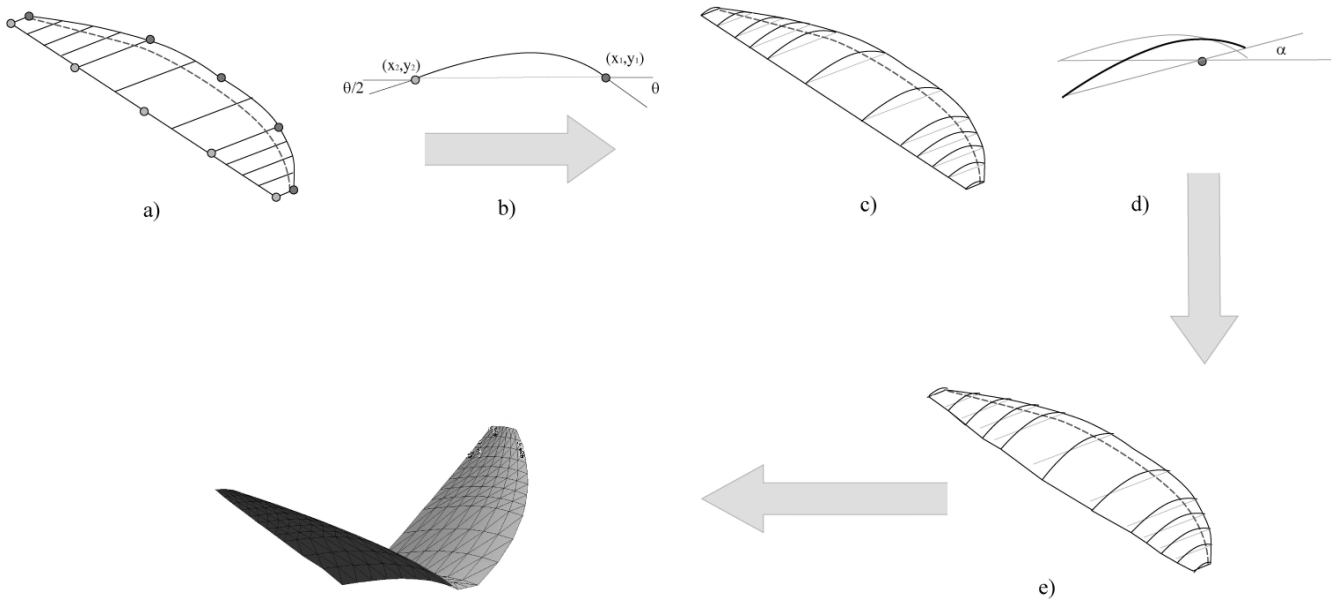

Figure 6: The QI-DLM geometry definition process: (a) the wing leading and trailing edges are defined; (b+c) the leading edge angle is used to generate the local wing camber; (d+e) the wing twist at each spanwise location is defined and the wing section is rotated through the twist angle about the twist axis; (f) the wings are rotated through the flapping amplitude.

OPTIMAL FLAPPING WINGS: LEADING EDGE ANGLE AND FLOW SEPARATION

We used the QI-DLM, *FastAero*, and the Discontinuous Galerkin solver to examine how leading edge angle impacts optimal flapping wing performance[6]. In our QI-DLM method the wing leading edge angle at any spanwise location is related to the camber at that location. We are able to explicitly prescribe the leading edge angle along the span or implicitly prescribe the angle by enforcing flow tangency at the leading edge (Figure 6). When the flow tangency condition is used, the leading edge angle varies both along the span and in time.

While inviscid methods such as *FastAero* and the QI-DLM predict similar time-dependent forces regardless of wing leading edge angle strategy, the Discontinuous Galerkin method results indicate that flow-leading edge alignment is a preferable strategy for mitigating flow separation (Figure 7). The results also indicate that fixed or constant curved leading edges with angles near to the flow tangency condition at mid-downstroke also work adequately. This result confirms our hypothesis that considering the leading edge angle is important in MAV wing design.

Following the initial study on leading edge separation, a second study was performed to preliminarily examine the effect of twist on the formation of flow structures on flapping wings. In this study, we examined the impact of more aggressive leading edge angles as a function of spanwise location (eg: the wing tip leading edge was less aligned with the flow than the wing root). The idea behind this study was to examine whether a stable leading edge vortex could be generated. The preliminary geometries that were developed were tested in the Discontinuous Galerkin solver. Initial results confirm the generation of a leading edge vortex using this strategy, however, the augmented stability of that vortex is still unconfirmed.

[6] P.-O. Persson and D. J. Willis, High Fidelity Simulations of Flapping Wings Designed for Energetically Optimal Flight, *Proc. of the 49th AIAA Aerospace Sciences Meeting and Exhibit*, January 2011, AIAA-2011-568.

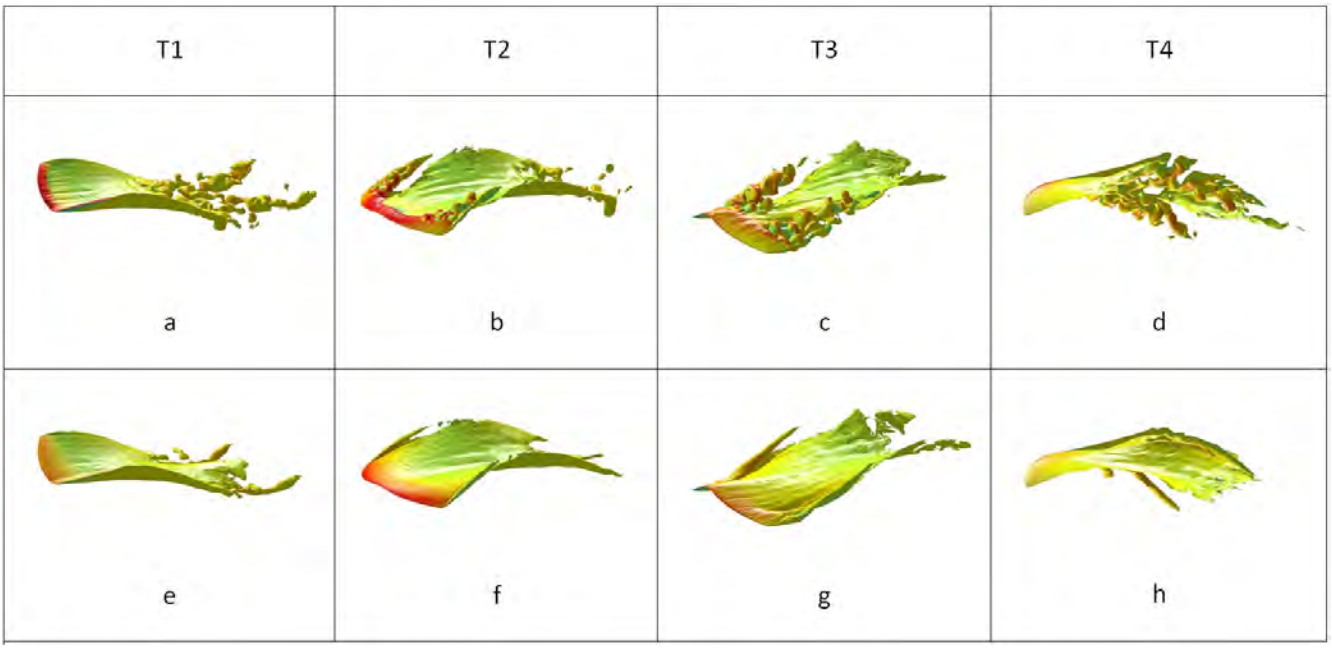

Figure 7: (a-d) QI-DLM designed wing with zero camber. (e-h) QI-DLM designed wing with leading edge aligned with the oncoming flow. The wing with the flow-aligned leading edge (e-h) has substantially less leading edge separation and has time dependent forces that compare well with the wake-only energetics method, the QI-DLM and *FastAero* predictions.

OPTIMAL FLAPPING WINGS: PLANFORM GEOMETRY

Our QI-DLM method has also been employed to understand how wing planform geometry, specifically wing taper ratio, impacts the wing twist distribution. We have examined a large collection of linearly tapered wings (Figure 8 shows a subset of candidate wings) to determine how wing taper correlates to wing twist distribution and spanwise angle of attack. This correlation is expected to shed some light onto potential structural strategies to passively accomplish the wing design. The wing planform geometry has a measurable effect on both wing twist and spanwise angle of attack. This suggests (1) that lower fidelity methods can provide valuable insight early in the design process, and (2) a strategy such as that offered by the QI-DLM will likely prove useful in the development of structurally compliant, flapping wings. We are presently integrating structural strategies with the quasi inverse design process, so we can develop optimal flapping wing structures based on both the required wing twist and the planform geometry.

We have also been developing a two-equation, two-dimensional, streamline integral boundary layer model similar to that used in XFOIL. The goal is to use this model in the QI-DLM method to predict separation likelihood and location in the design process, rather than using the discontinuous Galerkin solver to assess all candidate wing geometries. We have recently completed the development of this model and are now starting to couple it to simple 2-D airfoils and shapes. Once validated, we would like to be able to couple the boundary layer method to the QI-DLM or at least to the FastAero solver.

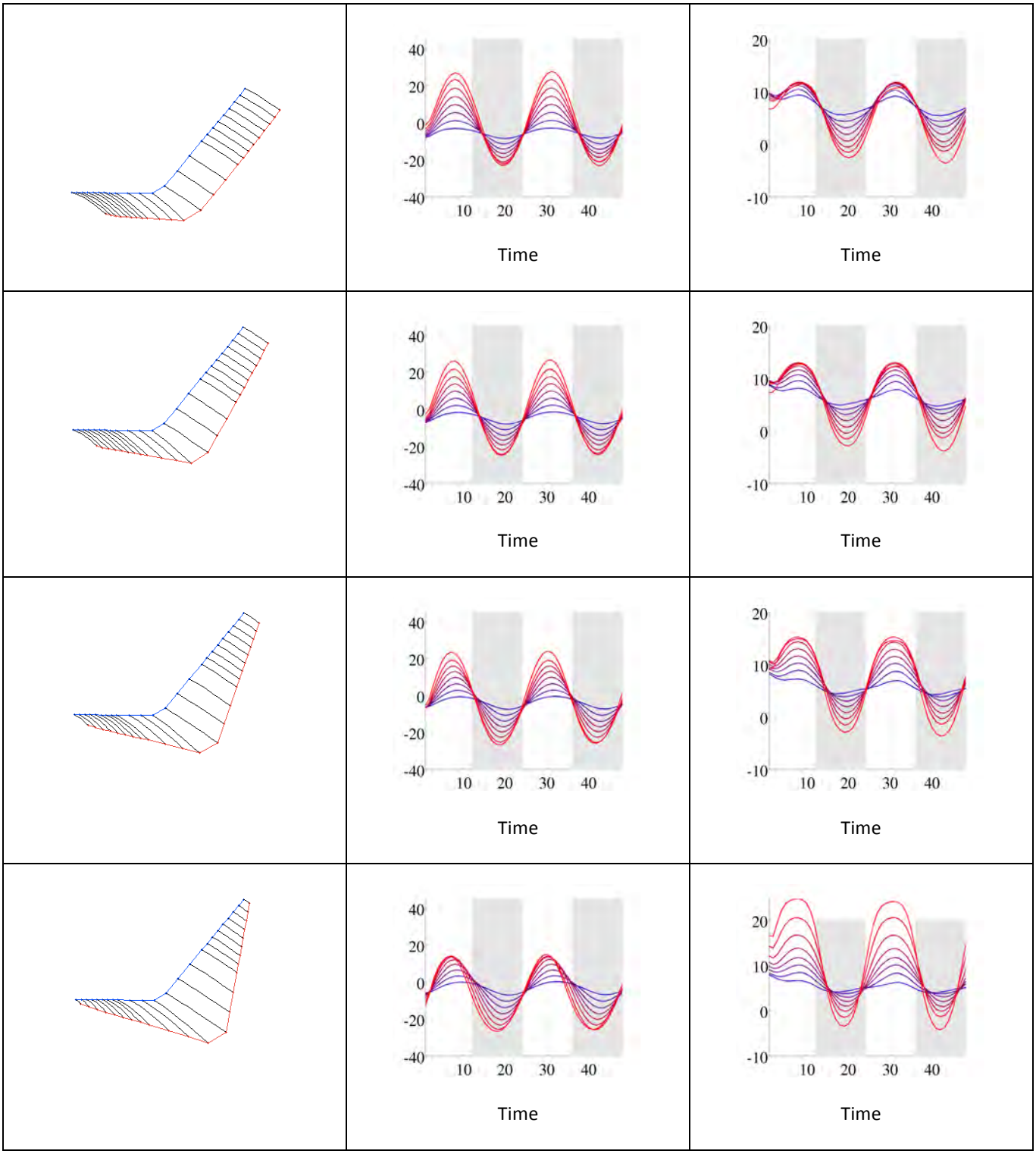

Figure 8: The wing twist (column 2) and wing local angle of attack (column 3) for a subset of the taper ratios examined using the QI-DLM code. The spanwise stations near the root of the wing are represented using blue, while the spanwise stations near the tips of the wing are represented using red.

PHYSICAL EXPERIMENT FOR EXPLORING AND TESTING STRUCTURALLY OPTIMAL WINGS

The computational effort to derive optimal wings leads to several questions:

(1) How physically realizable are the optimal wing shapes that have been determined?

(2) What structural strategies can be used to achieve the optimal flapping wing shapes?

(3) How do existing material options impact the achievement of optimal flapping wings?

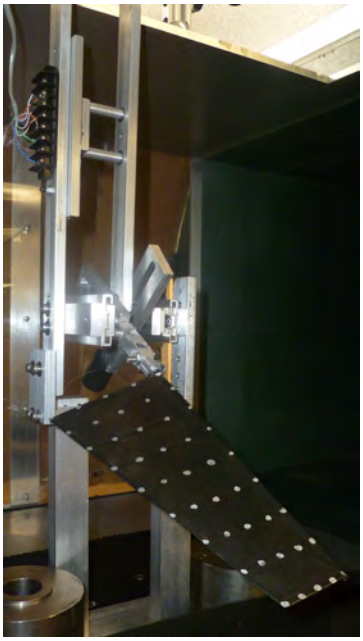

To start to address these questions we have commenced two physical experiments to explore our optimal flapping wing designs (**Error! Reference source not found.**). The aim of the first experiment was to examine wing structural compliance in air, while the second experiment will be performed in a small water tow tank. We have temporarily paused our experimental efforts in air and are focusing solely on water-based experiments.

Three students from the UMass Lowell research team visited Dr. Peter Ifju's lab in Fall 2011 to learn how to build lightweight, compliant, membrane and carbon fiber wings for flapping wing MAVs. The students learned wing manufacturing techniques that are currently being used and modified for the experimental study.

The flapping apparatus (**Error! Reference source not found.**) generates sinusoidal flapping motions with variable flapping frequencies (0-10Hz) and variable flapping amplitudes (30°-120° full stroke). This apparatus can be used to generate wing motions in air. Initial studies using this apparatus illustrated the challenge in capturing meaningful wing flapping data. Because of the high flapping frequency and the performance of the experiment in air, recording wing shape and using PIV to capture flow features was challenging. After getting preliminary data at WPAFB water tunnel during the faculty and graduate students' SFFP experience, we decided to switch to an experiment performed in water to prototype our initial optimal wing strategies. This experiment will continue, hopefully in collaboration with Michael Ol and Kenneth Grunland at AFRL, WPAFB. Using water as the test medium results in slower flapping motions for Reynolds number matching, allowing us to capture better experimental results using our lower speed cameras and PIV system. We expect to return to air testing once we have some meaningful and guiding results from our water tests. Our initial test cases in water will examine pure plunging cases akin to our early computational studies. Upon successful completion of these tests, we hope to explore hinged flapping cases, similar to flapping flight.

Figure 9: The variable frequency, variable amplitude flapping apparatus, and prototype wing installed in the UML wind tunnel.

In the experiments we will record:

- Wing shape data using a 120 FPS stereo-camera system. The wing shape will be determined using our own custom three-dimensional motion reconstruction and tracking tools.
- Flow visualization using the Particle Image Velocimetry system we have on loan from Natick Army Soldier Research Center. In addition we plan to use ink dye injection flow visualizations.

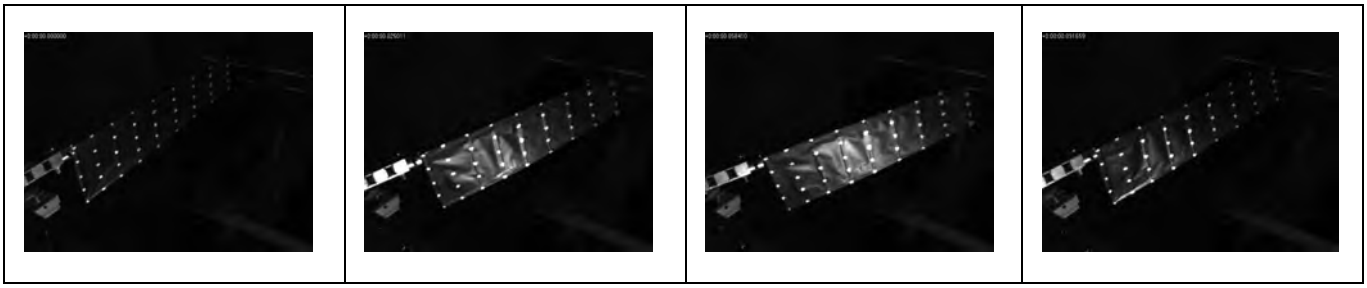

Figure 10: Several different video captures of an initial tapered geometry, flapping wing model using our air based experimental setup.

FUTURE EFFORTS

Our current and future efforts in the bottom-up study of flapping wings include integrating the effect of structural compliance in the determination of optimal wing designs. We aim to use both computation and physical experiment to determine minimally actuated structural strategies that generate the desired wing shape. These wing concepts will be characterized and shared amongst the community.

MULTI-FIDELITY SIMULATIONS OF BAT FLIGHT

We have performed several computations using bat wing kinematics data recorded by the Brown University research group. Our computations include both low-fidelity and high-fidelity simulations of the bat flight data.

FASTAERO SIMULATIONS OF BAT FLIGHT

We constructed meshes and performed a FastAero analysis of a kinematics dataset (Brown University) for a new bat species, *Tadarida brasiliensis*. We examined *Tadarida* due to the different flapping kinematics employed by this species compared with the previous *Cynopterus brachyotis* simulations. The bat mesh reconstruction for the *Tadarida brasiliensis* was performed by undergraduate summer interns at UMass Lowell.

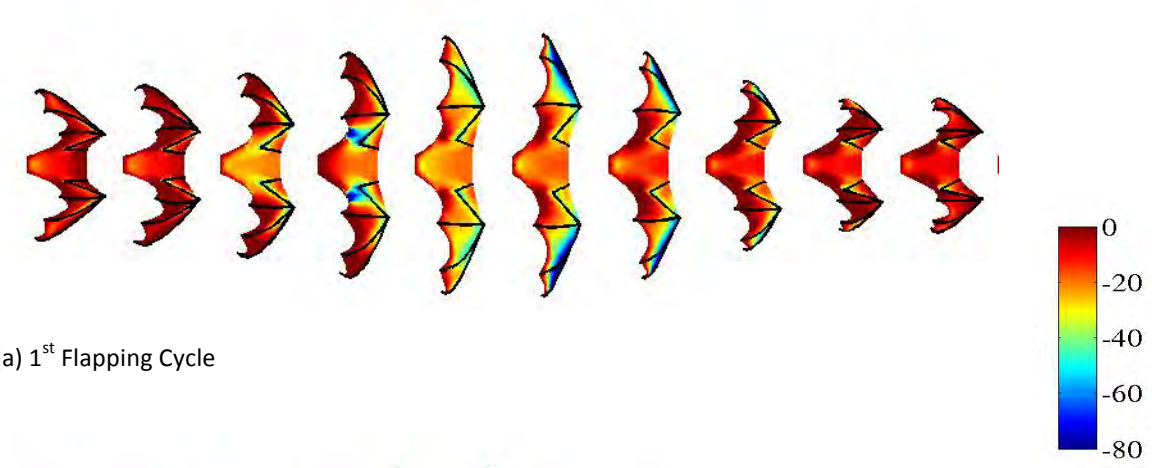

(a) 1st Flapping Cycle

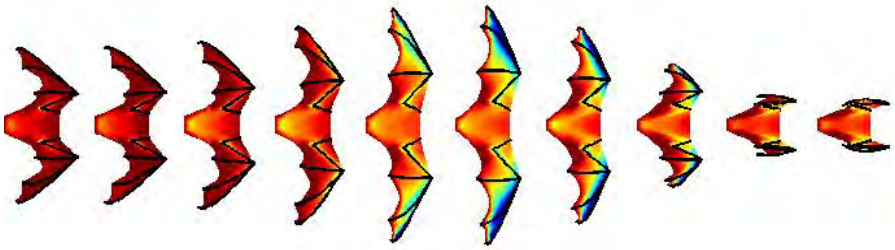

(b) 2nd Flapping Cycle

Figure 11: The pressure differential (upper surface minus lower surface pressures) for two consecutive flapping cycles of the *Tadarida* in a 7.5 m/s wind tunnel flight. Images are displayed at every 1/100th of a second.

The *FastAero* simulation results for two different wingbeat cycles of the 7.5 m/s flight are illustrated in Figure 11. Both wingbeat cycles show a similar outboard loading of the bat wing during moderate speed forward flight. This was also observed in our *FastAero* computations of the *Cynopterus brachyotis* aerodynamics earlier in the MURI effort. In addition, the wake computations (not shown here) show similar features as the Brown University PIV data measurements. We conclude from these computations as well as from the FastAero/DG computations that inviscid methods such as *FastAero* can be useful tools for analyzing biological and biologically-inspired flapping flight. We are somewhat cautious however, as *FastAero* will likely be inadequate for analysis of maneuver, hover and other flight regimes where flow separation is significant.

DISCONTINUOUS GALERKIN SIMULATIONS OF BAT FLIGHT

The numerical simulation of the bat wings presents two main additional challenges – the modeling of the complex geometry with very large domain deformations, and the efficient simulation of the resulting transitional flows. For the geometry, we have developed a new coarse-to-fine approach for efficient deformation of high-order volume meshes, which we employ to cheaply and robustly deform the volume mesh to fit every configuration of the bat wing over time. A nonlinear solid mechanics analogy is employed here to solve the deformed mesh state (as described for the optimal wings above), and a flow mesh is then constructed as a submesh of this coarser geometric mesh. We found that this approach was necessary to ensure valid (non-inverted) meshes for each wing configuration through the flapping cycle, due to the extreme nature of the wing displacement. Mesh deformation solutions for the coarse geometric mesh are shown below in Figure 12. A powerful feature of this meshing approach is the versatility in the kind of flow meshes that can be constructed as submeshes, simply by changing the refinement templates mapped to the coarse elements. Both uniform refinement and anisotropic boundary layer refinement are achievable through the use of different templates.

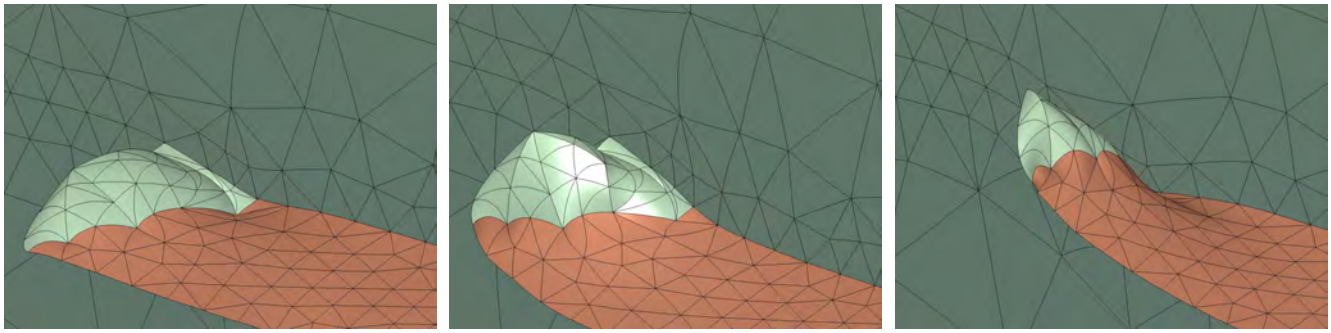

Figure 12: Coarse 3D volume mesh and time-dependent mesh deformation for biologically accurate flapping bat wing. The 3D mesh used for flow computations is generated as a submesh of this coarse high-order mesh, using our coarse-to-fine approach for efficient mesh deformation. Wing geometry and motion taken from motion capture data provided by collaborators at Brown University.

For the flow simulations, we have run a test simulation on a coarse mesh at a low Reynolds number of approximately 1,000. The pictures in Figure 13 visualize the flow field on the symmetry plane and the wing using Mach number color plots. A substantially refined simulation at higher Reynolds number with ILES turbulence modeling is currently being performed, making use of our new capabilities for mesh generation and robust deformation.

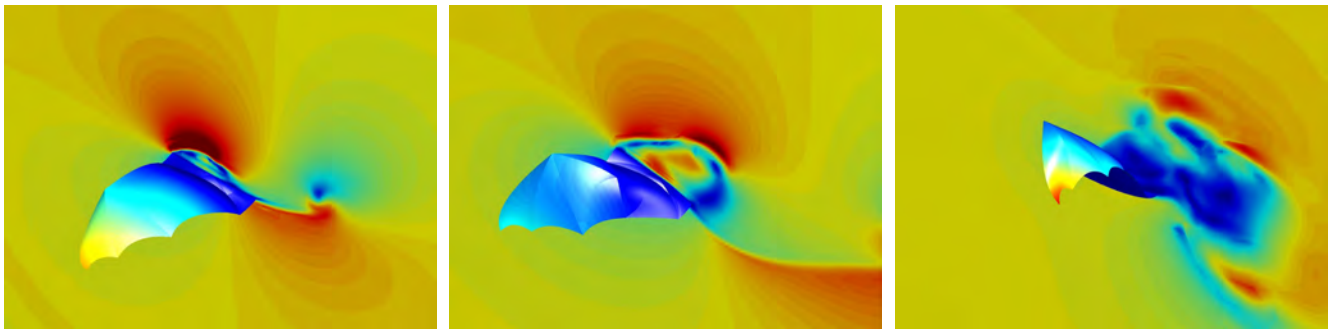

Figure 13: Preliminary simulation of flapping bat wing on coarse mesh, using wing geometry and motion data from biological measurements provided by collaborators at Brown University. A more refined simulation at higher Re is currently in progress.

2D simulations of a pitching and heaving foil have been used to explore flapping parameters that generate thrust efficiently. Specifically, here we have explored the effect of passive structural compliance on flapping wing performance, using a simple 2D model illustrated on the right. Structural compliance is modeled using a simple torsional spring at the pivot point (leading edge) of a heaving foil. The simulations were performed using our high-order Discontinuous Galerkin finite element solver for the compressible Navier-Stokes equations, coupled to a structural model to solve this fluid structure interaction problem.

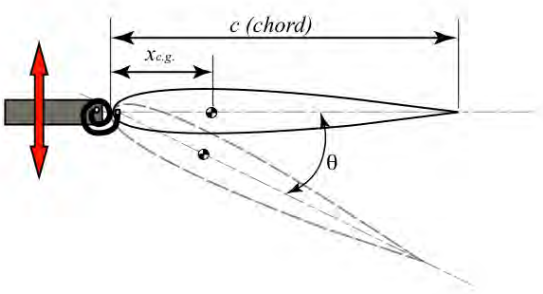

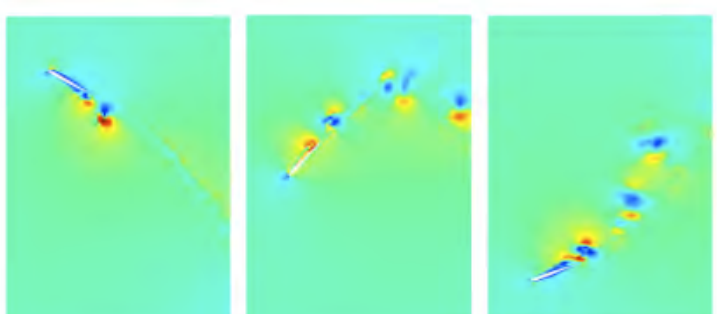

Figure 14: Mach contours for a flapping foil with k=0.4, Strouhal number 0.5, and spring constant C=0.3.

The model involves a torsional spring (characterized by spring constant C) that is placed at the foil's leading edge, thus enabling the airfoil's pitch to passively respond via the spring's compliance. We prescribe the harmonic heaving motion (h=ho*sin(w*t)) using the reduced frequency (k= w*c/(2*U)) and Strouhal number (or amplitude) as parameters. The airfoil pitch is governed by the moment balance equation. The fluid and structural equations are fully coupled and therefore must be solved simultaneously. The high fidelity design sweep examines the Strouhal number (St. = 0.1, ... , 0.5) and the spring constant (C = 0.1, ... , 0.5) at the reduced frequency k=0.4 which is representative of natural flyers. All simulations involve an HT13 airfoil (unit chord) and were conducted at Re=5000 and M=0.2.

For the design sweep, separation becomes a dominant factor in high amplitude heaving (St>0.3) and stiff springs (C>0.3). Despite the occurrence of separation, high amplitude heaving flappers have the ability to produce large thrust coefficients (Ct > 0.7) efficiently. Thus, stiffer springs and higher Strouhal numbers tend to lead to higher average thrust coefficients. However, once separation dominates, the propulsive efficiency is reduced, making these aggressive flapping parameters less desirable. This does, however, suggest that in extreme flight conditions (such as hover or maneuvering), large thrust and force production is possible at the expense of propulsive efficiency.

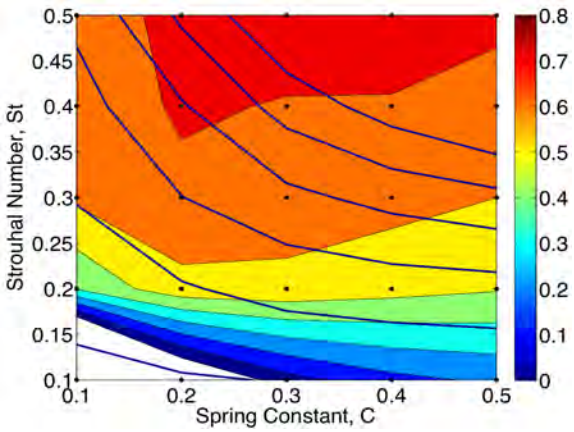

Figure 15: Contours represent the propulsive efficiency of the oscillating foil while the superimposed lines indicate constant thrust. For a given spring stiffness, the most efficient flapping strategy is determined by finding the region along a line of constant thrust at which the flapper's efficiency is optimized. (Plot shown for k=0.4.)

Also, the passive strategy is found to enhance the propulsive efficiency and period-averaged thrust production of the 2-D flappers specifically in cases where separation is encountered. The propulsive efficiency findings illustrate that there is a large region of the design space where flapping is efficient for thrust production. This indicates that flapping motions or leading edge torsional spring constants need not be exact to achieve high propulsive efficiency. A second result from this design space search indicates that a large range of thrust coefficients can be generate efficiently by simply choosing a single torsional spring constant and changing the flapping parameters.

HIGH-FIDELITY SIMULATIONS OF FLAPPING FLIGHT WITH HAIR SENSORS AND ACTIVE CONTROL

An important goal of this MURI project is to seek new insight into the special aeronautical features of bats that enable their great mastery of flight. One interesting feature of bat wings is the distributed array of fine hairs on their wings, each hair connected to a dome-like structure known to contain touch-sensitive cells. Too small to be regular pelage hair, biologists have hypothesized that these hairs are in fact flow sensors. They claim that bats use these "hair sensors" as part of a feedback control system, dynamically adjusting their wing motion in response to the boundary layer flow over their wings, and thus attaining superior flight performance. Our collaborators at the University of Maryland and Brown University have worked to address this hypothesis through biological experimentation, and have found strong evidence that the hairs do indeed provide aerodynamic sensory feedback that is used for flight control.[7]

At MIT, we have examined this hair sensor control concept from a computational perspective.[8] We have adapted our high-order Discontinuous Galerkin Navier-Stokes code to accommodate a simplified 2D model of a flapping wing, featuring both structural compliance and an active hair-sensor-based control system (see Figure 17). An Arbitrary Lagrangian-Eulerian formulation accounts for wing motion, and we compute flows with chord Reynolds number 5,000. Hair sensor dynamics are modeled using the approach of Dickinson[9]. Through this unique fluid-structure interaction model, we sought to gain new insight into the "hair sensor hypothesis" and also perform a useful characterization of the design space for active control schemes based on hair sensors.

PHYSICAL MODEL

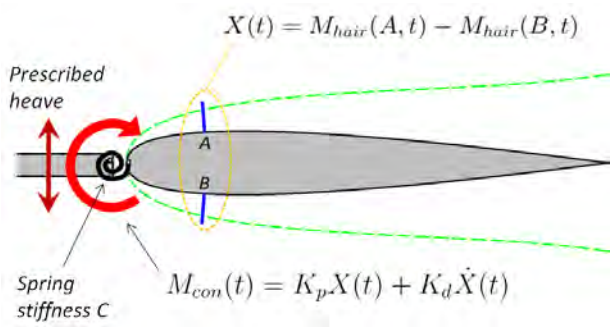

Figure 17: Diagram of 2D flapping wing model incorporating compliance and active control. Compliance is manifested via a torsional spring. An active control system is implemented via a proportional-derivative (PD) control law, taking an input signal *X* from a simplified array of two hair sensors.

Our model consists of a rigid symmetric 2D airfoil hinged at the leading edge with a torsional spring of a specified stiffness. This leading edge pivot is heaved up and down sinusoidally according to a prescribed Strouhal number and reduced frequency. The active control system is implemented as a proportional-derivative (PD) control law, which applies a control torque M_{con} to the leading edge of the airfoil. M_{con} is a function of a control signal *X*, which comes from a simple array of two hair sensors mounted on the surface of the wing. Aerodynamic drag on each hair results in a bending moment at the root, and the difference in this bending moment between the two hairs is taken to be the control signal *X*.

Note that high-fidelity methods are essential for accurately simulating this model, as the controller depends entirely on the hair sensor signal which in turn depends on the boundary layer flow over the wing. Flow in the boundary layer must therefore be correctly and accurately represented in our numerical simulations.

[7] Susanne Sterbing-D'Angelo *et al*, Bat wing sensors support flight control, *PNAS* 108: 11291-11296, June 20, 2011.
[8] H. K. Chaurasia, Active Pitch Control of an Oscillating Foil with Biologically-Inspired Boundary Layer Feedback, Master's Thesis, MIT, 2010.
[9] B. T. Dickinson, Hair receptor sensitivity to changes in laminar boundary layer shape, *Bioinspiration & Biomimetics*, 5(1):016002, 2010.

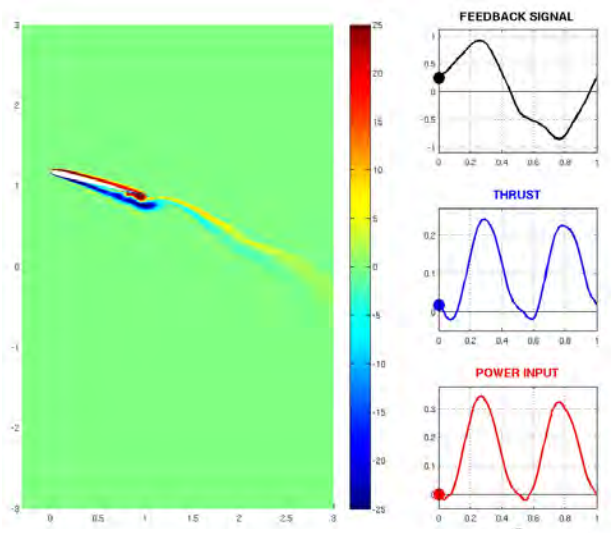

Figure 18: A typical example of our flapping wing simulations with hair-sensor-based active control. On the left is a snapshot of the pitching and heaving wing, colored by vorticity. Plots on the right show the hair sensor signal, total thrust and total power input over the entire flapping cycle.

A series of numerical experiments were performed with our model in a "cruising flapping flight" mode to characterize the effect of the controller on propulsive efficiency (the amount of power consumed to maintain a given thrust and velocity). An example of a typical simulation is provided in Figure 18. We found that an active controller with well-chosen gain parameters can enable up to 8% higher propulsive efficiency than a purely compliant flapper (i.e. a wing with torsional spring but no active controller). Quantified by a performance envelope in the thrust vs. efficiency space, the presence of a hair-sensor-based controller clearly improves the performance of our flapping wing model versus a purely compliant flapper (Figure 19). On closer analysis, this improvement appears to be derived from the fact that each hair sensor's root bending moment is well-correlated with the instantaneous boundary layer shape factor *H* at that location. This demonstrates that hair sensors are sensitive to important properties of the unsteady boundary layer, and a control law based on our hair sensor signal will be capable of responding to aerodynamically important events during the flapping cycle.

We also used our model to study the effect of hair sensor placement, by computing the performance of the flapping wing when hair sensors are placed at several different chordwise locations on the wing. Interestingly, we found a clear preference for placing sensors nearer to the leading edge. In our active feedback control experiments, sensors placed nearer the leading edge resulted in higher propulsive efficiency and smoother wing motion than sensors placed closer to the trailing edge. While this result may be limited to our chosen physical model and controller, it is an interesting observation to note.

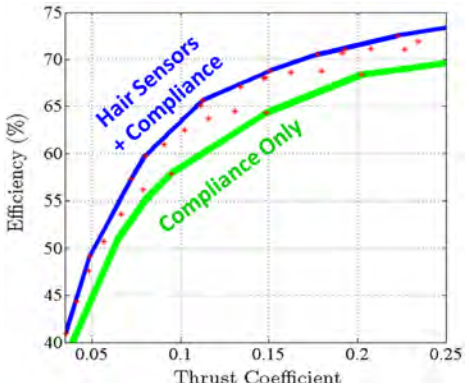

Figure 19: Computed performance envelopes in thrust vs. efficiency space, for a purely compliant (passive) flapper, and a compliant flapper augmented by an active hair-sensor-based controller.

Another series of experiments examined the behavior of our hair-sensor-based controller when the wing is subjected to a gust (see Figure 20). A large vortex was placed in the flow in front of the wing, which was previously in a steady flow state but free to pitch about its leading edge in response to flow forces, torsional spring stiffness and hair-sensor-based controller. As the vortex passes over the wing, it induces transient loads causing the wing to pitch up and down for a short period of time. This produces an oscillation in lift. As an illustrative test problem, we attempted to find an optimal hair-sensor-based controller that minimizes the transient lift deviation caused by the passage of the vortex. By an exhaustive search of the two-dimensional control law design space (proportional and derivative gain parameters), we were able to find a clear and unique optimum. This controller produced a 33% reduction in RMS lift deviation compared to a purely compliant wing (without a controller). This result illustrates the potential effectiveness of hair-sensor-based controllers for improving gust tolerance of flapping wings, and for responding to transient aerodynamic effects generally.

Full details of this research can be found in the associated Master's thesis.[10] Overall, our findings suggest that hair sensors are indeed useful for sensing important aerodynamic events such as flow separation and applying that information to a flight control system –complementing the findings of our biological collaborators at the University of Maryland and Brown University. There is now a range of compelling evidence to suggest that boundary layer feedback control via hair sensors contributes to the outstanding flight abilities of bats, and may also provide valuable clues for designing particularly robust and maneuverable Micro Air Vehicles.

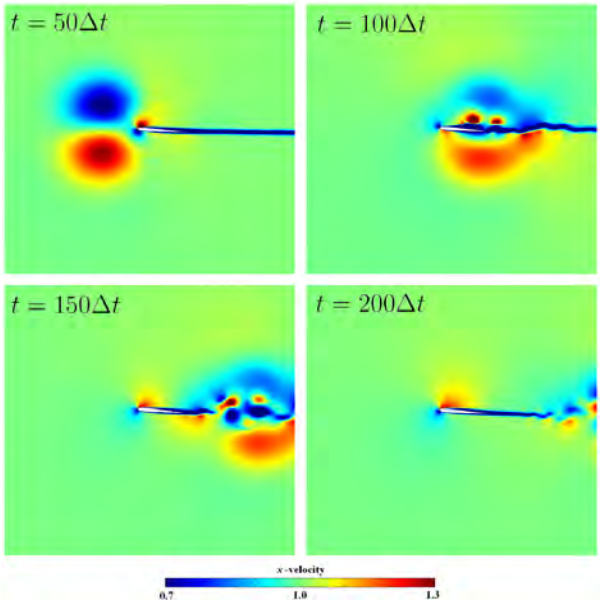

Figure 20: Example of wing subjected to a gust. A large vortex (visualized by x-velocity) passes over the wing, causing it to pitch in response to transient loads.

AEROSERVOELASTIC SIMULATIONS VIA LIFTING LINE METHOD (ASWING)

Our low fidelity approach to aeroservoelastic modeling makes use of the ASWING model developed by Mark Drela at MIT.[11] This model, illustrated in Figure 21, employs a lifting line method to represent aerodynamic effects. The structure is modeled by a series of one-dimensional beams with six degrees of freedom. The ASWING code has the capability to incorporate control laws, gust fields and propulsion elements. In particular, the model can be configured to represent a vehicle with flapping wings, such as the falcon model shown in Figure 22.

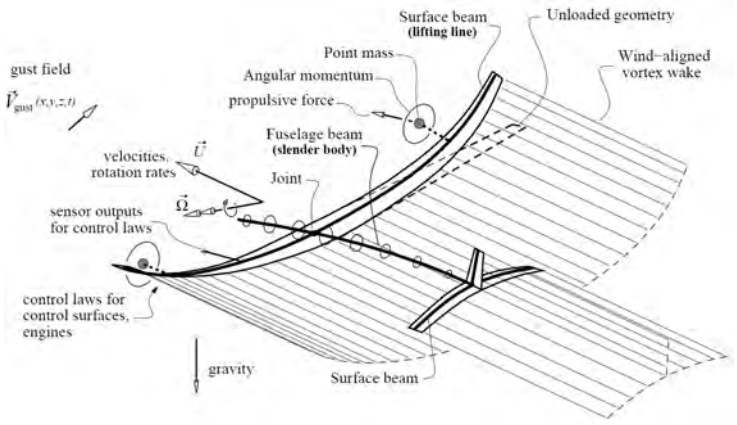

Figure 21: Aeroservoelastic model employed by ASWING code. Aerodynamics are incorporated by a lifting line method, and the structure is represented by a series of 1D, 6-dof beams.[11]

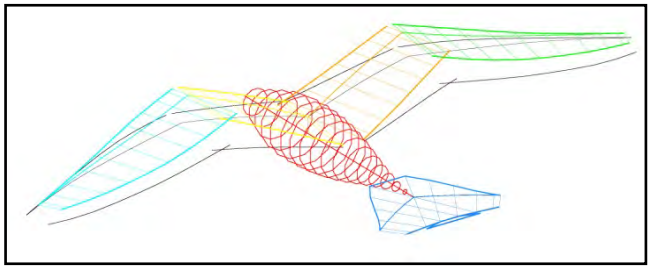

Figure 22: Falcon model produced for ASWING code.

The choice of a lifting line method inherently limits the validity of the ASWING approach, and it will not be an accurate means of directly simulating heavily loaded, very low Reynolds number flight such as in bats. However, we believe that the model captures a great enough portion of the true aeroelastic behavior to make ASWING useful as a first step for analyzing control schemes designed for cruising flight and maneuvering of flapping vehicles. The simplicity of the model makes it very inexpensive to run large numbers of cases, making ASWING amenable to optimization methods for simple flapping flight controllers. Relatively little work has been done in the area of flapping flight control schemes and associated computational tools, and we believe that the ASWING approach can make a useful contribution. This will be an active area of future research at MIT.

[10] H. K. Chaurasia, Active Pitch Control of an Oscillating Foil with Biologically-Inspired Boundary Layer Feedback, Master's Thesis, MIT, 2010.

[11] Mark Drela, Integrated Simulation Model for Preliminary Aerodynamic, Structural, and Control-Law Design of Aircraft, *Proc. of 40th AIAA SDM Conference*, St. Louis, MO, April 1999.

LOW REYNOLDS NUMBER AERODYNAMICS AND TRANSITION PREDICTION

At the low Reynolds numbers encountered in MAVs and animal locomotion, the boundary layer over the body remains laminar over large distances and is thus prone to separation, a phenomenon which is often detrimental to aerodynamic performance. Computational design strategies for low Reynolds number flying and swimming vehicles hence rely on the accurate prediction of separation. Furthermore, separation often induces transition to turbulence, which in turn can induce re-attachment. Separation, transition, and reattachment can take place over a significantly short distance, producing a laminar separation bubble (LSB) which can fluctuate in size and position. Thus, the prediction of separation and transition is of crucial importance in low Reynolds number flows.

Knowledge of the fundamental flow physics encountered in these regimes is still quite limited, and hence the development of a transition prediction method for low Reynolds number flows is necessarily accompanied by a study and an understanding of the fundamental flow phenomena involved, such as the formation of laminar separation bubbles and the mechanisms involved in the transition to turbulence. Having studied the transition which takes place along a laminar separation bubble in low Reynolds number flows, we quantified the growth of Tollmien-Schlichting waves. The second part of this work, completed in the last two years, focused on investigating the effects of having cross-flow present over swept wings – an area which had essentially remained unexplored.

The flow over an infinite SD7003 wing at an angle of attack of 4^{o} was considered at a chord Reynolds numbers of 60,000, and for sweep angles ranging between 0^{o} and 60^{o}, as illustrated in Figure 23. A separation bubble is present on the upper surface where the flow transitions to turbulence, and both Tollmien-Schlichting (TS) waves and cross-flow instabilities are observed.

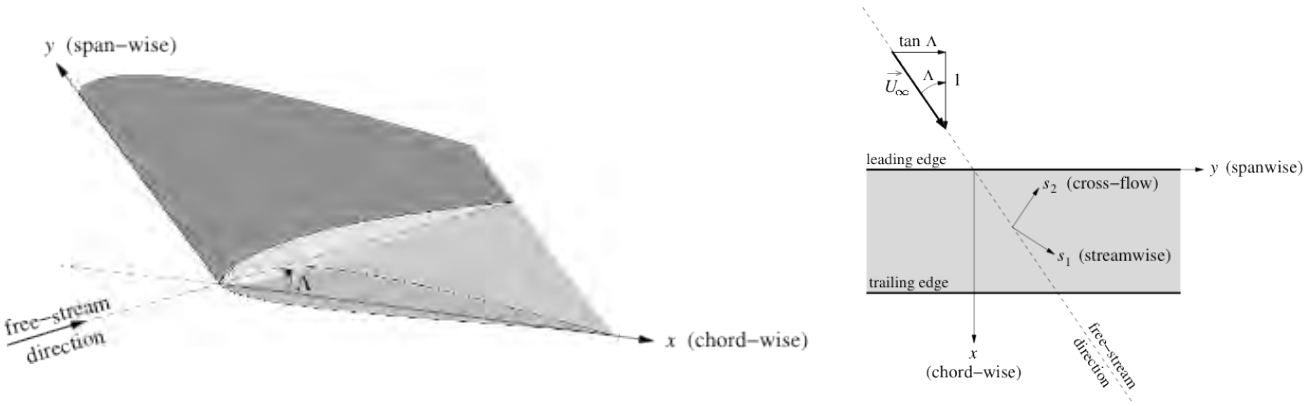

Figure 23: Illustration of the free-stream velocity, chord-wise direction x, and span-wise direction y for the swept-wing flow; Λ is the sweep angle.

Figure 25 provides a comparison of the boundary layer streamwise displacement thickness, momentum thickness, and shape factor for a straight and a 30^{o} swept wing. Separation and transition locations are defined at the locations where the shape factor reaches 4 and where it peaks, respectively. The separation location does not change significantly (5% farther downstream for the swept wing), but transition does occur significantly earlier (18%) in the presence of cross-flow.

Since the chord-wise characteristics are constant across all sweeps (same airfoil profile, angle of attack, chord-wise Reynolds number) the two-dimensional-equivalent boundary layer quantities can provide a meaningful comparison by decoupling the cross-flow components from the purely chord-wise boundary layer evolution. If the cross-flow and streamwise effects are only linearly coupled, the curves for different sweep angles should collapse into a single line (see details on the two-dimensional equivalent projection in the publications Uranga 2011; Uranga *et al* 2011).

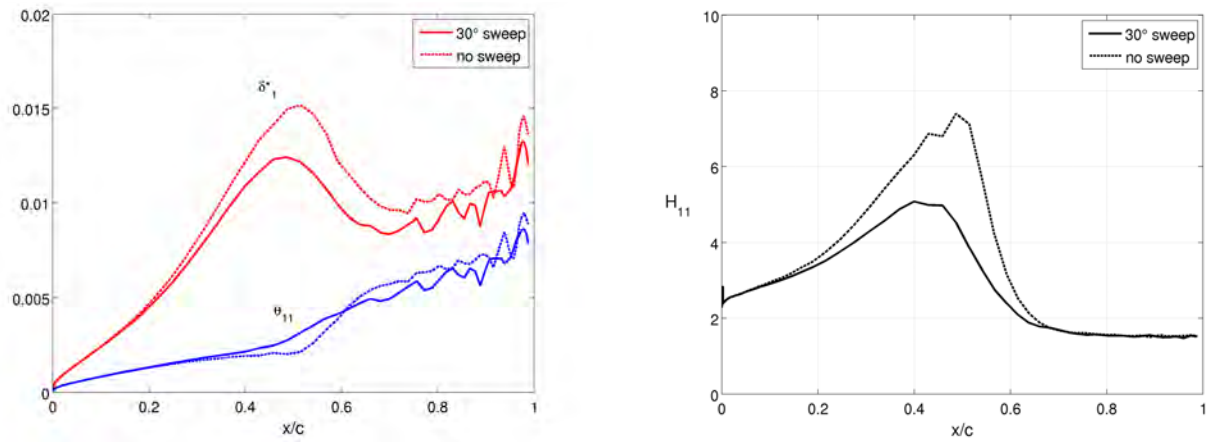

Figure 25: Boundary layer average streamwise displacement and momentum thicknesses (left), and shape factor (right) evolution along the chord-wise direction: comparison of un-swept and 30° sweep wing at fixed chord-wise Reynolds number of 60,000.

The right plot of Figure 24 shows the streamwise shape factor, while the left one gives the two-dimensional equivalent shape factor. The curves on the left demonstrate that span-wise/cross-flow effects cannot be considered independently of the chord-wise/streamwise evolution for sweep angles between 10° and 30°: the influence of the latter on the former is non-linear, and the two-dimensional equivalent boundary layer shape factors vary with sweep-angle. On the other hand, for $\Lambda = 1\circ$ and $\Lambda = 5\circ$, the two-dimensional equivalent boundary layer curves collapse, indicating that only linear interactions occur; the same happens for sweep angles of 40° and larger.

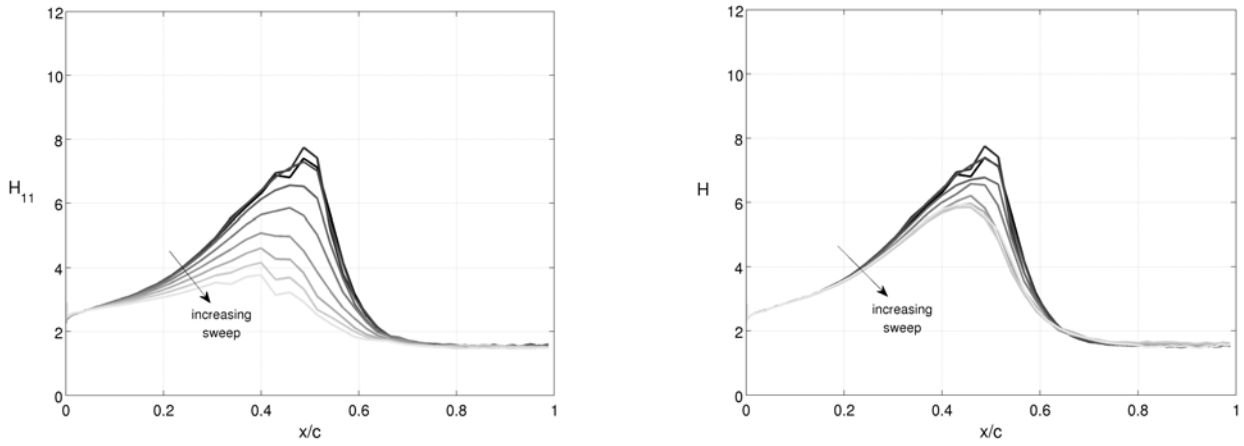

Figure 24: Boundary layer streamwise shape factor (left), and two-dimensional-equivalent shape factor (right), at fixed chord-wise Reynolds number of 60, 000 and for sweep angles of {0°, 1°, 5°, 10°, 20°, 30°, 40°, 50°, 60°}.

Hence, for separation-induced transition at low Reynolds numbers, it is not possible to treat streamwise and cross-flow instabilities independently for wings with sweep angles between about 10◦ and 40◦, and predicting the mixed transition cannot be reduced to treating the disturbances of each component separately. An important presumption to be adopted in the study of unsteady flows for MAVs and animal locomotion is thus that the type of transition (TS dominated, cross-flow dominated, or mixed) is a priori unknown as soon as the flow is slightly misaligned with the wing's chord.

HIGHLIGHTED INTERACTIONS WITH OTHER MURI TEAM MEMBERS

- Brown–UML: use of Brown University kinematics by U Mass Lowell for *FastAero* bat computations.
- Brown–MIT–Berkeley: ongoing use of Brown University bat kinematics data to develop high-fidelity flow simulations of flapping bat wings using 3DG.
- OSU–MIT: collaboration on applying hair sensor model developed by Dickinson[12] in active control simulations at MIT.[13]
- UML–MIT–Berkeley: worked in a highly collaborative manner to compare results of low-fidelity methods to high fidelity simulations of flapping flight.[14]
- UML–MIT–Berkeley: collaborative study to assess optimal flapping wing shapes and understand the effect of leading edge angle and camber on flight performance.[15]
- MIT–Berkeley: ongoing collaborative development of 3D high-fidelity aeroelastic simulation tools.
- UML–MIT: collaborations to define and examine structural strategies that will be useful for achieving optimal flapping wing shapes passively.
- UML–MIT: collaborations to collate animal flight data and define flapping flight regimes from an engineering perspective.
- Brown–MIT: Preliminary collaboration on coordinated physical and numerical experiments for a flapping plate.

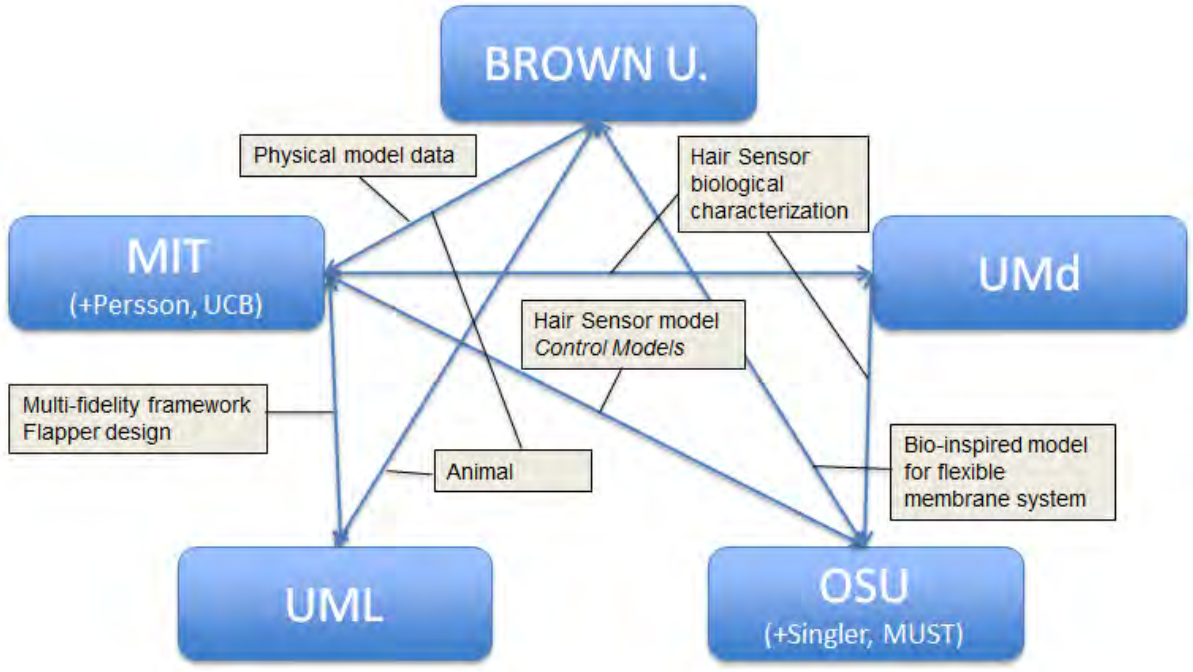

[12] B. T. Dickinson, Hair receptor sensitivity to changes in laminar boundary layer shape, *Bioinspiration & Biomimetics*, 5(1):016002, 2010.
[13] H. K. Chaurasia, Active Pitch Control of an Oscillating Foil with Biologically-Inspired Boundary Layer Feedback, Master's Thesis, MIT, 2010.
[14] P.-O. Persson, D. J. Willis and J. Peraire, Numerical Simulation of Flapping Wings using a Panel Method and a High-Order Navier-Stokes Solver, *Int. J. Num. Meth. Engrg.,vol. 89, issue 10, pp. 1296-1316, 2012.*
[15] P.-O. Persson and D. J. Willis, High Fidelity Simulations of Flapping Wings Designed for Energetically Optimal Flight, *Proc. of the 49th AIAA Aerospace Sciences Meeting and Exhibit*, January 2011, AIAA-2011-568.

FUTURE RESEARCH PLANS

Here we briefly highlight some of our plans for future research relevant to the MURI effort.

- 3D bat computations: in the near term we will complete highly resolved Navier-Stokes simulations of a flapping bat wing, using our high-order Discontinuous Galerkin solver and our new coarse-to-fine mesh deformation approach featuring a nonlinear elasticity solver. Early results from this approach have shown great promise and we expect to have refined results very soon.

- Experiments in a water tank are currently being developed to examine wing compliance and the effect on flight performance. These experiments will tie in with computational predictions at lower fidelity levels, to understand how passive structural compliance can be used in flapping flight.

PERSONNEL & PUBLICATIONS

Personnel (MIT)

Faculty:	Jaime Peraire	
	Mark Drela	
	David J. Willis	(Research Scientist '07-'08, Visiting Assistant Professor('08-'10))
	P.-O. Persson	(Applied Mathematics Instructor 6/08 – 7/08)
Research Scientist:	Ngoc Cuong Nguyen	
Graduate Students:	Alejandra Uranga	
	Hemant Chaurasia	
	Emily Israeli	6/08 – 9/08
Undergraduate Students :	Isaac Ascher (UROP)	
	Andy Huang (UROP)	
External Collaboration	P.-O. Persson (Berkeley)	

Personnel (UML)

Faculty:	David J. Willis	(09-12)
Graduate Students:	Hesam Salehipour	(MURI: 01/09-05/10)
	Paul Bevillard	(MURI: 01/09-01/11)
	Raghu Gowda	(MURI: 1/11-7/12)
	Justin Sousa	(MURI: 9/11-7/12)
	Christopher Pitocchelli	(MURI: 04/11 - 12/11)
	Guy Crescenzo	(MURI: 04/11 - 12/11)
	Milo DiPaola	(Not supported, but working on IBLM)
Undergraduate Students :	Bradley Olson	
	Richard Poillucci	
	Jeremy Vaillant	
External Collaborations :	Peter Ifju, UF-Gainesville, MAV Wing Construction	

PUBLICATIONS RELEVANT TO MURI PROJECT

Archival Publications, Theses and Published Conference Proceedings

- P.-O.Persson, D.J.Willis, J. Peraire, Numerical Simulation of Flapping Wings using a Panel Method and a High-Order Navier-Stokes Solver, International Journal for Numerical Methods in Engineering, vol. 89, issue 10, pp. 1296-1316. 2012
- P.-O. Persson and D. J. Willis, High Fidelity Simulations of Flapping Wings Designed for Energetically Optimal Flight, Proc. of the 49th AIAA Aerospace Sciences Meeting and Exhibit, January 2011. AIAA-2011-568.
- D.J.Willis, Using Enriched Basis Functions for Automatically Handling Wake-Body Intersections in Source-Doublet Potential Panel Methods, in the proceedings of and presented at the 50th AIAA-ASM Meeting, January 2012.
- J. Peraire and P.-O. Persson, High-Order Discontinuous Galerkin Methods for CFD, in Adaptive High-Order Methods in Computational Fluid Dynamics, World Scientific series in Advances in Computational Fluid Dynamics, Vol. 2, editor Z.J. Wang, 2011.
- A. Uranga, P.-O. Persson, M. Drela and J. Peraire, Preliminary Investigation Into the Effects of Cross-Flow on Low Reynolds Number Transition, Proc. of the 20th AIAA Computational Fluid Dynamics Conference, June 2011.
- S.M.Swartz, K.S.Breuer, and D.J.Willis, Aeromechanics in Aeroecology: Flight Biology in the Aerosphere, Integrative and Comparative Biology, volume 48, number 1, pp. 8598, 2011.
- P.-O. Persson and D. J. Willis, High Fidelity Simulations of Flapping Wings Designed for Energetically Optimal Flight, Proc. of the 49th AIAA Aerospace Sciences Meeting and Exhibit, January 2011, AIAA-2011-568.
- P.-O. Persson, High-Order LES Simulations using Implicit-Explicit Runge-Kutta Schemes, Proc. of the 49th AIAA Aerospace Sciences Meeting and Exhibit, January 2011, AIAA-2011-684.
- D. Moro, N.C. Nguyen, J. Peraire and J. Gopalakrishnan, A Hybridized Discontinuous Petrov-Galerkin Method for Compressible Flows, Proc. of the 49th AIAA Aerospace Sciences Meeting and Exhibit, January 2011. AIAA-2011-197.
- J. Iriarte-Díaz, D. K. Riskin, D. J. Willis, K. S. Breuer and S. M. Swartz, Whole-body kinematics of a fruit bat reveal the influence of wing inertia on body accelerations, The Journal of Experimental Biology 214, 1546-1553, May 2011.
- D. Willis, J. Bahlman, K. Breuer and S. Swartz, Energetically Optimal Short-Range Gliding Trajectories for Gliding Animals, AIAA Journal, accepted for publication, 2011.
- A. Uranga, P.-O. Persson, M. Drela, and J. Peraire, Implicit Large Eddy Simulation of Transition to Turbulence at Low Reynolds Numbers using a Discontinuous Galerkin Method, Int. J. Num. Meth. Engrg., vol. 87, No. 1-5, pp 232-261, published online October 2010.
- D.J. Willis, P.-O. Persson, H. Salehipour, J. Peraire, A multi-fidelity framework for designing compliant flapping wings, Invited Paper presented at the Fifth European Conference on Computational Fluid Dynamics ECCOMAS CFD 2010, June 14th - 17th, 2010, Lisbon, Portugal
- H. Salehipour, D. J. Willis, A Novel Energetics Model for Examining Flapping Flight in Nature and Engineering, presented at the 2010 ECCOMAS CFD Conference, Lisbon, Portugal, 2010.
- P.-O.Persson, D.J.Willis, J. Peraire The Numerical Simulation of Flapping Wings at Low Reynolds Numbers, submitted and presented at the 2010 Aerospace Sciences Meeting and Exhibit in Orlando Florida, January 2010.
- H. Salehipour, D. J. Willis, A Wake-Only Energetics Model for Preliminary Design of Biologically-Inspired Micro Air Vehicles, AIAA Atmospheric Flight Mechanics Conference, Toronto, Canada, August 2010.
- D.J. Willis, and H. Salehipour, Preliminary Design of Three-Dimensional Flapping Wings from a Wake-Only Energetics Model, Invited Paper, AIAA Atmospheric Flight Mechanics Conference, Toronto, Canada, August 2010.
- D.J.Willis, Bahlman, J., Swartz, S.M., Breuer, K.S., Energetically Optimal Flight Trajectories for Short Range Gliding

Animals, Presented at the AIAA Applied Aerodynamics Conference, San Antonio TX, June 2009.

- Salehipour, H., and Willis, D. J., A coupled kinematics and energetics model for flapping flight, submitted and presented at the 2010 Aerospace Sciences Meeting and Exhibit in Orlando Florida, January 2010.
- P.-O. Persson, J. Peraire and J. Bonet, 'Discontinuous Galerkin solution of the Navier-Stokes equations on deformable domains', Comp. Methods Appl. Mech. and Engrg, 198, p. 1585-1595, 2009.
- P.-O. Persson and J. Peraire, 'Curved mesh generation and mesh refinement using Lagrangian solid mechanics', presented at the 47th AIAA Aerospace Sciences Meeting and Exhibit, January 2009, AIAA-2009-949.
- P.-O. Persson, 'Scalable Parallel Newton-Krylov Solvers for Discontinuous Galerkin Discretizations', presented at the 47th AIAA Aerospace Sciences Meeting and Exhibit, January 2009. AIAA-2009-606.
- A. Uranga, P.O. Persson, M. Drela and J. Peraire, 'Implicit large eddy simulation of transitional flows over airfoils and wings', presented at AIAA Conference, AIAA-2009-4131, San Antonio, TX, June 2009.
- M. Drela, 'Power balance in aerodynamic flows', presented at AIAA Conference, AIAA 09-3762, San Antonio, TX, June 2009.
- David J. Willis, Emily R. Israeli, Jaime Peraire "Computational Investigation and Design of Compliant Wings for Biologically Inspired Flight Vehicles", ICAS 08, 26th International Congress of the Aeronautical Sciences, Alaska, September 2008.
- D.J. Willis, E.R. Israeli, and J.Peraire, Computational Investigation and Design of Compliant Wings for Biologically Inspired Flight Vehicles, Presented at the 26th Congress of International Council of the Aeronautical Science , ICAS, Anchorage, Alaska, September 2008.
- Riskin, D.K., Willis, D.J., Diaz, J.-I., Hedrick, T.L., Kostandov, M., Chen, J., Laidlaw, D.H., Breuer K.S., and Swartz, S.M., Quantifying the complexity of bat wing kinematics, Journal of Theoretical Biology, 254 (2008) 604-615.
- D.J. Willis, P.O.Persson, E.R.Israeli, K.S.Breuer, S.M.Swartz, J. Peraire, Multifidelity Approaches for the Computational Analysis and Design of E_ective Flapping Wing Vehicles, Invited Paper, Proceedings of the 46th AIAA Aerospace Sciences Meeting and Exhibit, Reno, Nevada, January 2008.

Papers in Review

- Hesam Salehipour, David J. Willis, A Coupled Kinematics-Energetics Model for Predicting Energy Efficient Flapping Flight, Submitted to the Journal of Theoretical Biology, 2012

Theses (Completed)

- A. Uranga, Investigation of Transition to Turbulence at Low Reynolds Numbers using Implicit Large Eddy Simulations with a Discontinuous Galerkin Method, PhD Thesis, Massachusetts Institute of Technology, February 2011.
- H. K. Chaurasia, Active Pitch Control of an Oscillating Foil with Biologically-Inspired Boundary Layer Feedback, Master's Thesis, Massachusetts Institute of Technology, 2010.
- Salehipour, H., "A Fast, Low Fidelity Computational Model for Analyzing Flapping Flight Energetics in Nature and Engineering", *Master's thesis*, UML, 2010.
- E. Israeli, Simulations of a passively actuated oscillating airfoil using a discontinuous Galerkin method,Master's Thesis, Massachusetts Institute of Technology, 2008.

Presentations (without archival papers)

- H. Chaurasia, X. Roca, P.-O. Persson, J. Peraire, A Coarse-To-Fine Approach for Efficient Deformation of High-Order Meshes, 21st International Meshing Roundtable, San Jose, CA, October 9, 2012.P.-O. Persson, Sparse Line-Based

Discontinuous Galerkin Discretizations and Efficient Time-Integration,
High-Order Methods I, 20th AIAA Computational Fluid Dynamics Conference, June 27, 2011.

- J. Peraire, Hybridized Discontinuous Galerkin Methods, INI/WIMCS - Computational Challenges in Partial Differential Equations, Swansea University, 4-8 April 2011.
- J. Peraire, Hybridized Discontinuous Galerkin Methods, Fluid-Structure Interaction 2011, iHPC, Singapore, 27-29, April 2011.
- P.-O. Persson, High-Order Discontinuous Galerkin Simulation of Flapping Wings, 16th International Conference on Finite Elements in Flow Problems, Munich, Germany, March 2011.
  Also: UC Berkeley Matrix Computations and Scientific Computing Seminar, March 9, 2011.

  SIAM CSE11, March 3, 2011.
  NASA Ames Applied Modeling & Simulation (AMS) Seminar Series, January 25, 2011.
- H. K. Chaurasia, N.C. Nguyen, J. Peraire and P.-O. Persson, A Discontinuous Galerkin Method for Fluid Structure Interaction Problems, 16th International Conference on Finite Elements in Flow Problems, Munich, Germany, March 2011.
- D. Moro, N.C. Nguyen and J. Peraire, A Hybrid Discontinuous Petrov-Galerkin Method for Compressible Flows, 16th International Conference on Finite Elements in Flow Problems, Munich, Germany, March 2011.
- J. Peraire, N.C. Nguyen and B. Cockburn, An Embedded Discontinuous Galerkin Method for the Compressible Euler and Navier-Stokes Equations, 16th International Conference on Finite Elements in Flow Problems, Munich, Germany, March 2011.
- J. Peraire - ASME IMECE 2008 Minisymposium on Reduced Order Models, “Reduced Order Modelling for Nonlinear Parametrized PDE’s”, Boston MA, October, 2008
- J. Peraire - Inauguration Lecture, Course 2008-2009, School of Civil Engineering, Polytechnic University of Catalonia, October, 2008
- J. Peraire - iCME Colloquium (Institute for Computational and Mathematical Engineering), "High order discontinuous Galerkin methods for systems of conservation laws", Stanford University, February, 2009.
- J. Peraire - "High order discontinuous Galerkin methods for systems of conservation laws", National University of Singapore, January, 2009.
- H. Chaurasia – “A Hybridizable Discontinuous Galerkin Method for Nonlinear Inviscid Conservation Laws”, presented at the 5th MIT Conference on Computational Fluid and Solid Mechanics, Cambridge MA, June 2009.
- D. J. Willis ,”Boundary Element Methods for the Preliminary Design, Analysis and Optimization of Compliant Flapping Wings”, WCCM-Eccomas July 2008
- D.J. Willis, “Computational modeling of the aeromechanics of a bat (Cynopterus brachyotis)”, SICB January 2009
- D. J. Willis “Computation for Understanding (aero-structural aspects of) Biologically Inspired Flight”, IMAV09: June 2009

Theses (Near Completion)

- P. Bevillard
- H. Chaurasia
- J. Sousa
- Milo DiPaola

UNIVERSITY OF MARYLAND

CONTENTS

INTRODUCTION

Bat flight – the only true, powered flight found in mammals – is characterized by remarkable aerial maneuvers like steep banking, hovering and landing upside-down. Skeletal specializations, muscular control of wing shape, e.g., camber, and the highly compliant characteristics of the wing membrane are the basis of maneuverability and energy efficiency (Swartz *et al.* 1996, Winter *et al.* 1998, Voigt and Winter 1999, Stockwell 2001). Moreover, bat flight is very robust in turbulent, gusty, and low Reynold number air flow conditions, for example during low-speed flight and hovering. While earlier studies relied on high-speed video tracking and modeling to characterize bat flight (Rayner 1979a, b), recent particle image velocimetry (PIV) experiments showed that these animals produce complex aerodynamic wake patterns (Hedenstrom *et al.* 2007, Muijres *et al.* 2008).

However, the sensory-motor mechanisms that underlie the robustness of bats' flight have not been studied in detail, and despite the fact that the wing is well represented in the primary somatosensory cortex of echolocating bats (Big Brown Bat - *Eptesicus fuscus (E.f.)*: Chadha *et al.* 2010, Pallid Bat - *Anthrozous pallidus (A.p.)*: Zook and Fowler 1986, Ghost Bat - *Macroderma gigas (M.g.)*: Wise *et al.* 1986), we know only little about the nature and function of the cutaneous tactile receptors located in the wing membrane. To the naked eye, the bats' wing membrane appears hairless in contrast to the head and body of the animals, which are densely covered with fine hair. At first thought this appears odd, because fur surfaces are known to stabilize (microlaminarize) the boundary layer airflow by breaking up large vortices into microturbulences (Nachtigall 1979). However, a sparse grid of microscopically small hairs, many of which are protruding from domed structures, is found on both surfaces of the bat wing. These hairs have been described first in the early 20th century (Maxim 1912), but their role for bat flight has never been studied until recently (Sterbing-D'Angelo *et al.* 2012, Zook and Fowler 1986).

The Maryland group's contribution to this project has been three-fold: 1) Scanning electron microscope studies of the morphology and distribution of wing hairs of different bat species, 2) Neurophysiological studies of somatosensory signaling from the wing membrane to the cortex of the bat brain, and 3) Behavioral studies of obstacle avoidance and response to air turbulence in bats following wing hair removal. Collectively, this research contributes to our understanding of somatosensory signaling for flight control, and the results of our experiments have immediate implications for the design of autonomous micro-air-vehicles.

I. SENSORY HAIRS ON THE WINGS OF BATS – MORPHOLOGY AND DISTRIBUTION

The morphology and distribution of wing hairs was examined for three echolocating species, the Big Brown Bat (*Eptesicus fuscus, E.f.*), the Short-Tailed Fruit Bat (*Carollia perspicillata, C.p.*), and Pallas's Long-Tongued Bat (*Glossophaga soricina, G.s.)* using scanning electron microscopy. The ecological niches and diets of these three bat species differ and consequently impact requirements for flight control. In particular, the insectivorous *E.f.* must make sharp turns in flight to pursue and capture evasive insect prey, the frugi-/nectarivorous *C.p.* must maneuver through dense vegetation to find fruit, and the nectarivorous *G.s.* must hover over flowers to take nectar. In all three species, the short hairs are sparsely distributed along dorsal and ventral surfaces of the wing, and are morphologically distinct from the long pelage hairs. The pelage hairs were only found on SEM samples that were cut close to the limbs. They were up to several mm long, relatively thick at the base (6 - 18 μm) found close to the ventral forearm, around the leg, and on the tail membrane, sometimes referred to as inter-femoral

membrane (IFM) or uropatagium. In all three species, on the membraneous parts of the wing, a second type of hair was found, which is invisible to the naked eye. These hairs are so thin that only one follicle cell builds each segment of the hair, resulting in a coronal scale pattern (Figure 1A). The tip diameter of these hairs is only 200 to 900 nm (Figure 1B).

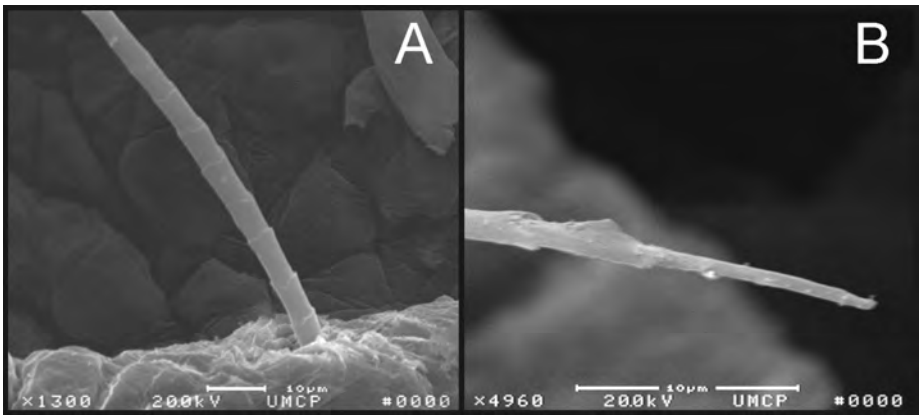

Figure 1. Scanning Electron Microscope photographs of hairs taken from wing membrane of *Eptesicus fuscus*. A – hair base protruding from a dome (x 1300), B – hair tip (x 4960). calibration bars located on the bottom of both images indicate 10 um.

These small hairs are typically found in rows, generating a sparse grid of about one hair per mm^2. In the two phyllostomid species, C.p. and G.s., the distribution of the hairs, as well as their length and thickness, are similar to E.f. except that in some areas of their wing membrane, particularly on the dorsal plagiopatagium at the trailing edge, several hairs protrude from one dome (Fig. 2), a finding that has been previously described for A.p. (Zook 2006). Theoretical considerations and modeling of boundary layer detection of the Batten group (OSU) revealed that the measured hair lengths we provided are in very good agreement with the theoretical ideal length of hair for maximum shear-force sensitivity to boundary layer shape and avoidance of viscous coupling (Dickinson, 2010).

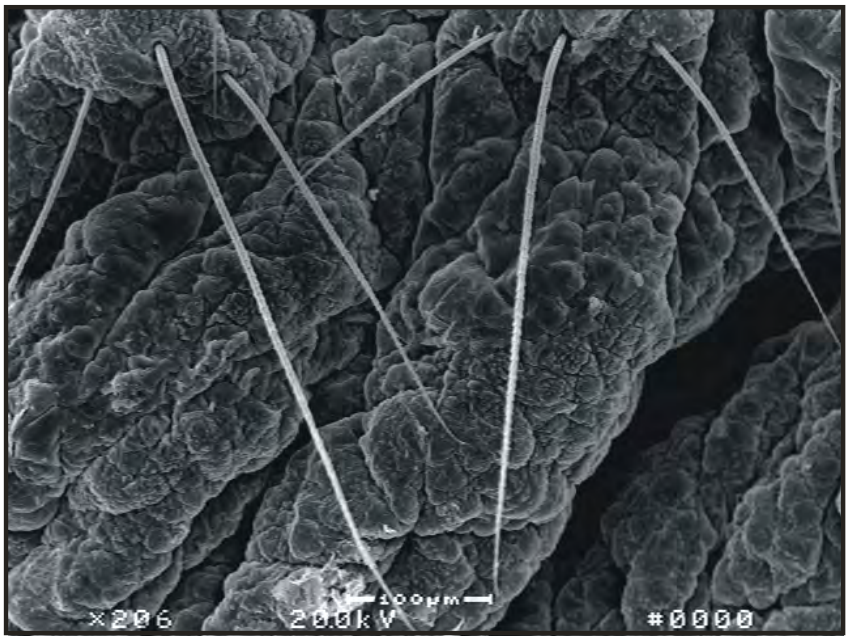

Figure 2. Scanning Electron Microscope photograph of hairs taken from the dorsal plagiopatagium of the frugi-/nectarivorous neotropical bat Carollia perspicillata. Note the groups of three hairs each protruding from a dome. The center hair is consistently longer than the sideways pointing hairs.

II. SOMATOSENSORY PHYSIOLOGY: CORTICAL MAPPING OF WING REPRESENTATION AND NEURAL RESPONSES TO AIR PUFF STIMULATION

A. TOPOGRAPHIC MAPPING OF PRIMARY SOMATOSENSORY CORTEX

The existence of orderly representations of the sensory surface in somatosensory cortex and other brain regions has long been known. Earliest observations of correspondence between peripheral tactile stimulation and cortical excitation were reported during the late 1930's and early 1940's (Marshall et al. 1938; Adrian 1941) in cats and monkeys. Since then, tremendous progress has been made in our understanding of the development and organization of representations of sensory surfaces in cortical and subcortical structures. Studies of animals with specialized sensory systems are especially useful, as they not only provide information on how sensory systems operate, but they also reveal the evolutionary forces that shape brain organization and function.

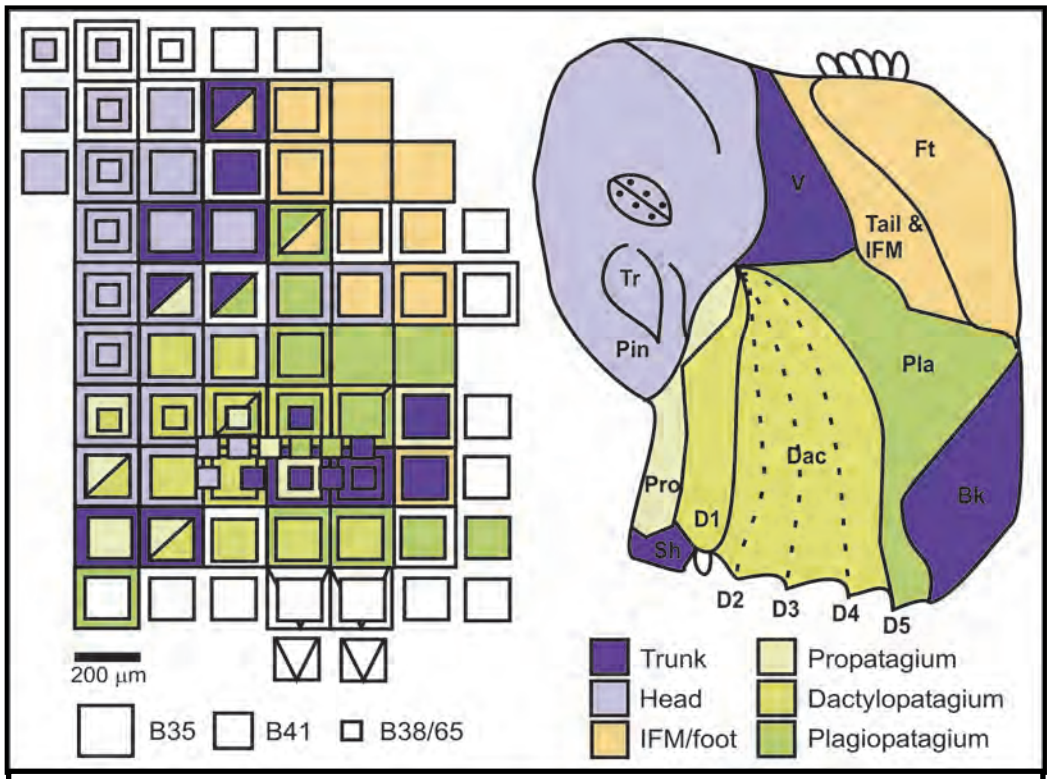

Figure 3. Average cortical surface map or "homunculus" obtained from pooling data from 5 bats. The representation of the wing is marked in color shades to indicate the functional regions, leading edge, trailing edge and mid-wing.

We studied the neuronal representation of the wing membrane in the primary somatosensory cortex (S1) of the anesthetized Big Brown Bat, *Eptesicus fuscus*, using tactile stimulation with calibrated monofilaments (von Frey hairs) while recording from multi-neuron clusters. The body surface is mapped topographically across the surface of S1, with the head, foot, and wing being overrepresented. Also in this bat species, the orientation of the wing representation is rotated compared to terrestrial mammals. Although different wing membrane parts derive embryologically from different body parts, including the flank, the tactile sensitivity of the entire flight membrane is remarkably close the tactile sensitivity of the human fingertip.

B. CORTICAL RESPONSES TO AIR PUFF STIMULATION

To characterize the function of the domed hairs on the wing of the Big Brown Bat (*Eptesicus fuscus*) for flight control, a series of electrophysiological experiments were conducted using air flow stimulation of the wing membrane while recording from the bat's primary somatosensory cortex, S1.

The air puff stimuli were generated by a glue workstation (EFD Ultra® 2400) that allows one to vary the duration and amplitude of the air puffs. The external trigger to the workstation also triggered the data acquisition board that recorded the waveform of the neural responses after amplification using a differential amplifier (Bak Electronics) and band-pass filtering (400 – 4000 Hz; Stanford Research Systems). The neural response was also monitored on an oscilloscope and played through a loudspeaker. For stimulation of the dorsal and ventral wing surface, the airflow was directed at the center of the receptive field from the front at a vertical angle of 30 – 45 degrees using syringes. A set of valves allowed us to present the same magnitude of airflow to either surface of the wing or to both surfaces during simultaneous stimulation without having to move the syringes. In the case of stimulation of either side alone, a valve was opened to split the airflow, resulting in the same amount of air reaching the stimulated area as in the simultaneous condition. The airflow was calibrated using an anemometer (Datametrics Model: 100VT-A). Airflow stimulation experiments were conducted on four bats. Each recording session lasted 4-6 hours and each animal underwent 2-6 recording sessions spread over a period of 1-4 weeks. Once the high-impedance (15-20 MOhm) microelectrode was advanced into the cortex, the contralateral wing was spread and taped by the tip to the recording table. The wing surface was then stimulated with the air puffs, and to determine the size and center of the receptive fields by using a set of calibrated von Frey monofilaments (North Coast), which allow for a more localized stimulation than air puffs.

Five different types of experiments were performed of different subsets of neuronal cell clusters (units):

1. The duration of the airflow was varied to study the temporal dynamics of responses.

2. The magnitude of airflow was varied to obtain input/output functions (I/O) of the units. The goal was to measure the neuronal output from threshold to the stage of saturation to determine the unit's dynamic range and the range of airflow that generated the linear part of the I/O function, so that experiment B (see next) could be conducted in a controlled fashion.

3. The dorsal and ventral surfaces were stimulated either separately or simultaneously with equal magnitude to assess possible modes of interaction between the surfaces at the same location. It is imperative for this experiment that the magnitude of airflow is kept within the linear portion of the I/O function close to threshold. In the case of suprathreshold airflow, the membrane could get indented with every stimulation, which would make recruiting of cutaneous receptors that are not associated with the sensory hairs possible. Furthermore, possible non-linear interactions between the dorsal and ventral surfaces, like facilitation, could not be detected if the operating range was close to the level of saturation.

4. The neuronal activity was tested before and after hair removal. In this experiment, baseline activity of neuronal clusters, which respond to stimulation of different wing areas, was measured; the tactile receptive field, and tactile thresholds were characterized. Then, the bat was removed from the setup, and the hairs were epilated on the entire dorsal surface of the wing using epilatory cream. The bat was allowed to recover from this

manipulation for at least one day. Then, we recorded from the same locations (+/- 50 µm) again, using stereotaxic benchmarks and digital micromanipulators (Mitutoyo). If the location of the tactile receptive field still matched (the tactile cutaneous receptors should be unaffected by the hair removal), we proceeded with the air puff stimulation.

5. Directionality of responses to airflow was characterized by measuring response magnitude to airflow direction with respect to the wing surface. The neuronal response to air puffs from eight directions (20 trials each) was recorded. In all of these experiments, Air flow velocity was calibrated with an anemometer (Datametrics 100VT-A) at 3 mm distance to the syringe opening, the same distance (syringe opening to wing membrane) that was used during the experiments. The area of the wing affected by the air puff was estimated using the displacement of talc powder on a paper surface as reference. At air puff magnitudes close to the neuronal threshold (20-30 mm/s, 2 PSI), the diameter of the affected area is about 8 mm in direction of the syringe, as well as orthogonally. With a known density of 1 hair/ mm2 (our SEM analysis), we conclude that maximally 64 hairs were deflected. In comparison the average size of the tactile receptive fields of the wing membrane, this area is small.

1. TEMPORAL CHARACTERISTICS OF CORTICAL RESPONSES

Recordings with chronically implanted floating microelectrode arrays (Microprobes) allowed us to collect responses from various sites on the wing membrane. The multi-neuron responses at each array electrode were sorted (Neuroexplorer, Plexon Inc.) for single neuron activity. Figure 4 shows responses of a single neuron to 40 ms air puffs presented from the neuron's preferred direction (135 deg) at different air flow velocities. Latencies at 0.029 m/s, close to threshold velocity (top panel), are significantly longer than at higher air flow rates. Above 0.17 m/s, latencies usually don't change. The responses are largely independent of the duration of stimulation, indicating a rather short integration time window, and a "snapshot type" of response, comparable to the visual system.

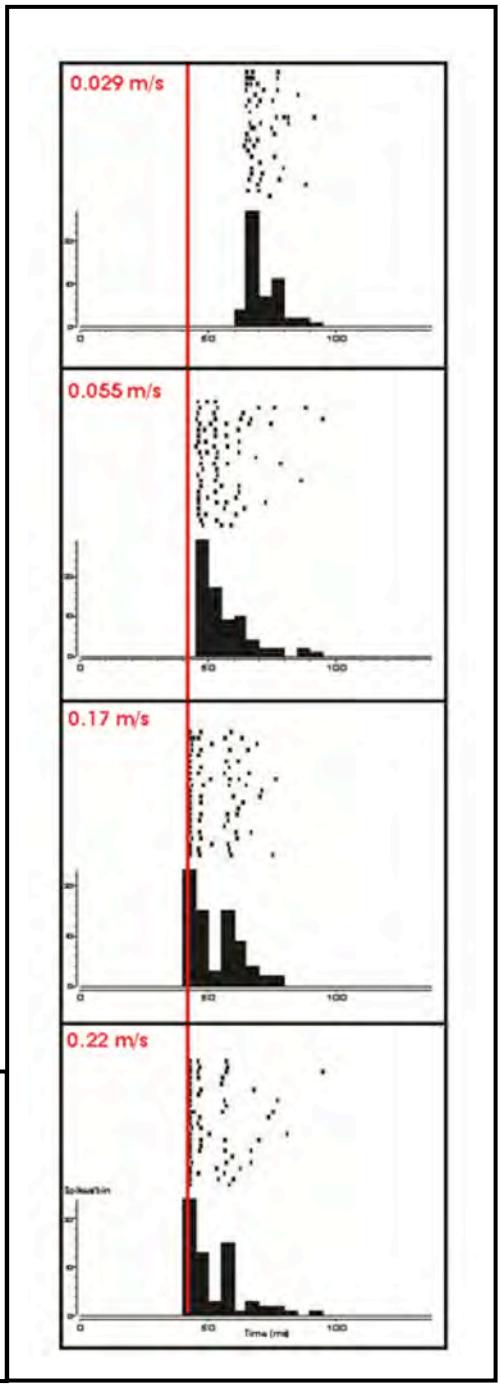

Figure 4. Response latencies to air puff stimulation shortens with increasing air flow velocity. Note that the response of this particular neuron is strongest for close to threshold airflow. Other neurons exhibit an even more sparse response – with only one or two spikes per trial - that has to be regarded as a sub-poisson process.

2. I/O FUNCTIONS

Stimulated with increasing air puff magnitudes, the units usually increased the response magnitude. Figure 5 shows the average input/output function of the neuronal activity to different PSI values of 9 multi-units. The average I/O function has a monotonic sigmoidal shape, however, some single units have non-monotonic I/O functions.

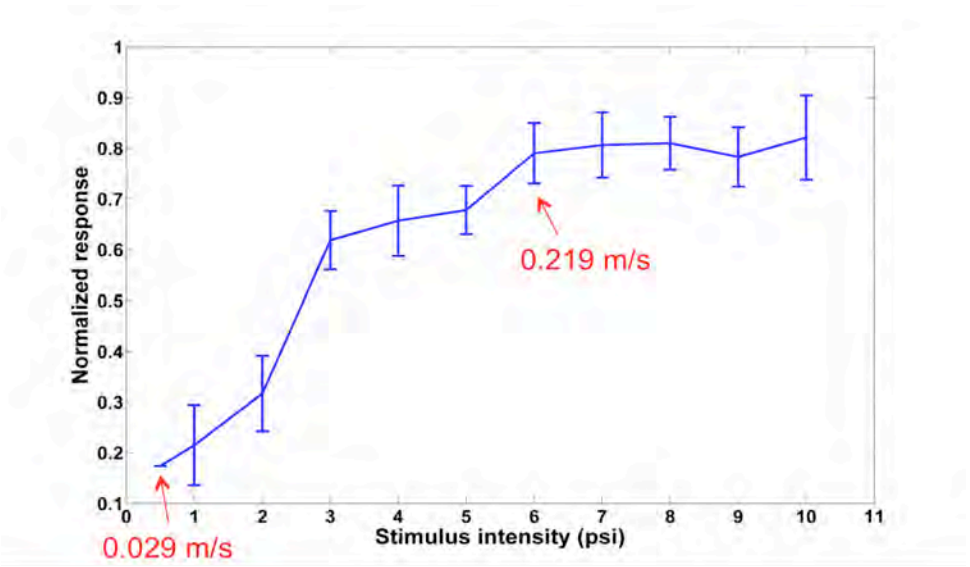

Figure 5. Average I/O functions for multi-neuron S1 clusters stimulated with changing air flow velocity.

3. INTERACTION BETWEEN DORSAL AND VENTRAL WING SURFACES

When a receptive field was found whose center was located on the wing membrane, two blunt syringe needles were positioned so that their openings pointed to the same location on the wing, one from the dorsal and one from the ventral side at a fixed measured distance (for most units 3 mm) from the surface. An air flow magnitude that just elicited a weak response, and therefore was close to threshold was chosen and delivered to either side of the membrane alone of to both sides simultaneously. For most units (7/9 recorded from two animals) analyzed so far we found evidence for facilitation if both surfaces were stimulated simultaneously, which means that the unit's response was stronger than the sum of the responses to stimulation of either side alone would predict. Figure 2 shows two examples of facilitation recorded from two different bats using different air pressure at either wing surface. The facilitation effect appears to be strongest close to threshold of the respective neuronal cluster (Fig. 6 A, D). As mentioned above, at suprathreshold air stimulation levels it cannot be ruled out that cutaneous receptors other than the hair follicle surrounding lanceolate and Merkel-receptors are contributing to the response, because the wing membrane is deflected instead of the hairs alone.

Figure 6. Cortical responses of two neurons (upper and lower rows) stimulated on the dorsal surface of the wing (red), ventral surface of the wing (green) and simultaneously on both the dorsal and ventral surfaces of the wing (blue).

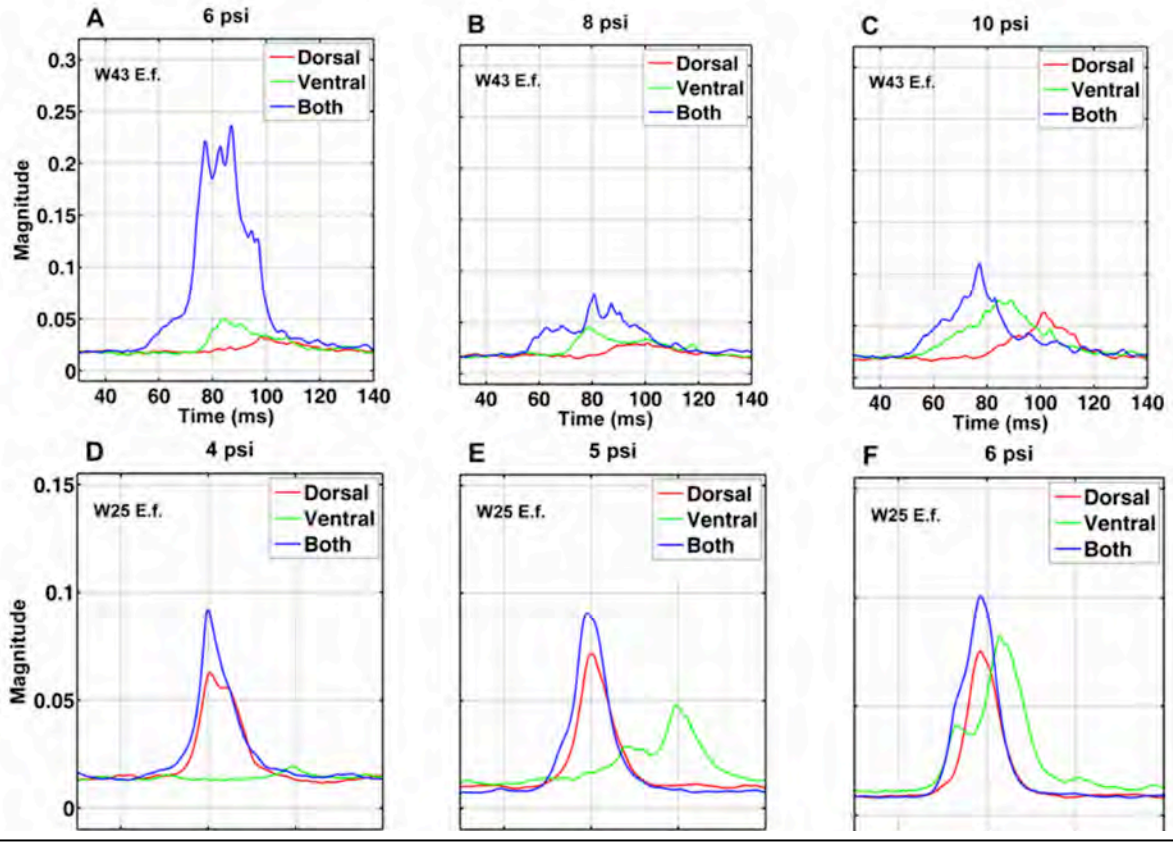

4. AIR PUFF RESPONSES BEFORE/AFTER HAIR DEPILATION

Also for this experiment it was assured that the magnitude of the air puff was chosen close to threshold of the unit/location as measured before depilation to exclude activation of other cutaneous tactile receptors than

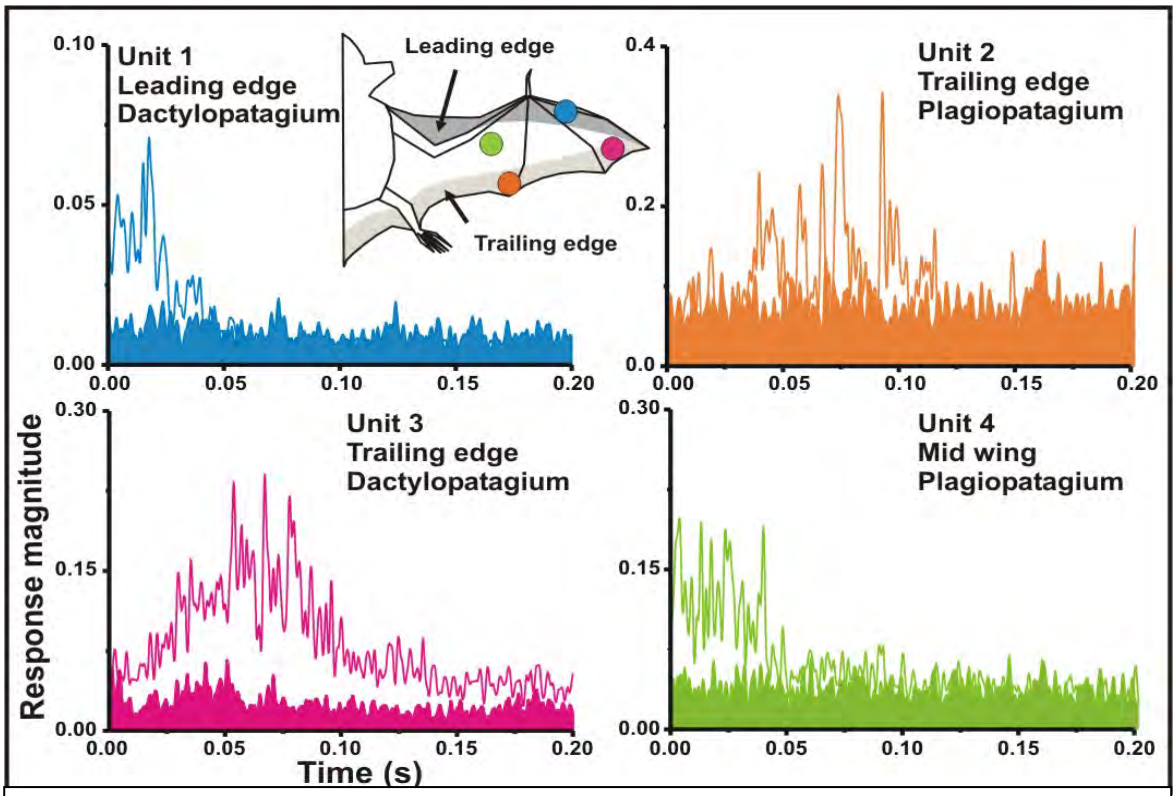

Fig. 7. Cortical responses to air puffs are diminished after depilation. The averaged post-stimulus multi-unit responses (time 0: end of air puff) to 10 air puff stimulations are shown for 4 different wing locations (see color-matched circles in bat schematic, open line- before depilation, filled area – after depilation).

those associated with the hairs. Since at least one day passed between the before/after experimental session, we can only assume that the same cortical column (same module) was studied based on our stereotaxic measurement and the location of the receptive field. It is questionable, that we recorded from the exact same cluster of neurons. However, neurons within one column and layer share inputs. Because of this well-known fact we conclude that these preliminary data hold some validity. Figure 7 shows examples of the result of one of those experiments. The upper panel shows the averaged response of the unit to 10 presentations of a close-to-threshold air puff. The lower panel shows the averaged response at the same recording location to the same strength air puff after depilation. The response is largely reduced. To address the problem of a most perfect match of contributing neurons at each location, we have begun using chronically inserted microelectrode arrays. With a fixed array, and appropriate spike sorting, we are now able to follow single neurons over time, before and after depilation of the wing membrane.

5. DIRECTIONAL SELECTIVITY TO AIRFLOW STIMULATION

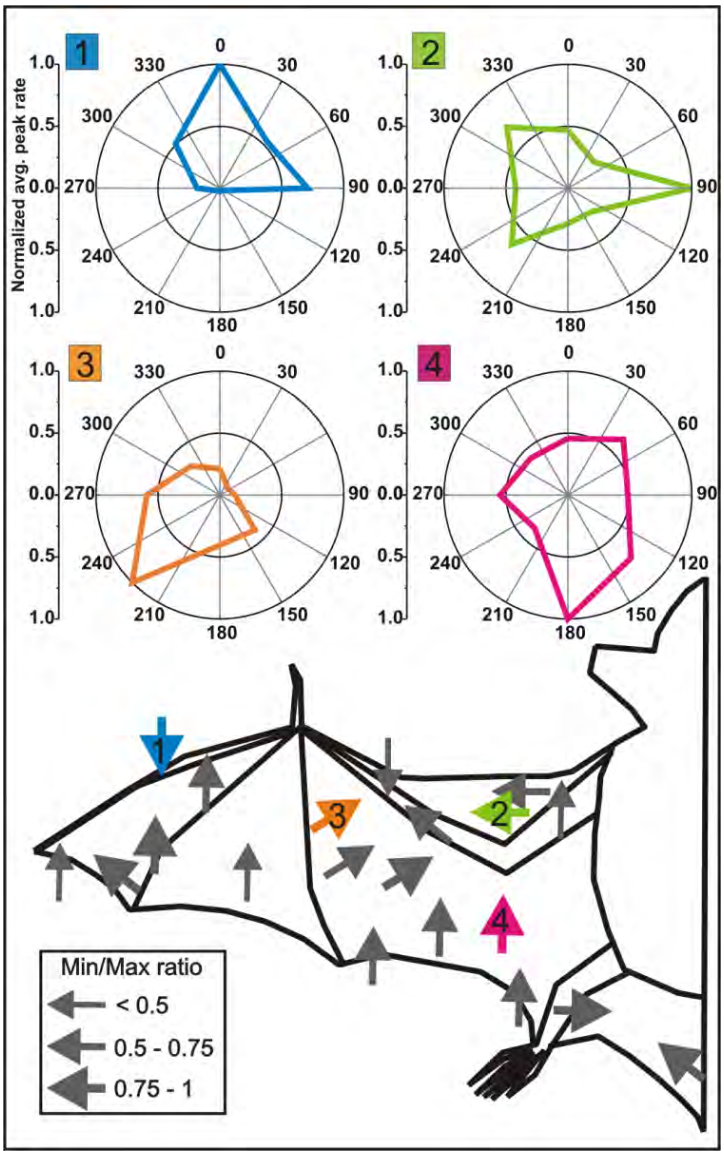

We provide here for the first time empirical evidence that the tactile receptors associated with these hairs are involved in sensorimotor flight control by providing aerodynamic feedback. We found that neurons in bat primary somatosensory cortex respond with directional sensitivity to stimulation of the wing hairs with low-speed air flow. Wing hairs mostly preferred reversed airflow, which occurs under flight conditions when the air flow separates and vortices form. This finding suggests that the hairs act as an array of sensors to monitor flight speed and/or stall. Depilation of different functional regions of the bats' wing membrane altered the flight behavior in obstacle avoidance tasks by reducing aerial maneuverability, as indicated by decreased turning angles and increased flight speed.

Figure 8. Directionality of responses to air flow in primary somatosensory cortex of *Eptesicus fuscus*. Top panels show the directional responses of 4 multi-neuron clusters as polar plots. Air flow from each of the 8 directions (every 45 degrees) was presented 20 times. The polar plots show the averages of the neuronal peak response, normalized to the peak. The lower panel shows the locations of the center of the receptive field (tip of arrow) for all tested neurons (N=20). The arrows point in the direction of air flow that excites the neurons at each location most. The 4 colored arrows indicate the wing locations for the neuronal responses shown in the upper panels. Arrow thickness indicates the minimum-maximum ratio of the directional response strength. For example, a value of 0.5 indicates that for the non-preferred direction the neuronal response was reduced by half compared to the preferred direction. Note that most neuronal clusters are tuned strongly with ratios between 0.5 and 1.

III. BEHAVIORAL STUDIES OF SOMATOSENSORY SIGNALING FOR FLIGHT CONTROL

A series of experiments is underway to study in detail the role of sensory dome-hairs in flight control. Baseline behavioral experiments are used to characterize the natural adjustments bats make in flight to avoid obstacle avoidance. Experimental manipulation of dome-hairs on the bat's wings reveals how signals from these receptors contribute to the motor adjustments in flight.

A. STUDIES OF BATS ENGAGED IN OBSTACLE AVOIDANCE IN FREE FLIGHT

The schematics (see Figure 9) below illustrate the setups used to study the role of wing hairs in flight control for obstacle avoidance in two bat species, *Eptesicus fuscus* and *Carollia perspicillata*. *Eptesicus fuscus* was trained to fly through an artificial forest (left) and *Carollia perspicillata* was trained to fly though openings in a series of nets to create a maze (right). Both species gained access to a food reward for successfully maneuvering around obstacles. Flight behavior was monitored with two high-speed video cameras mounted in corners of the room. With the stereo video recordings, we are able to reconstruct the 3-D flight paths of the bats as they perform the tasks. In the past year, we have combined high speed video image recordings with Photron cameras with high speed Vicon motion tracking of reflective markers on the bats' wings.

Originally, we planned to test both species with the net maze, but we discovered during baseline experiments that only *Carollia*, a species that maneuvers often through close spaces in the wild, was able to perform successfully in this task. Therefore, we are studying obstacle avoidance by *Eptesicus fuscus* with the artificial forest (schematic shown on left), which does not require such tight maneuvering, but nonetheless demands adjustments in flight direction to avoid collision with the trees. The artificial trees are cylindrical, constructed out of visually transparent nets, to allow us to continuously monitor the bat's flight path with our high speed video cameras.

Figure 9. Schematic of setups to record flight behavior of *Eptesicus fuscus* through an artificial forest (left) and of *Carollia perspicillata* through a net maze (right). Both tasks required turning in flight to avoid obstacles. In both setups, two high-speed video cameras recorded flight behavior, and 3-D flight paths were reconstructed.

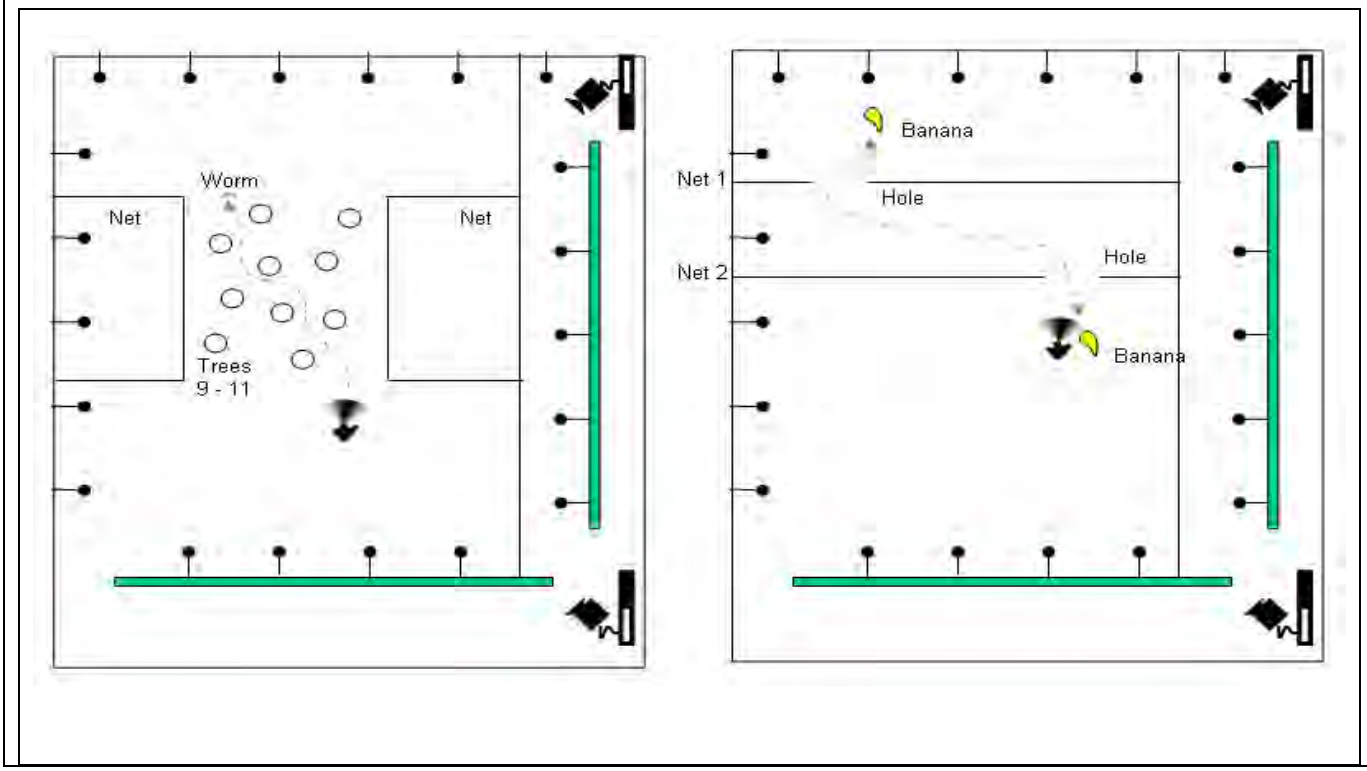

In all of the behavioral experiments, bats are run under baseline, control and experimental conditions. Baseline recordings are conducted over a minimum of twenty trials, to establish the norms of the bat's flight behavior. After baseline recordings are taken, a minimum of twenty control trials are run, in which water is applied to the bat's wings. This manipulation introduces extra handling and application of a substance to the wing, but does not affect the wing hairs. Finally, the experimental trials are conducted, in which hairs are removed from selected regions of the wings, using a depilatory cream.

1. OBSTACLE AVOIDANCE BY *EPTESICUS*

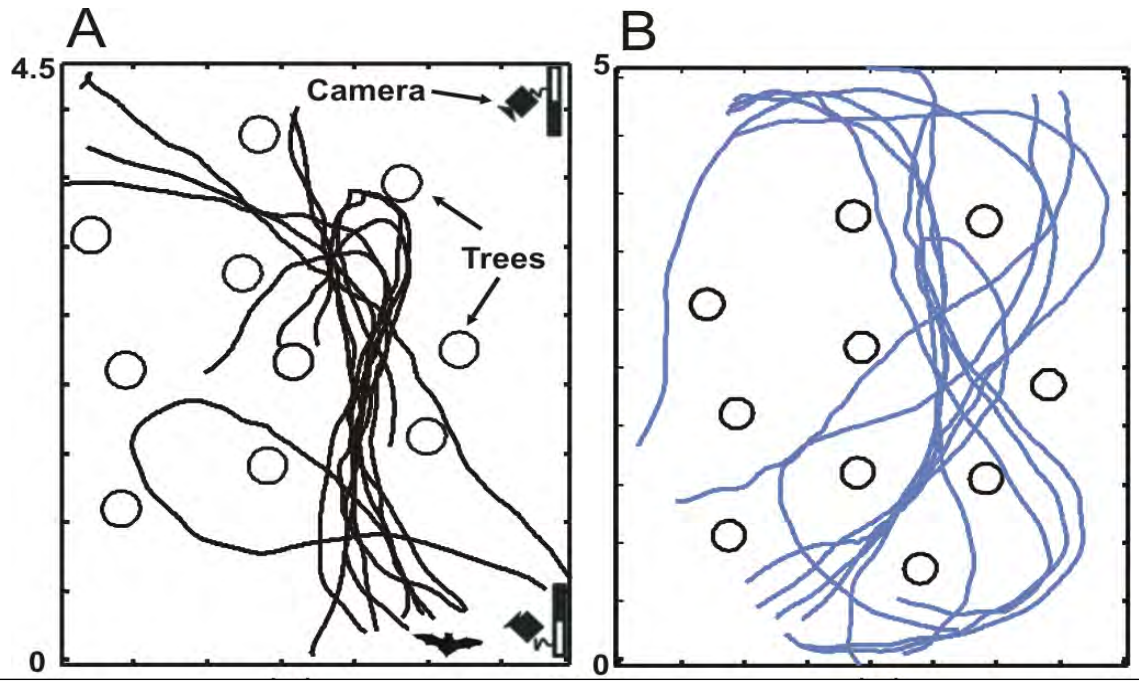

Figure 10. Overhead view of flight paths of *Eptesicus fuscus* navigating an artificial forest before (left) and after (right) wing hair depilation. The flight paths were reconstructed using high speed IR stereo video cameras. Note that the bat makes wider turns following wing hair depilation.

Shown in Figure 10 above are flight paths before and after wing hair removal in *Eptesicus fuscus*. The bat was trained to fly through a group of artificial trees to catch a tethered mealworm. Videos from two infrared-sensitive high-speed cameras were used to reconstruct the flight paths. Left panel: Ten subsequent flight paths before hair removal (viewed from top). Right panel: Ten flight paths after removal of all tactile hairs along dorsal and ventral trailing edge (2 cm width of depilated wing membrane on each side). Note that following wing hair depilation, the bat makes wider turns, i.e. the turn angle per frame decreased.

B. OBSTACLE AVOIDANCE BY *CAROLLIA*

Removing the tactile wing hairs of the trailing edge results in higher average flight speed and reduced angular turn rate angle (i.e., make wider turns) as the treated bat approaches an obstacle, compared to baseline. Although comparing bat flight to fixed-wing aircraft flight is problematic, increasing air speed is also

recommended to pilots to recover from stalls. We interpret the depilated bats' increase average flight speed as the result of the lack of input from the domed hair receptors to the somatosensory system. Our findings that neural responses to airflow are directional suggest that wing sensors may play a role in stall detection. In the behavioral task, a depilated animal may fly faster and make wider turns compared to baseline attempt to avoid a stall by speeding up, because reverse airflow signals have been disrupted, and the treated animal may have experienced that it is more vulnerable to stall. Alternatively, the hairs may simply function as flight velocity sensors, and the depilated bat would interpret a lack of input from the hairs as low speed, and consequently increase the flight speed. Of course, also kinesthetic and proprioceptive inputs are still available, and it remains an open question whether a bat can adapt to the absence of wing hairs. We tested the flight performance within two days of depilation. It is unclear if, and in which time frame the domed hairs grow back.

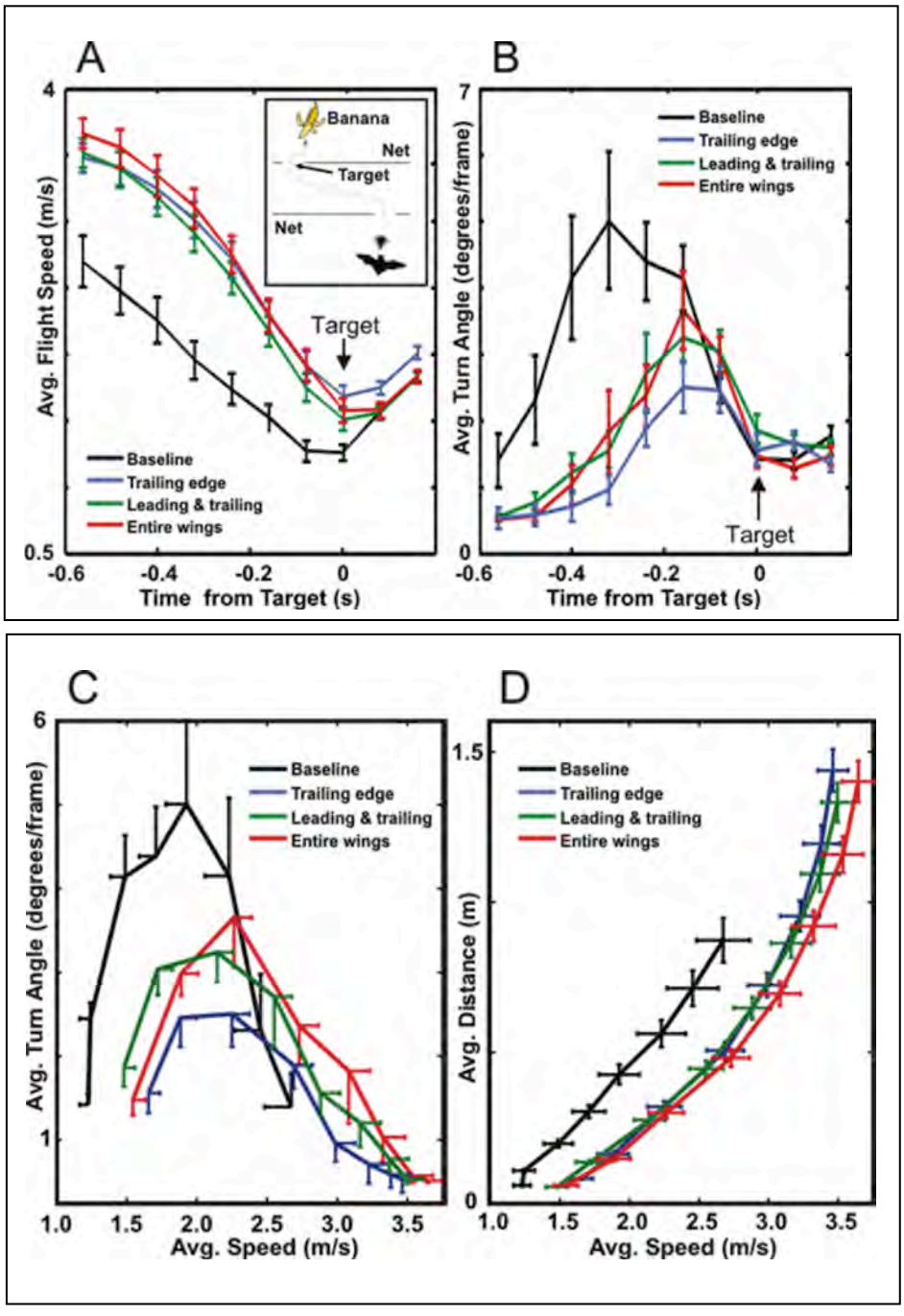

Figure 11. Flight experiments before and after wing hair removal in C.p.: The bats had to fly through openings in two nets to get a food reward (banana, see inset). A: average flight speed was increased higher after hair removal along the trailing edge (black vs. blue line), (2 animals, 117 trials, mean +/- SE). Additional depilation of the leading edge (red) and mid wing areas (green) did not further increase affect flight speed. B: conversely, the average angular turn angle rate of the bats decreased after depilation, indicating that maneuverability was negatively affected (same trials as for A). C: Flight speed versus turn angle. After treatment the average maximum speed (mean +/- SE) is increased higher, and the maximum angular turn rate angle reduced (degree/video frame). Depilated bats generally make wider turns. D. Flight speed versus obstacle distance. Maximum distance to obstacles is 16 - 25% greater after treatment.

B. BEHAVIORAL RESPONSES TO WIND GUSTS

Studies of behavioral responses to wind gusts are now underway. Big brown bats are trained to fly through an opening in a net to gain access to a mealworm. Surrounding the opening are three fans, one to the left and right of the opening, and one below the opening. The direction of wind gusts was experimentally manipulated by activating only one of these fans, following a random sequence. Control trials were included in this experiment in which no fan was activated. IR reflective markers on the bats' wings permitted high speed motion tracking of these points using a 10-camera Vicon system. These data will be used to study wing kinematics.

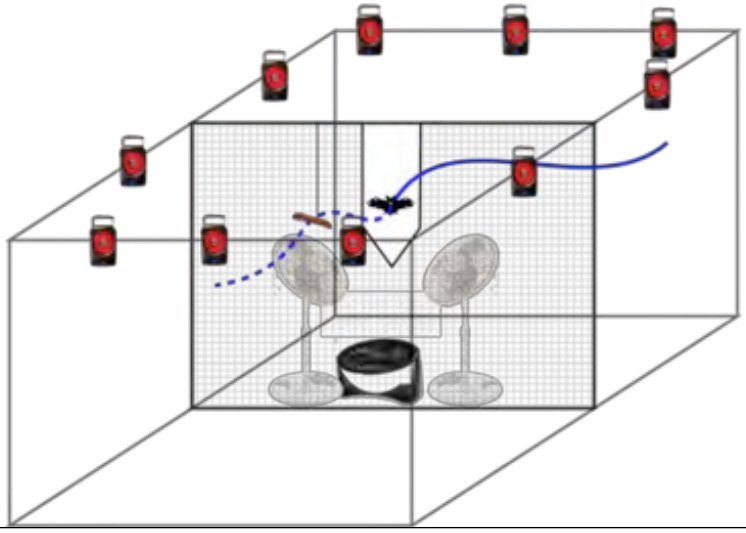

Figure 12. Schematic showing net opening that allows bat access to tethered insect reward. Three fans are positioned by the net opening to deliver wind gusts to bats as they fly through the net. 10 Vicon high speed cameras mounted on the walls of the flight room to track IR reflective markers attached to fixed locations on

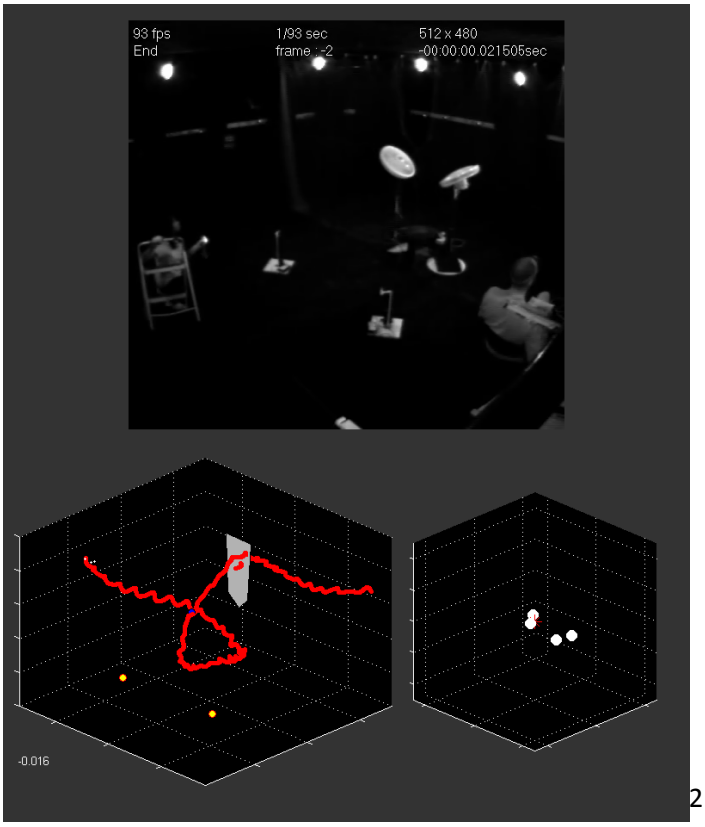

Figure 13. Raw video frame showing experimental set-up for wind gust experiments (above), flight path measured with high speed Vicon system in one behavioral trial (bottom left), and snapshot showing four marked points on the wings of the bat in one frame (bottom right).

REFERENCES:

Adrian ED (1941). J Physiol 100: 159-191

Chadha M, Moss CF, Sterbing-D'Angelo SJ (2010) *J Comp Physiol A* 197: 89-96.

Dickinson BT (2010) BIOINSPIR. BIOMIM. 5, 1-11.

Hedenström A, Johansson LC, Wolf M, von Busse R, Winter Y, Spedding GR (2007) Bat Flight Generates Complex Aerodynamic Tracks. *Science* 316: 894-897.

Maxim H (1912) *Sci Am* 27: 80-81.

Muijres FT, Johansson LC, Barfield R, Wolf M, Spedding GR, Hedenström A (2008) *Science* 319, 1250-1253.

Sterbing-D'Angelo, S., Chadha, M., Chiu, C., Falk, B., Xian, W., Barcelo, J., Zook J.M., Moss, C.F. (2011). PNAS 108: 11291-11296.

Swartz SM, Bishop K, Ismael-Aguirre MF. (2005) In Functional and evolutionary ecology of bats. Oxford Press, 2005.

Swartz SM, Groves MS, Kim HD, Walsh WR (1996) J Zool 239:357-378

Voigt CC, Winter Y. (1999). Journal of Comparative Physiology B – Biochemical Systemic and Environmental Physiology, 169(1):38–48.

Winter Y, Voigt C, Von Helversen O (1998) Journal of Experimental Biology, 201(2):237–244.

Zook JM, Fowler BC (1986) *Myotis* 23-24: 31-36.

Zook JM (2005) Soc Neurosci Abstr 78.21.

Zook JM (2006) *Evolution of Nervous Systems. Vol. 3: Somatosensory adaptations of flying mammals*, ed Kaas JH (Academic Press, Oxford), pp. 215-226.

IV. COLLABORATIONS WITH OTHER MURI TEAM MEMBERS

- Collaboration 1: Instrumentation for neurophysiological studies: Design of controlled air flow stimulus device with Brown (Breuer) group
- Collaboration 2: Behavior: Flight studies using wind tunnel facilities, with Brown (Swartz and Breuer) groups
- Collaboration 3: Modeling: Provided hair data distribution/dimensions/stiffness for OSU (Batten) group

SUMMARY DATA

Period covered: July 2008 - June 2012

Personnel

Faculty:	Cynthia Moss
	Susanne Sterbing-D'Angelo
Postdocs:	Chen Chiu
Graduate Students:	Mohit Chadha
	Ben Falk
Undergraduate Students:	Delphia Varadarajan.
	Tanvi Thakkar
	Ashlea Glickstein
	Joe Kasnadi
	Lindsay Gil
Research Assistants:	Janna Barcelo
	Wei Xian

Patents: None

Publications and Published Conference Proceedings (relevant to project)

- Sterbing-D'Angelo, S., Moss, C.F. (in prep.) Functional role of air flow sensors on the bat wing. In: „Flow Sensing in Air and Water – Behavioral, Neural and Engineering Principles of Operation". (Bleckmann, H., Mogdans, J., Coombs, S.L.,eds.) Springer Verlag, New York, Heidelberg.

- Sterbing-D'Angelo, S., Reynolds, A., Moss, C.F. (in prep.) Structural analysis of tactile hairs on the wing membrane of bats.

- Chadha, M., Marshall, K., Sterbing-D'Angelo, S., Lumpkin, E., Moss, C.F. (in prep.) Air flow receptor responses and morphology along the wing of the echolocating bat.

- Sterbing-D'Angelo, S.J., Chadha, M., Falk, B. Barcelo, J, Zook, J.M. and Moss, C.F., Bats sense air flow with specialized wing hairs, *Proceedings of the National Academy of Sciences*, 2011, 108 (27): 11291-11296.

- Chadha, M., Moss, C.F., and Sterbing-D'Angelo, S. Organization of the primary somatosensory cortex and wing representation in the big brown bat, *Eptesicus fuscus*, *Journal of Comparative Physiology*, *A*., 2011, 197, Number 1, 89-96.

- Chiu, C., Puduru, V.R. Xian, W., Krishnaprasad, P.S., and Moss, C.F. Effects of competitive prey capture on flight behavior and sonar beam pattern in paired big brown bats, *Eptesicus fuscus, J. Exp. Biol.*, 2010, 213: 3348-3356. (best paper award)

Presentations (without archival papers)

- Chadha, M., Marshall, K.L., Sterbing-D'Angelo, S.J., Lumpkin, E.A., and Moss, C.F. Tactile sensing along the wing of the echolocating bat, *Eptesicus fuscus*, Society for Neuroscience Meeting, Abstract 523.03, 2012.
- Chadha, M., Marshall, K.L., Sterbing-D'Angelo, S., Lumpkin, E.A., and Moss, C.F. Tactile sensing along the wing of the echolocating bat, *Eptesicus fuscus,* International Society for Neuroethology Congress, College Park, MD, 2012.
- Falk, B., Varadarajan, D., and Moss, C.F. The role of wing airflow sensors in bat flight control under wind gust conditions. International Society for Neuroethology Congress, College Park, MD ,2012.
- Moss, C.F., Adaptive echolocation behavior in a complex sonar scene. Acoustics 2012, Hong Kong, Animal Bioacoustics Session (invited).
- Moss, C.F. What the bat's voice tells the bat's brain. International Workshop in Auditory Neuroscience, Beijing, 2012 (invited).
- Moss, C.F. Adaptive behaviors for scene analysis in echolocating bats. 14th International Behavioral Ecology Congress, Lund, Sweden, 2012 (invited).
- Moss, C.F., Chiu, C., Barcelo, J., Xian, W., Falk, B., Chadha, M., and Sterbing-D'Angelo, S.J. Echolocation and flight behavior in three-dimensional space. Neurosensing and Bionavigation Research Center Symposium, Doshisha University, Biwako Retreat Center, Japan, 2011 (invited).

- Sterbing-D'Angelo S.J., Chadha M., Chiu C., Falk B., Xian W., Barcelo J., Moss C.F. Bat Wing Sensors Improve Flight Maneuverability, 31st meeting of the J.B. Johnston Club, Washington, D.C. (invited), *Brain Behavior and Evolution*, 2011;78:190.
- Chadha, M, Sterbing-D'Angelo, S.J., Falk, B., Barcelo, J., Xian, W. Moss, C.F. Somatosensory signaling for flight control in bats, 41st Meeting of the Society for Neuroscience, Washington, D.C., 2011, abstract number 385.12.
- Moss, C.F. Adaptive sensorimotor behaviors in the free-flying echolocating bat. Conference on Animal Migration, The Sven Lovén Centre for Marine Sciences, Kristineberg/Fiskebäckskil Sweden, 2011 (invited).
- Moss, C.F. Multimodal sensing for 3-D spatial navigation, Neural Systems and Behavior, Konishi Lecture, Woods Hole, MA, 2011 (invited).
- Sterbing-D'Angelo S.J., Chadha M., Chiu C., Falk B., Xian W., Barcelo J., Zook J.M., Moss C.F., Bat wing sensors support flight control, Conference on flow sensing in air and water, Bonn, Germany, 2011 (invited).
- Moss, C.F., Chiu, C., Barcelo, J., Xian, W., Falk, B., Chadha, M. and Sterbing-D'Angelo, S. Auditory and tactile sensing support 3-D spatial navigation in echolocating bats. Joint Meeting of the Animal Behavior Society and International Ethological Conference, Indiana University, Bloomington, IN, 2011 (invited).
- Moss, C.F. Multisensory signaling in free-flying bats. Neuroethology: Behavior, Evolution, and Neurobiology, Gordon Conference, Stonehill College, Easton, MA, 2011 (invited).
- Falk, B., Jakobsen, L., Varadarajan, D., and Moss, C.F. Adaptive sonar and flight behavior in the echolocating bat, *Eptesicus fuscus, 34th Midwinter Meeting of the Association for Research in Otolaryngolgy, 2011.*
- Moss, C.F. Active sensing for analysis of natural auditory scenes. Plenary lecture at the International Society for Neuroethology Meeting, Salamanca, Spain, 2010 (invited).
- Moss, C.F. Perception of complex auditory scenes: A glimpse of the world through the voice of the bat. Gordon Conference on the Auditory System. New Hampshire, 2010 (invited).
- Moss, CF. Active listening in a complex scene. Salk Institute Symposium on Biological Complexity. Sensory Systems. San Diego, CA 2010 (invited).
- Moss, C.F. Perceptual, cognitive and adaptive motor behaviors enable the echolocating bat, *Eptesicus fuscus*, to negotiate a complex environment Fifth international animal sonar symposium, Kyoto, Japan, 2009 (invited).
- Sterbing-D'Angelo, S.J., Chadha, M., Falk, B. Barcelo, J, Zook, J.M. and Moss, C.F. Role of somatosensory signaling for flight control in the echolocating bat, *Eptesicus fuscus*. Fifth international animal sonar symposium, Kyoto, Japan, 2009.
- Moss, C.F. and Surlykke, A. Action and audition for spatial orientation in bats. Gordon Conference on Sensory Coding and the Natural Environment, Il Ciocco, Italy, 2008 (invited).
- Zook, J.M., Falk, B., Sterbing-D'Angelo, S.J., Moss, C.F. Separate contributions of dorsal and ventral wing-surface tactile receptors to bat flight behavior. Thirty-eighth Meeting of the Society for Neuroscience, Washington, D.C., 2008.

- Sterbing-D'Angelo, S.J., Chadha, M., and Moss, C.F. Representation of the wing membrane in somatosensory cortex of the bat, *Eptesicus fuscus*, Thirty-eighth Meeting of the Society for Neuroscience, Washington, D.C., 2008.

OREGON STATE UNIVERSITY

CONTENTS

INTRODUCTION

The primary goal of the Oregon State University (OSU) group during the MURI funding was to understand how bats control their flight, focusing on the inner loop control (e.g., movement of the bat including stabilization, not navigation). This included understanding local control mechanisms—e.g., control of wing shape for aerodynamic performance—as well as global control of propulsion and how bats accommodate disturbances such as gusts.

The approach taken by the OSU team has been to use mathematical modeling tools from the partial differential equations (PDE) control community to form a hierarchy of models that can be used to understand the physical underpinnings of bat flight. This includes the high fidelity PDE model as well as varying levels of fidelity of reduced order models that capture salient features of the full order model. We have developed a new approach to reduced order modeling that provides convergence results not normally obtainable for popular reduced order methodology. The control methods used include both model based control such as linear quadratic, MinMax and central controller, as well as learning based methods applied to multi-agent systems.

Over the five years of funding, research has focused on developing and analyzing algorithms for model reduction and feedback control design for partial differential equation (PDE) systems, modeling hair cell sensors, modeling membrane-bone structures, and utilizing a variety of control methods—both model based and learning methods—that can be used to understand the role of flexibility in the control loops used in bat flight. The team focused on the following tasks; the specific PIs involved in each task are noted in parentheses:

1. Reduced order model development/reduced order compensators (Singler/Batten/Merritt)
2. Role of hair cells as flow sensors (Dickinson)
3. Multi-agent methods for multiple actuator coordination (Salichon)
4. Structural Modeling for Flexible Wings (Ray/Batten)
5. Smart Wing Shaping (Ray/Batten)
6. Digital image correlation for parameter estimation in composite structures (Chuang/Ray/Albertani/Batten)

An overview of accomplishments during the funded research period is given under each task.

REDUCED ORDER MODEL DEVELOPMENT AND REDUCED ORDER COMPENSATORS

Research in this task spanned the entire funding period. Accomplishments within this task include:

- Focused on computing control laws and reduced order models for PDE systems, concentrating on efficient and accurate algorithms for linear PDE systems that will be extended to nonlinear systems. We have developed a variety of computational tools including: a new low storage snapshot algorithms for infinite dimensional Lyapunov and Riccati equations; a new POD-based algorithm for LQG balanced model reduction; proved convergence theory for Lyapunov algorithms and POD-based algorithm for balanced model reduction of parabolic systems; established a POD-like optimal data reconstruction property for “balanced POD” of two general datasets.
- Used proper orthogonal decomposition (POD) in a new way to develop model reduction and control algorithms for linear PDE systems. Specifically, we are applying POD in a novel and systematic fashion to derive efficient algorithms with convergence theory and error bounds. Using this method, we have obtained preliminary results for feedback control design using a snapshot algorithm for a linear incompressible flow system.
- Developed a generalized computational method, termed the group-POD method, as a way to represent and compute nonlinear terms of truncated Galerkin projections with a proper orthogonal decomposition (POD) basis in a more computationally efficient form. The computational efficiency and accuracy of the group-POD method was supported with experiments using a two-dimensional Burgers’ equation, which captures some of the computationally challenging aspects of Navier-Stokes equations, as a model problem.
- Initiated development and extensions of linear control laws and linear model reduction techniques to nonlinear PDE

systems. Such extensions have great potential for controlling fluid flows. And extending the algorithms in these directions will enable development of realistic controllers for systems modeled by PDE systems, such as a fluid-structure interaction in the bat wing.

- In the final funding period, the team applied the algorithms that had been developed for test cases to the structural simulation codes that Ray developed for morphing wing estimation and control. This work has been submitted for publication in 2013 American Control Conference, and is currently under review.

MODELING HAIR CELL SENSORS FOR FLOW ESTIMATION AND CONTROL

Within the MURI project, the team developed models of hair-cell sensors for control applications. Specifically, we focused on creating a model of the hair-cell sensor, characterizing its response to an unsteady separating flow, and from that characterization, constructing a model for use in optimal control designs. Particular advances in the hair-cell modeling include: Increased understanding of the detection of boundary layer flows with hair sensors; Development of simplified hair sensor models suitable for control design; and Initial investigations into hair cell sensors for observer design in an unsteady Stokes flow control problem. Research into construction of artificial hair cell sensors based on this task is underway at the Air Force Research Lab Materials Directorate.

MULTIAGENT CONTROL TECHNIQUES FOR MICRO AIR VEHICLES

Within this task, the team concentrated on leveraging multi-agent control techniques to accommodate a higher number of control surfaces on a Micro Air Vehicle (MAV) with the goal of designing a more robust and efficient MAV control. The results show that MAV performances are improved both in terms of reduced deflection angles and reduced drag (up to 4%) over a simplified model in two sets of experiments with different objective functions.

STRUCTURAL MODELING FOR FLEXIBLE WINGS

Work within this task had two focus areas. The first looked at modeling and control of a flexible hub/beam/mass structure that rotates at the hub. This structure served as an idealization of a flexible flapping structure and the project arose out of initial discussions with Sharon Swartz and Johnny Evers at the inception of the project. As the project evolved, we decided to focus on control of shape morphing (such as camber) instead of flapping, as this fit better with the hair cell sensor work within the team. This project came to be known as smart wing shaping.

SMART WING SHAPING

The smart wing shaping work began with developing finite element codes that could be used to simulate, control, and estimate behavior of a morphing wing with smart sensors and actuators. During the MURI funding period, the following progress was made under this task:

- Derived and extended thin plate theory for anisotropic materials with distributed smart material sensors and actuators.
- Designed and constructed a versatile finite element code that admits any initial conditions, anisotropic material parameters, sensor and actuator positions, and external loading inputs, and solves for both open- and closed-loop system response for full state as well as partial state feedback linear quadratic control. While not discussed in detail in this report, this code has been and is being utilized in a variety of additional projects and investigations, including model reduction, sensor placement and system identification investigations.
- Demonstrated that piezoceramic patches can be effectively used to control wing shape.

These results have been previously reported on. The following results are new to the last funding increment, and will be discussed further below:

- Derived a membrane and stretch sensor model from basic principles to investigate membrane wing dynamics.

- Constructed a second finite element code for the simulation of membrane wing dynamics to estimate aerodynamic load inputs to a membrane wing system.
- Derived a novel load identification method for membrane wings with distributed stretch, or strain, sensors, and investigated its efficacy via numerical simulation and experimental wind tunnel tests.

LOAD IDENTIFICATION

Motivated by the previous wing morphing studies and a surge of interest in membrane wing micro air vehicles, a novel means of estimating aerodynamic load was formulated and studied. Fundamentally, the approach utilizes a joint extended Kalman filter and an important form of regularization to approximate the pressure distribution on a membrane wing from a few nonlinear strain measurements.

The measurements were assumed to be of a form similar to what the bat might sense during flight using muscle spindles (stretch sensors) due to deformation of its wing membrane. Assuming the muscles sense stretch, one can derive a nonlinear strain model to approximate such feedback for use in approximating solutions to the nonlinear load identification problem. However, even with such sensors, the problem is still ill posed. A major contribution of this work was determining how to enforce smooth solutions, and therefore unique solutions, to this problem. This was done by assuming the aerodynamic loads vary smoothly, and by formulating a modified form of the joint extended Kalman filter, to yield a regularized solution. Through extensive numerical experiments, it was determined that this was sufficient to consistently solve the load identification problem for a variety of load distributions.

Figures 1 and 2 depict an estimated load with 1% and 5% noise, respectively, while the exact load is illustrated in Figure 3. This is a quadratic load with maximum value of 200 Pa pressure occurring in the center of the membrane, decreasing to zero along the boundaries.

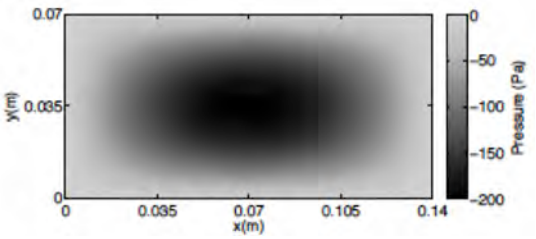

Figure 1 Estimated load distribution, 1% noise

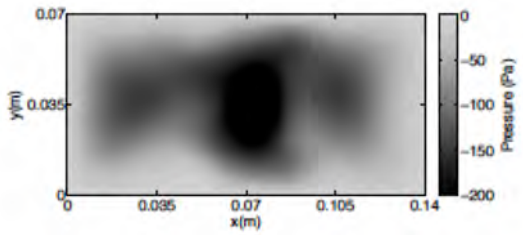

Figure 2 Estimated load distribution, 5% noise

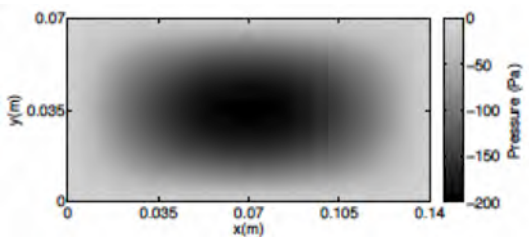

Figure 3 Exact load, P = 200sin(pi*x)sin(pi*y)

The resulting estimated membrane deformation for each noise case is illustrated in Figures 4 and 5. The error in membrane position and velocity states is hardly visible in these images; to the careful eye, a slight discrepancy can be seen in the 5% noise case, Figure 5, in which the mesh lines between the exact solution and estimated position are not perfectly aligned.

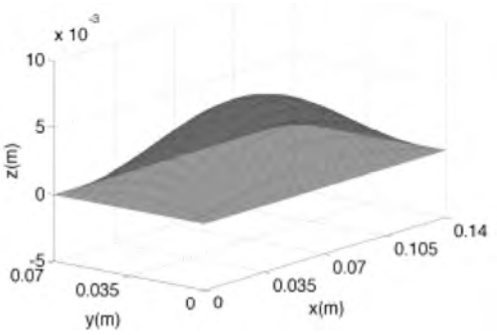

Figure 4 Final membrane position, 1% noise

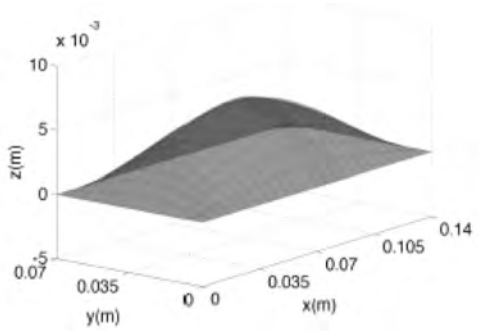

Figure 5 Final membrane position, 5% noise

This load identification approach was also investigated experimentally, yielding some exciting preliminary results. Figures 6 and 7 respectively depict the membrane wing being manufactured and tested in the wind tunnel. The wing is composed of latex that is glued securely to a steel frame (constructed to ensure a nearly rigid support and, therefore, appropriate Dirichlet boundary conditions). The wing was tested at an angle of attack of 4 degrees with 18 m/s free stream velocity.

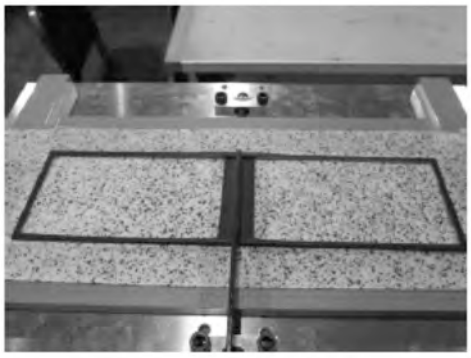

Figure 6 Membrane wing fabrication

Figure 7 Wing tunnel testing

Speckled before testing, the wing was photographed with high-speed cameras to allow a digital image correlation system to reconstruct the membrane deformation and strain fields that developed. Using the computed strain fields to approximate appropriate nonlinear strain sensors, the load identification algorithm was applied directly to the laboratory data to yield the results displayed in Figures 8 and 9. Figure 8 illustrates the identified load, appearing quadratic in nature. Figure 9 depicts the reconstructed membrane position as a mesh, and the actual measured digital image correlation position as a surface.

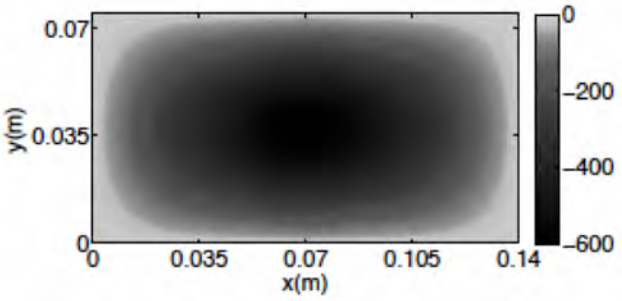

Figure 8 Estimated load distribution, on membrane wing

More interesting is the comparison between the sting balance measurement of lift and the integrated estimate of pressure distribution. These data are in agreement within 5% and illustrated in Figure 10.

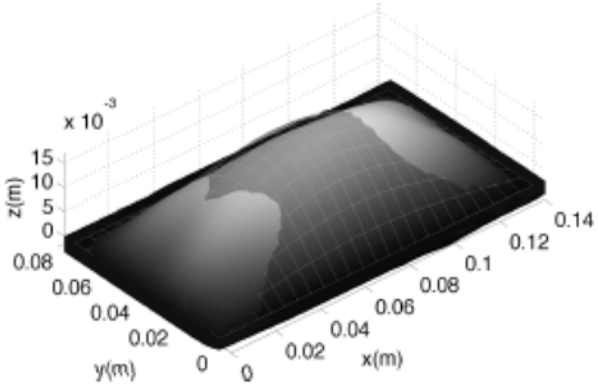

Figure 9 Estimated (mesh) and measured (interpolated surface) membrane deformation

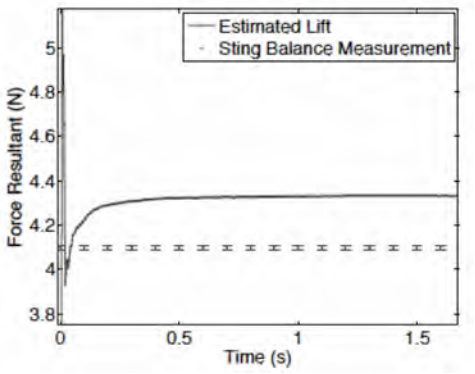

Figure 10 Time-varying lift resultant estimate

The results obtained under the smart material wing task have laid the foundation for further work in this area that could integrate the hair cell sensors, piezoceramic actuators and flexible wings for a variety of missions. While the research has been performed in the context of micro air vehicles as the motivating application, the results apply to larger scale aircraft as well. Further work on real-time estimation based on reduced order models that incorporate nonlinear effects is merited, and should prove to enhance the performance of air vehicles more widely.

DIGITAL IMAGE CORRELATION FOR PARAMETER ESTIMATION IN COMPOSITE STRUCTURES

Work within this task was done within the last funding period, and therefore does not appear in other annual reports.

Identifying material parameters in composite plates is a necessary first step in order to develop accurate models of composite wings suitable for control development and sensor/actuator placement. Traditional testing methods for finding material parameters such as stiffness and damping require multiple types of experiments such as tensile tests and shaker tests. These tests are not without complications. Tensile testing can be destructive to the test specimens while use of strain gages and accelerometers can be inappropriate due to the lightweight nature of the structures.

In this task, the team investigated inverse problem testing methods using digital image correlation (DIC) via high-speed cameras. This approach can potentially eliminate the disadvantages of traditional methods as well as determine the required material parameters by conducting only one type of experiment. These material parameters include stiffness and damping for both isotropic and orthotropic materials, and ply angle layup specifically for carbon fiber materials. A finite element model based on the Kirchoff-Love thin plate theory was used to produce theoretical data for comparison with experimental data collected using DIC. Shaker experiments were also carried out using DIC to investigate the modal frequencies as validation of the results of the inverse problem.

These techniques were first applied to an aluminum plate for which material parameters were known, to test the performance and efficiency of the method. We then applied the method to composite plates to determine these parameters, as well as the layup angle. Specifically, three types of plate samples were made and tested: 6061 aluminum plates, 0◦ carbon fiber plates, and 15◦ carbon fiber plates.

A stationary vice was used to hold the plates, and releasing the plates from a corner displacement provided an initial displacement. The results of the dynamic displacements of the plates recorded by DIC were used for the inverse problem. The inverse problem successfully estimated the Young's modulus and damping for the aluminum material. Shaker tests were also performed on all test specimens as a validation for the material parameters obtained from the inverse problem as well as a validation of the accuracy of the finite element model for all test samples. The vibration analysis produced consistent resonance frequencies for the first two modes for both theoretical and experimental data. However, carbon fiber plates presented challenges.

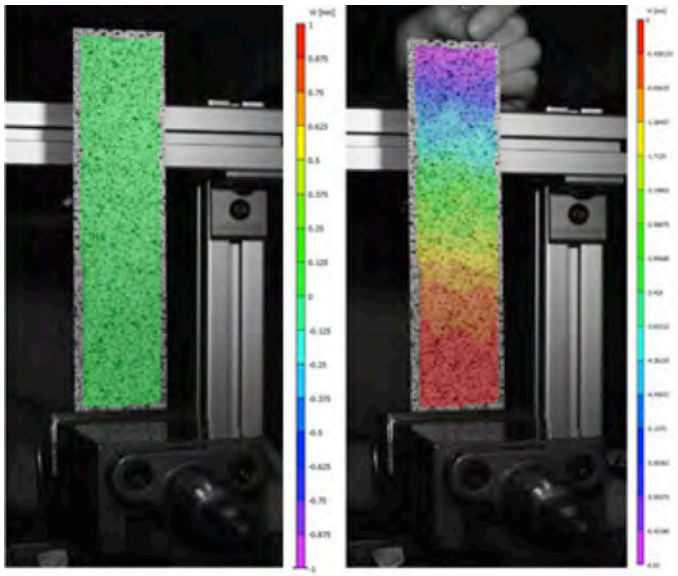

Figure 11 Left: initial image with zero displacement; right: the plate after it is released from an initial displacement of the corner

In seeking to identify the material parameters for the 0◦ and 15◦ carbon fiber plates, the inverse problem was not able to estimate the parameters. In addition, even with known results found from the tensile tests, the finite element model could not accurately represent the dynamic behavior of either type of carbon fiber test specimens during vibration analysis. We expect a primary source of difficulty was due to limitations of the Kirchoff-Love plate theory used as the underlining theoretical model for the finite element approximation in the inverse problem, resulting in a persistent mismatch of resonance frequencies in experimental data.

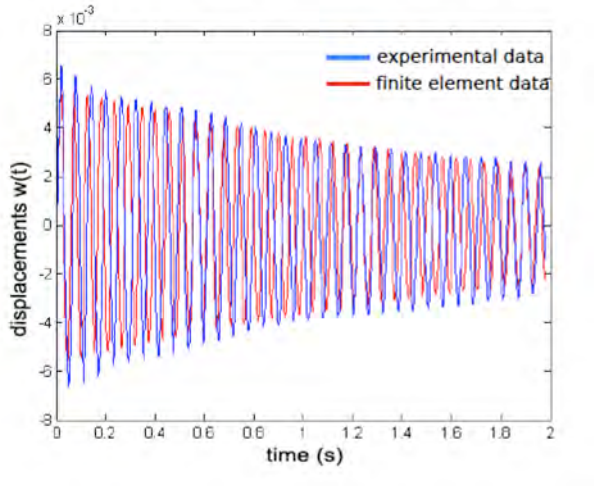

Figure 12 Displacement matching results for center of aluminum plate between finite element data (red) and experimental data (blue). Finite element data and experimental data match fairly well in terms of both vibrational amplitude and frequency

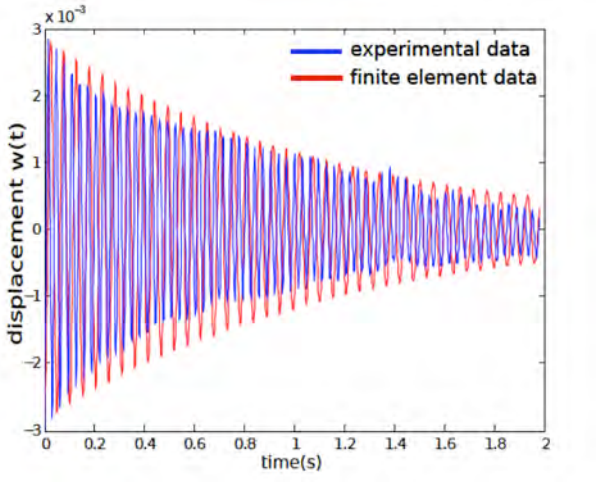

Figure 13 An example of inconsistent displacement matching results between finite element data (red) and experimental data (blue) collected from DIC. The frequency mismatch is approximately a factor of two

Despite the difficulties in estimating the carbon fiber material parameters, the results found in the vibration analysis were consistent with the prediction of plates' dynamic behavior based on their stiffness and layup angles. In terms of experimental data collection, DIC proved to be reliable in measuring full field displacement data and also capturing modal

frequencies in vibration analysis.

For future material characterization of carbon fiber using the inverse problem approach, greater attention in modeling damping might alleviate the challenges faced within this project, as well as using quasi-isotropic or less non-isotropic laminates for validation. Other plate models may be used for predicting the material parameters as well. In particular, additional parameters associated with nonlinear terms might be implemented for more accurate model estimation since this task used only a linear plate model.

COLLABORATIONS WITH OTHER MURI TEAM MEMBERS

1. Collaboration with Brown University: joint work, visits, and weekly meetings via Skype.
2. Graduate Student (Ben Dickinson) visited MIT; discussions with M. Drela refined paper on optimal hair length
3. Ben Dickinson accepted AFOSR funded NRC postdoc at AFRL/RW (Eglin) to work with G. Abate; begins October 2009.

SUMMARY AND PLANS FOR FUTURE WORK

Significant progress was made during the funded MURI research in the algorithms for model formulation and controller design, and in characterizing the hair cell sensor for use in flow estimation. Research in artificial hair cell sensors has transitioned to the Air Force Research Lab Materials Directorate, where fabrication of such sensors for use in enhanced airplane flight control is underway. Integrating the sensor work, reduced order modeling task, and the extensive work on structural modeling, a holistic task on smart material wing developed to integrate the work. This task lays the foundation for future work that could apply to air vehicles in a variety of scales and flight domains. In addition, some foundational work in using digital image correlation to identify material parameters was undertaken. The method shows promise for conventional materials, but still has challenges for composites—we expect that model shortcomings had more to do with the underwhelming performance than did the digital image correlation approach itself.

Future areas for research from this part of the MURI team include:

- Extensions of the reduced order model framework to nonlinear systems.
- Characterization of different reduced order controller methodologies based on Riccati sensitivities
- Continuation of the work on observers for use in controllers
- Continued development of smart wing, to include more sophisticated sensor placement approaches.
- Incorporation of better composite material models into digital image correlation to investigate performance in composite structures.

SUMMARY DATA

Period covered: July 2007 - July 2012

Personnel

Faculty: Belinda Batten, John Singler (transitioned from Postdoctoral Associate to Assistant Professor, Department of Mathematics, Missouri University of Science and Technology, 8/2008)

Graduate Students: Ben Dickinson (MS, PhD), Cody Ray (MS, PhD), Max Salichon (PhD), Joshua Merritt (MS), Jasmine Chuang (MS)

Undergraduate Students: Andreas Simonis

Other Visitors and Collaborations (outside MURI team members): Dr. Yue Zhang

Patents: none

Awards and Recognition: Ben Dickinson received the award in School of Mechanical, Industrial, and Manufacturing Engineering at OSU for the Outstanding Graduate Research Assistant in 2008-09 for his work supported on this MURI; Ben Dickinson was selected as a National Research Council Postdoctoral Research Associate at Air Force Research Lab.

Publications in refereed journals

1. J.R. Singler and B.A. Batten, "A Proper Orthogonal Decomposition Approach to Approximate Balanced Truncation of Infinite Dimensional Linear Systems", *International Journal of Computer Mathematics*, vol. 86, no. 2, 2009, pp. 355–371.
2. B. T. Dickinson and J. R. Singler, "Nonlinear Model Reduction Using Group Proper Orthogonal Decomposition," *International Journal of Numerical Analysis and Modeling*, vol. 7, no. 2, pp. 356-372, 2010.
3. K. A. Evans and B. A. Batten, Reduced Order Compensators via Balancing and Central Control Design for a Structural Control Problem, *International Journal of Control*, vol. 83, 563–574, 2010.
4. J.R. Singler and B.A Batten, Balanced POD for Linear PDE Robust Control Computations, *Computational Optimization and Applications* 2011, 1–22.
5. B.T. Dickinson, J.R. Singler and B.A. Batten, Mathematical Modeling and Simulation of Biologically Inspired Hair Receptor Arrays in Laminar Unsteady Flow Separation, Journal of Fluids and Structures, 29, 1–17, 2012.
6. Max Salichon and Kagan Tumer. A neuro-evolutionary approach to control surface segmentation for micro aerial vehicles. International Journal of General Systems to appear, 2012.

In review

7. J. R. Singler, "Convergent Snapshot Algorithms for Infinite Dimensional Lyapunov Equations," *IMA Journal of Numerical Analysis*, in review.
8. J. R. Singler, "Optimality of Standard and Balanced Proper Orthogonal Decomposition for Data Reconstruction," *Numerical Functional Analysis and Optimization*, in review.
9. J. R. Singler, "Snapshot Algorithm for Balanced Model Reduction of Linear Parabolic Systems: Convergence Theory," *Numerische Mathematik*, in review.
10. J.R. Singler, J. Merritt, C.W. Ray, and B. A. Batten, Reduced Order Controllers for an Anisotropic Composite Plate with Smart Actuation and Sensing, *Proceedings of the 2013 American Control Conference*, in review.

Publications in refereed conference proceedings:

1. J.R. Singler and B.A. Batten, "Balanced Proper Orthogonal Decomposition for Model Reduction of Infinite Dimensional Linear Systems", in *Proceedings of the 7th International Conference on Computational and Mathematical Methods in Science and Engineering (CMMSE)*, 2007, pp. 361-371.
2. J.R. Singler "Approximate Low Rank Solutions of Lyapunov Equations via Proper Orthogonal Decomposition," *Proceedings of the 2008 American Control Conference*, Seattle, WA, June 2008, pp. 267 – 272.
3. B. T. Dickinson, J.R. Singler and B.A. Batten, "The Detection of Unsteady Flow Separation with Bioinspired Hair Cell Sensors", 26th AIAA Aerodynamic Measurement Technology and Ground Testing Conference, June 2008, Seattle, WA, Paper AIAA-2008-3937.
4. M. Salichon and K. Tumer, "A Neuro-evolutionary Approach to Micro Aerial Vehicle Control", In Intelligent Engineering Systems Through Artificial Neural Networks Conference, Vol. 18, pp. 11-18, ASME Press, 2008. (ANNIE 08).
5. J. R. Singler and B. A. Batten, "A Comparison of Balanced Truncation Methods for Closed Loop Systems", Proceedings of the American Control Conference, 2009, pp. 820-825.
6. B. T. Dickinson, John R. Singler, and Belinda A. Batten, "A Snapshot Algorithm for Linear Feedback Flow Control

Design," *Proceedings of the AIAA Infotech@Aerospace Conference and AIAA Unmanned...Unlimited Conference*, 2009, AIAA paper number 2009-1961.

7. J. R. Singler and B. A. Batten, Balanced POD Algorithm for Robust Control Design for Linear Distributed Systems, *Proceedings of the American Control Conference,* June 2010, Baltimore, 4881–4886.
8. C. W. Ray, B. A. Batten, and J. R. Singler, Feedback Control of a Bioinspired Membrane-Beam Systems, *Proceedings of the IEEE Control and Decision Conference,* December 2010, Atlanta, 1719–1724.
9. C. W. Ray, B. A. Batten, and J. R. Singler, A Model Based Feedback Controller for Wing-Twist via Piezoceramic Actuation, *Proceedings of the American Control Conference*, June 2011, San Francisco CA, 2362–2367.

Presentations (without archival papers)

1. B. A. Batten and *J. R. Singler*, "A New Algorithm for Balanced Truncation", ASME International Mechanical Engineering Congress and Exposition, Boston MA, November 2008.
2. B. T. Dickinson, ""A mathematical model of the detection of unsteady flow separation by hairs on a bat wing", *Society for Integrative and Comparative Biology,* Boston MA January 2009.
3. J. R. Singler, "New POD-Based Algorithms for Model Reduction and Control of PDEs," Colloquium presentation, Department of Mathematics, Virginia Tech, Blacksburg, VA, January 2009.
4. *Benjamin T. Dickinson*, John R. Singler, and Belinda A. Batten, "Biologically inspired hair sensor arrays for flow control", invited minisymposium presentation, AIAA Infotech@Aerospace Conference and AIAA Unmanned...Unlimited Conference, Seattle, WA, April 2009.
5. B. A. Batten and J. R. Singler, "Comparison of Truncation Methods for Low Order Estimators", 2009 SIAM Conference on Control and Its Applications, Denver CO, July 2009.
6. B. T. Dickinson, "Observer Design for an Unsteady Oseen Flow with Hair Sensor Arrays", 2009 SIAM Conference on Control and Its Applications, Denver CO, July 2009.
7. J. R. Singler, 'Convergent Snapshot Algorithms for Model Reduction and Feedback Control of PDE Systems", 2009 SIAM Conference on Control and Its Applications, Denver CO, July 2009.
8. *J. Chuang*, C.W. Ray, R. Albertani, B.A. Batten, Material Characterization and Modal Analysis of Composite Plates via Digital Image Correlation, Society for the Advancement of Material and Process Engineering, Baltimore, MD, May 2012.

(speaker in italics, when more than one author listed)

Dissertations and Theses Produced

Cody W. Ray, *Modeling Control and Estimation of Flexible Aerodynamic Structures*, M.S. Thesis, 2008

Benjamin T. Dickinson, *Detecting Fluid Flows with Bioinspired Hair Sensors*, Ph.D. Dissertation, Oregon State University, 2009

Max Salichon, *Learning Based Methods Applied to the MAV Control Problem*, Ph.D. Dissertation, Oregon State University, 2009.

Cody W. Ray, *Modeling and Control of a Biologically Inspired Compliant Structure*, Ph.D. Dissertation, Oregon State University, 2012.

Chuang, Chih-Lan (Jasmine), *Application of Digital Image Correlation in Material Parameter Estimation and Vibration Analysis of Carbon Fiber Composite and Aluminum Plates,* M.S. thesis, Oregon State University, 2012.